THE MASS OF L-PYRROLYSINE IN METHYLAMINE METHYLTRANSFERASES AND THE ROLE OF ITS IMINE BOND IN CATALYSIS

DISSERTATION

Presented in Partial Fulfillment of the Requirements for the Degree of Doctor of Philosophy in the Graduate School of The Ohio State University

by

Jitesh Anthony Aloysius Soares, M.S.

The Ohio State University

2008

Dissertation Committee:

Dr. Joseph A. Krzycki, Advisor

Dr. Charles J. Daniels

Dr. Mark Morrison

Dr. F. Robert Tabita

Approved by

_____

Advisor

Graduate Program in Microbiology

ABSTRACT

Methanosarcina barkeri is an archaeon capable of producing methane from methylamines. Methylamine methyltransferases initiate methanogenesis from methylamines by transferring methyl groups to a cognate corrinoid protein. Each gene encoding a methylamine methyltransferase has been shown to contain a single in-frame amber codon. Further studies have shown that in the monomethylamine methyltransferase, *mtmB*, the amber codon encodes a novel amino acid, *L*-pyrrolysine. X-ray crystal structures of MtmB have shown that the structure of this amino acid is a lysine residue with the epsilon-nitrogen in amide linkage to a (4R, 5R)-4-substituted pyrrolyine-5-carboxylate ring. However, these structures did not allow an assignment of the pyrroline ring C4 substituent as a methyl or amine group. In this thesis (Chapter 2) mass spectrometry of chymotryptic digests of methylamine methyltransferases is employed to show that pyrrolysine in present in all three types of methylamine methyltransferase at the position corresponding to the amber codon in their respective genes. The mass of this amber-encoded residue was observed to coincide with the predicted mass of pyrrolysine with a methyl- group at the C4 position.

The x-ray crystal structures showed that pyrrolysine had electrophilic character suggesting the presence of an imine bond which could play a role in catalysis. In Chapter 3, the role of this imine bond in catalysis is probed with $NaBH_4$. Treatment of methylamine methyltransferases with $NaBH_4$ was found to inhibit their enzymatic activity. Mass spectrometry showed that *L*-pyrrolysine was the only detectable site of $NaBH_4$ reduction in these methylamine methyltransferases. These data were consistent with the hypothesis that *L*-pyrrolysine plays a role in catalysis.

During methanogenesis from methylamines, methylamine methyltransferases methylate cognate corrinoid proteins. During catalysis, the corrinoids oscillate between a supernucleophilic Co(I)-form and the CH_3-Co(III) state. When in the Co(I)-form, the cobalt center is prone to oxidative inactivation to the Co(II)-form in methyltransferases. In Chapter 4 of this dissertation, a novel ATP-dependent redox activator, RAM is shown to play a role in the direct reduction of these corrinoid proteins.

This work is dedicated to my wonderful parents

Joseph and Vilma Soares

ACKNOWLEDGMENTS

I would like to thank my wonderful family for all the love and support through my graduate career. I wish to thank my committee members, Dr. Charles Daniels, Dr. Mark Morrison and Dr. Robert Tabita for their suggestions and advice on this project. I am especially grateful to my lab mates both past and present for their council and friendship. I greatly appreciate all the help given to me by the people at the campus chemical and instrumentation center, especially Dr. Kari Green-Church and Dr. Liwen Zhang. Finally, I would like to thank my advisor Dr. Joseph Krzycki for his guidance and immeasurable help that made this possible.

VITA

November 27, 1976……...Born, Frankfurt, Germany

1997……...B.S. in Microbiology/Biochemistry

St. Xavier's College, Mumbai

1999……..M.S. in Biochemistry

University of Mumbai

2007……..M.S. in Microbiology

The Ohio State University

2000-2008…….....Graduate Teaching and Research Associate

The Ohio State University

PUBLICATIONS

Hao, B., G. Zhao, P. T. Kang, J. A. Soares, T. K. Ferguson, J. Gallucci, J. A. Krzycki, and M. K. Chan. 2004. Reactivity and chemical synthesis of L-pyrrolysine- the 22(nd) genetically encoded amino acid. Chem Biol **11:**1317-24.

Soares, J. A., L. Zhang, R. L. Pitsch, N. M. Kleinholz, R. B. Jones, J. J. Wolff, J. Amster, K. B. Green-Church, and J. A. Krzycki. 2005. The residue mass of L-pyrrolysine in three distinct methylamine methyltransferases. J Biol Chem **280:**36962-9.

Mahapatra, A., A. Patel, J. A. Soares, R. C. Larue, J. K. Zhang, W. W. Metcalf, and J. A. Krzycki. 2006. Characterization of a Methanosarcina acetivorans mutant unable to translate UAG as pyrrolysine. Mol Microbiol **59:**56-66.

FIELD OF STUDY

Major Field: Microbiology

TABLE OF CONTENTS

LIST OF FIGURES

LIST OF TABLES

LIST OF ABBREVIATIONS

AdoMet	s-adenosyl-L-methionine
ADP	adenosine diphosphate
AMP-PNP	5'-adenylyl-β, γ-imidodiphosphate
ATP	adenosine triphosphate
BES	bromoethanesulfonic acid
BSA	bovine serum albumin
CAM	carbamidomethylated
CFeSP	corrinoid iron-sulfur protein
CH_3-THF	methyltetrahydrofolate
CID	collision induced dissociation
CoM	coenzyme M
CoB	coenzyme B
DMA	dimethylamine
DTNB	5,5'-dithio-bis(2-nitrobenzoic acid)
DTT	dithiothreitol
E. coli	*Escherichia coli*
EPR	electron paramagnetic resonance
FTICR	fourier transform ion cyclotron resonance
HAL	histidine ammonia lyase

H_4MPt	tetrahydromethanopterin
HPLC	high performance liquid chromatography
H_4SPt	tetrahydrosarcinopterin
kDa	kilodaltons
M. acetivorans	*Methanosarcina acetivorans*
MALDI	matrix-assisted laser desorption ionization
MAP	methanol activating protein
M. barkeri	*Methanosarcina barkeri*
MetH	methionine synthase
MFR	methanofuran
MIO	5-methylene-3,5-dihydroimidazol-4-one
MMA	monomethylamine
MtaA	methanol and trimethylamine CoM methylase
MtaB	methanol specific methyltranferase
MtbA	methylamine CoM methylase
MtbB	dimethylamine specific methyltransferase
MtaC	methanol corrinoid protein
MtbC	dimethylamine corrinoid protein
MtmB	monomethylamine specific methyltransferase
MtmC	monomethylamine corrinoid protein
MOPS	3-[N-morpholino]propanesulfonic acid
MttB	trimethylamine specific methyltransferase
MttC	trimethylamine corrinoid protein

MV	methyl viologen
OX	oxidized methionine residue
PAGE	polyacrylamide gel electrophoresis
PCR	polymerase chain reaction
PYLIS	pyrrolysine insertion sequence
PylS	pyrrolysyl-tRNA synthetase
RAM	redox activation of methylamines
SDS	sodium dodecyl sulfate
SECIS	selenocysteine insertion sequence
THF	tetrahydrofolate
TMA	trimethylamine
TOF	time of flight
Tris	tris(hydroxymethyl)aminomethane
tRNA	transfer RNA
UTR	untranslated region
UV/Vis	ultraviolet/visible light

CHAPTER 1

GENERAL INTRODUCTION

1.1 The methanogens

Methanogenesis refers to the production of methane by prokaryotic microorganisms known as methanogens. In many environments, the generation of methane is the final step in the anaerobic degradation of organic matter (Zinder, 1993). The methane thus produced may serve as substrate for methane-oxidizing microorganisms or escape into the atmosphere, where it is a greenhouse gas (Rogers *et. al.* 1991). Methanogens are found in a diverse range of environments such as; sanitary landfills, deep sea hydrothermal vents, animal gastrointestinal tracts, freshwater and saline sediments, etc. (Boone *et. al* 1993).

A large number of methanogenic strains have been identified. Based on 16S ribosomal RNA sequences, these strains have been found to be phylogenetically distinct, and are classified into a separate domain known as the

Archaea (Woese *et. al.* 1990). This domain includes all of the mesophilic, thermophilic and halophilic methanogenic microorganisms (Woese *et. al.* 1978, 1990). In recent times, a wide variety of novel cofactors and enzymes have been discovered in these organisms (White & Zhou 1993). The advent of genetic manipulation of these organisms has aided in the study these microorganisms.

Methanogens utilize a small number of simple compounds, consisting of one to three carbons, in the production of methane (Blaut, 1994). Most of the methanogens known grow autotrophically in the presence of CO_2 with H_2 providing the necessary reducing equivalents. However, certain microorganisms such as members of the family *Methanosarcinacea*, can grow on a wider array of substrates such as acetate, methanol, methylated amines, dimethylsulfide apart from CO_2 and H_2. (Boone *et. al.* 1993, Zinder, 1993).

1.2 *Methanosarcina barkeri*

M. barkeri is part of the order *Methanosarcinales*, family *Methanosarcinaceae*, and belongs to the genus *Methanosarcina*. *M. barkeri* strain MS is one such strain of the species. *M. barkeri* was originally isolated from freshwater lake sediments. It is mesophilic with optimal growth temperatures ranging between 35°C to 42 ^{o}C, and similar to all methanogens, is a strict anaerobe. *M. barkeri* MS can grow on a wide range of substrates such as acetate, methanol, methylated amines, pyruvate, and H_2/CO_2. When grown on acetate, *M. barkeri* MS can also convert dimethylsulfide and methylmercaptopropionate to methane (Tallant *et. al.* 1997). In fact, *M. barkeri*

has been shown to catabolize all known methylotrophic substrates except for tetramethylammonium, which was demonstrated to be utilized by the *Methanococcoides sp.* While studying the methylated amines metabolism of this organism, *L*-pyrrolysine, the 22nd genetically-encoded amino acid was discovered (Srinivasan *et. al.* 2002, Hao *et. al.* 2002).

1.3 Methanogenesis from methylamines

Methanogens can accomplish methanogenesis by three major ways. One way is by utilizing the hydrogenotrophic pathway, which involves the reduction of carbon dioxide to methane coupled with the oxidation of H_2 to provide the necessary reducing equivalents. A second pathway for methanogenesis is the acetoclastic pathway. Here, acetate is initially activated to form acetyl-CoA, following which the carbonyl group is oxidized to carbon dioxide, with a methyl group transferred to tetrahydromethanopterin (H_4MPt). In *M. barkeri*, a tetrahydrosarcinopterin (H_4SPt) performs the function of H_4MPt. The methyl group on H_4MPt is then reduced to methane. A third methanogenesis pathway is the methylotrophic pathway. This pathway involves the disproportionation of C_1 substrates such as methanol, monomethylamine (MMA), dimethylamine (DMA), trimethylamine (TMA) and methylthiols to carbon dioxide and H_2. (Deppenmeier, 2002, Deppenmeier *et. al.* 1999, Galagan *et. al.* 2002)

The most common precursors for methanogenesis are known to be either $H_2 + CO_2$ or acetate. However in marine and brackish environments, methylated compounds are thought to predominate due to the anaerobic breakdown of

common cellular osmolytes such as betaine, trimethylamine-N-oxide and dimethylsulfoniopropionate, originating from plants and phytoplankton (Deppenmeier, 2002). *Methanosarcinaceae* are unique in their ability to utilize methanol and methylated amines as a sole energy source (Blaut, 1994). When utilizing methanol or methylamines towards methanogenesis, four substrate molecules are disproportionately converted into one molecule of CO_2 and three molecules of CH_4 (Figure 1.1). The oxidation step to CO_2 results in the production of six electrons for the reduction of methyl moieties from the substrate to methane (Thauer, 1998). Distinct soluble methyltransferase systems are involved in binding methanol or methylamines culminating in the synthesis of methylated CoM. This important intermediate is reduced to CH_4 by a pathway involving the enzyme, methyl-CoM reductase (Shima *et. al.* 2005).

The MMA, DMA and TMA-dependent methylation of CoM is catalyzed by three distinct methyltransferases (Figure 1.2). The first enzyme in the pathway is a substrate-binding methyltransferase such as MMA methyltransferase, MtmB, DMA methyltransferase, MtbB and TMA methyltransferase, MttB which methylates a cognate corrinoid protein MtmC, MtbC and MttC respectively. The last step of CoM methylation is catalyzed by a CoM methylase, MtbA, which transfers the methyl moiety from the corrinoid protein to CoM (Burke *et. al.* 1997, Ferguson *et. al.*, 1997, 2000)

MtmB has been shown to exist in a hexameric structure comprised of a dimer of trimers (Burke *et. al.* 1995, 1997, Hao *et. al.* 2002). Each monomer is of approximately 50 kDa in size. MtmB transfers a methyl group to the prosthetic

group of the 29 kDa cognate-corrinoid protein MtmC. The methyl group from MtmC is subsequently transferred to CoM via a 36 kDa zinc-containing CoM methylase, MtbA. The residue sequence of MtmC shows the presence of all the signature residues for a motif involved in binding a B_{12} cofactor similar to that found in methionine synthase in *E. coli*. This includes a DXHXXG conserved motif, of which the histidine residue can be the lower ligand of the corrinoid cofactor. This histidine likely plays a role in controlling the coordination state of the cobalt center.

The overall scheme for the DMA and TMA methyltransferase systems are very similar to the MMA methyltransferase pathway. The three functionally similar proteins, MtmB, MtbB and MttB surprisingly do not share any sequence similarity. These proteins show the presence of an in frame amber (UAG) codon in their respective genes, with an opal or ochre stop codon downstream of the amber codon (Paul *et. al.* 1996, Burke *et al.* 1998). If these amber codons functioned as stop codons, their respective gene products would be approximately 23 kDa (MtmB), 38 kDa (MtbB), and 32 kDa (MttB), respectively. In the case of MtmB, the 23 kDa truncated product is detectable in trace amounts in cell extracts. Instead the great majority of these proteins are isolated as their full-length products, all of which are approximately 50 kDa in size as monomers. On further analysis of MtmB using a combination of tryptic digestion and mass spectrometry indicated that the amino acid residue encoded by the UAG was lysine (James *et. al.* 2001). The reason for the detection of a lysine residue

present in MtmB coded for by the UAG is likely due to the acidic conditions that were used for the isolation of the tryptic peptides.

1.4 *L*-Pyrrolysine

The crystal structure of MtmB from *M. barkeri* MS was determined and showed the presence of a novel amino acid in the form of a modified lysine at the position encoded by the in-frame amber codon. Two crystal structures determined at 1.5- 2.0 ^{o}A resolution deduced the structure of the amino acid as a lysine with $^{\varepsilon}$N in amide linkage with (4R, 5R)-4-substituted-pyrroline-5-carboxylate (Hao *et. al.* 2002). The identity of the C4-substituent on the pyrroline ring of this amino acid could not be determined, but was proposed to be either, a methyl, hydroxyl, or an amino group. Subsequent crystallography of MtmB indicated that a methyl group was the most probable substituent, with an amine group also a possibility (Hao *et. al.* 2004).

The current hypothesis for the existence of this novel amino acid is that it has electrophilic properties that may play a role in catalysis. The C2 position of the pyrroline ring of pyrrolysine was found to have an additional amino group when MtmB crystals were grown in the presence of 2 M $(NH_4)_2SO_4$. The pyrroline ring was determined to have rotated 90° when forming an adduct with this amino group. Thus it was proposed that this amino acid may play a role in binding substrate and orienting the methyl group of the substrate to the cognate corrinoid protein (Hao *et. al.* 2002, 2004). *L*-pyrrolysine has been predicted to be present in a few methanogenic Archaea, and the bacterium, *Desulfitobacterium*

Figure 1.1: The pathways for the oxidation and reduction of methylamines and methanol. The oxidation of methylamines and methanol to CO_2 provides the reducing equivalents necessary for the reduction of methyl moieties from substrate to methane. The C1-unit carriers shown in have been identified to be methanofuran (MFR) (Leigh *et. al.* 1985), tetrahydrosarcinopterin (H_4SPt) (van Beelen *et. al.* 1984 (a), (b)), and coenzyme M (CoM) (Taylor *et. al.* 1974). MFR functions as a carrier of formyl- groups (White and Zhou 1993, DiMarco et. *al.* 1990). Figure adapted from Keltjens and Vogels, 1993.

Figure 1.1

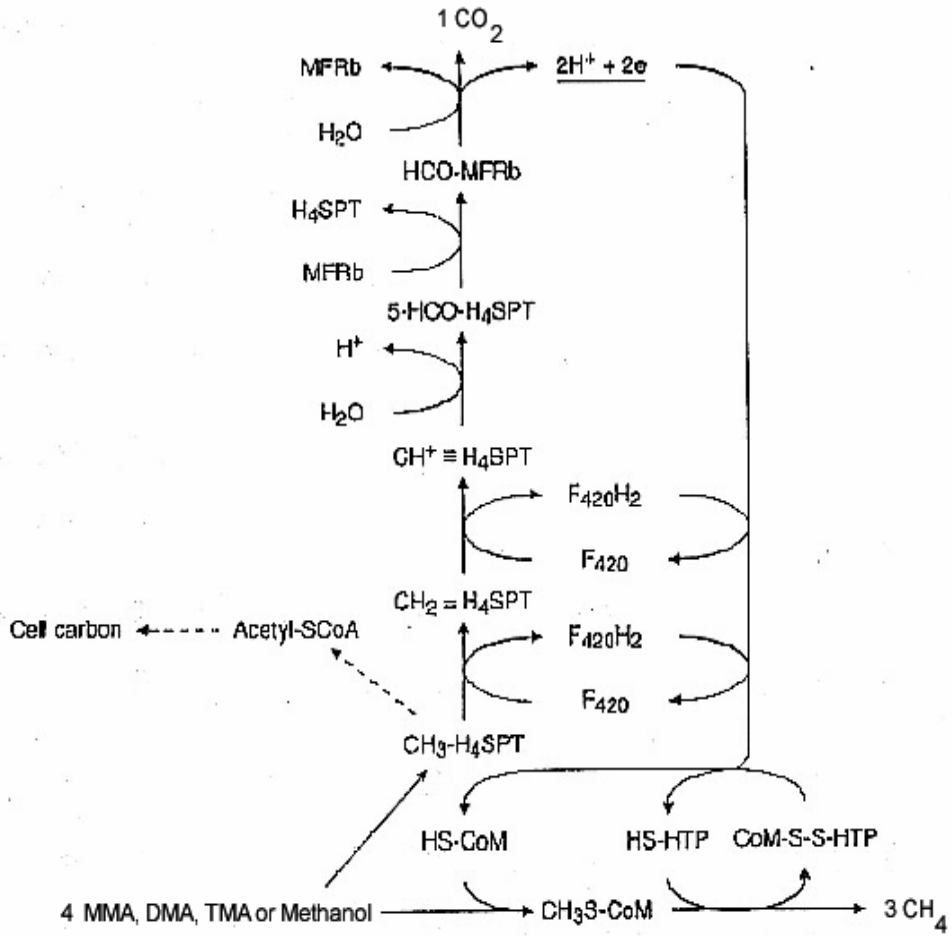
1 CO2
MFRb
2H+ + 2e
H2O
HCO-MFRb
H4SPT
MFRb
5-HCO-H4SPT
H+
H2O
CH+ ≡ H4SPT
F420H2
F420
CH2 = H4SPT
Cell carbon
Acetyl-SCoA
F420H2
F420
CH3-H4SPT
HS-CoM
HS-HTP
CoM-S-S-HTP
4 MMA, DMA, TMA or Methanol
CH3S-CoM
3 CH4

Figure 1.2: The biochemical pathways for the methylation of CoM with MMA, DMA and TMA. MtmB, MtbB and MttB show the presence of in-frame amber codons in their respective genes, *mtmB*, *mtbB* and *mttB*. MtmC, MtbC and MttC are homologous cognate corrinoid proteins, whereas MtbA is common to all three pathways and catalyzes CoM methylation.

Figure 1.2

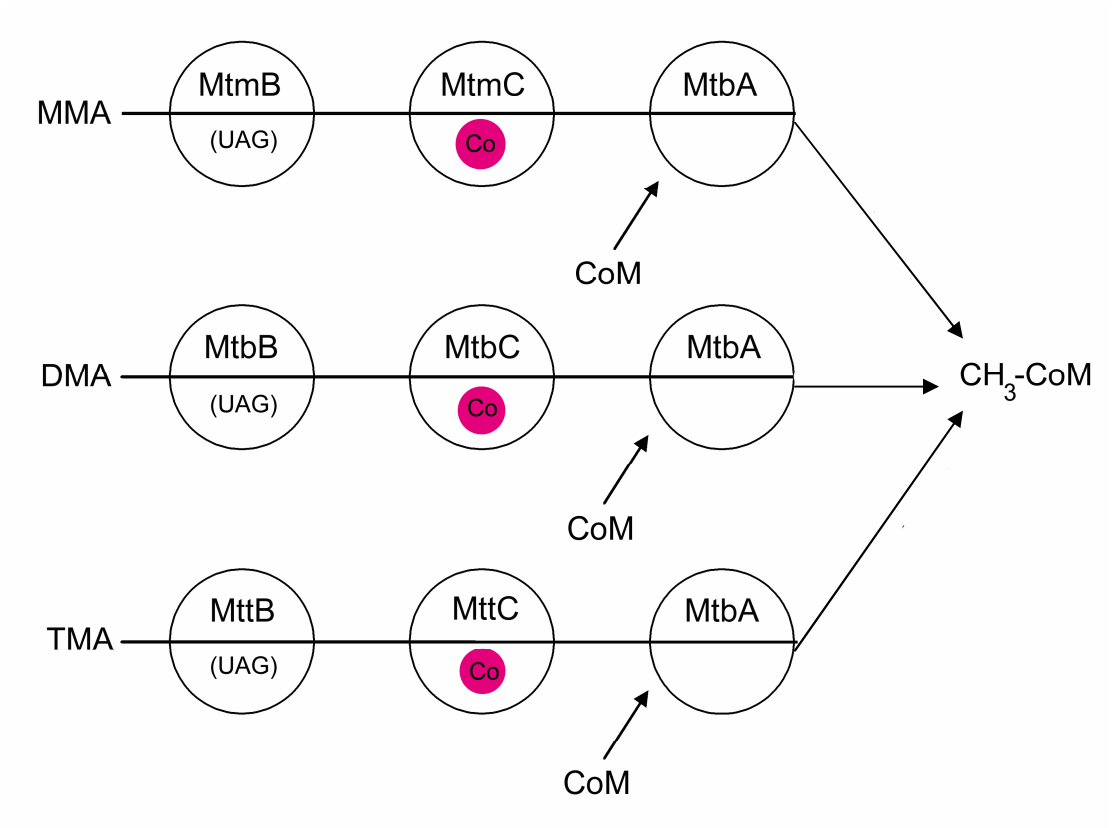
MMA
MtmB
(UAG)
MtmC
Co
MtbA
CoM
DMA
MtbB
(UAG)
MtbC
Co
MtbA
CoM
TMA
MttB
(UAG)
MttC
Co
MtbA
CoM
CH3-CoM

hafniense. (Srinivasan *et. al.* 2002, Galagan *et. al.* 2002). This prediction is based on the presence of a cluster of genes called the *pyl* operon. The operon includes *pylT*, the gene encoding a specific $tRNA^{pyl}$ and *pylS*, the pyrrolysyl-tRNA synthetase, which has been shown to charge $tRNA^{pyl}$ with pyrrolysine (Blight *et. al.* 2004). It has been demonstrated that a deletion of *pylT* results in *M. acetivorans* results in the inability of this organism to grow on methylamines (Mahapatra *et. al.* 2006). Downstream of *pylS*, are three genes, *pylB*, *pylC* and *pylD*, which have been shown to be involved in the biosynthesis of pyrrolysine (Longstaff *et. al.* 2007(a)).

Pyrrolysine and selenocysteine are unusual amino acids as the incorporation of these residues into peptides is dependent on the translation of canonical termination codons. Initial experimentation has shown that the mechanism of incorporation of pyrrolysine into proteins may involve the pyrrolysine insertion sequence (PYLIS) element which is present just downstream of the UAG codon in *mtmB* transcripts (Longstaff *et. al.* 2007(b)). Untranslated regions flanking *mtmB* were shown not to be involved in UAG readthrough. However, the deletion of this PYLIS element resulted in a significant increase in the translation of the truncated product as compared to the translated full-length product, but did not completely abolish readthrough. Thus, while there may be some contextual requirements for the incorporation of pyrrolysine into proteins, the PYLIS element is not an absolute requirement for translation (Longstaff *et. al*. 2007(b)). Variations of the PYLIS element appear to be present in the genes encoding MtbB and MttB.

1.5 Vitamin B12 structure and function in enzymes

The complex structure of the organometallic cofactor Vitamin B12 was first elucidated by Hodgkin D.C. (Hodgkin *et. al.* 1956). The overall structure was determined to include a central cobalt atom coordinated with a tetrapyrrole structure through four equatorial nitrogen ligands. The tetrapyrrole structure of this cofactor is shown in Figure 1.3. A modified ribonucleoside with dimethylbenzimidazole as a base is found tethered to the tetrapyrrole ring through pyrrole D. The upper ligand of the corrinoid cofactor is known to bind several ligands, most commonly, either an adenosyl- or a methyl- group. Over the years, the cobalt cofactor has been shown to be involved in the functioning of three different classes of enzymes; the adenosylcobalamin-dependent enzymes, methylcobalamin-dependent methyltransferases, and the dehalogenases (Banerjee, *et. al.* 2003). Adenosylcobalamin-containing enzymes are typically involved in catalyzing carbon skeleton rearrangements and reductions, whereas methylcobalamin-containing enzymes catalyze the transfer of methyl-groups.

1.6 Methionine synthase

Amongst the enzymes catalyzing the transfer of methyl-groups in a cobalamin-dependent manner, methionine synthase (MetH) is perhaps the best characterized. An understanding of the functioning of the MetH system is important as the cobalamin-binding domain of MetH is homologous to the methylamine corrinoid proteins. The methylcobalamin-dependent MetH catalyzes the last step in the biosynthesis of methionine. This reaction involves the transfer

of a methyl group from methyl-tetrahydrofolate (CH_3-THF) to homocysteine resulting in the synthesis of methionine and tetrahydrofolate (THF). The overall reaction consists of two half-reactions (Banerjee *et al.*, 1990(a), (b)). In the first half reaction, the highly nucleophilic cob(I)alamin prosthetic group of MetH takes up the methyl group of CH_3-THF to form methyl(III)cobalamin and THF. In the second half reaction, the methyl-Co(III) undergoes a heterolytic cleavage of the methyl-cobalt bond that results in the methylation of homocysteine, forming methionine and Co(I) (Figure 1.4).

The 136-kDa MetH monomer is a modular enzyme consisting of separate binding domains for CH_3-THF, corrinoid cofactor, homocysteine and adenosyl-methionine (AdoMet) (Drummond *et. al.* 1993(a), Goulding *et. al.* 1997, Evans *et. al.* 2004). Depending on the oxidation state of the corrinoid cofactor, B_{12}-binding domain of MetH has to interact with different methyltransferase domains of MetH towards the biosynthesis of methionine. In the Co(I) form, the B_{12}-binding domain interacts with the CH_3-THF methyltranferase domain, in the Co(II) form, it interacts with the AdoMet-binding domain. When in the Co(III) state, the B_{12}-binding domain interacts with the homocysteine-binding domain of MetH. The cobalt cofactor, when in the Co(I) form, is prone to oxidative inactivation. The mechanism by which this cofactor is reductively activated will be discussed in the section covering the reductive activation of corrinoid proteins.

The crystal structure of the cobalamin-binding domain of MetH was determined and brought to light some interesting insights into the way this

Figure 1.3: A detailed structure of cobalamin showing the cobalt atom coordinated with a corrin ring via the four equatorial nitrogen atoms. The lower ligand of the cobalt center is coordinated with a 5,6-dimethylbenzimidazole ribonucleotide, which is tethered to the corrin ring system via a phosphodiester linkage. The figure shows the different functional groups (R) that may bind the cobalt atom as the upper ligand.

Figure 1.3

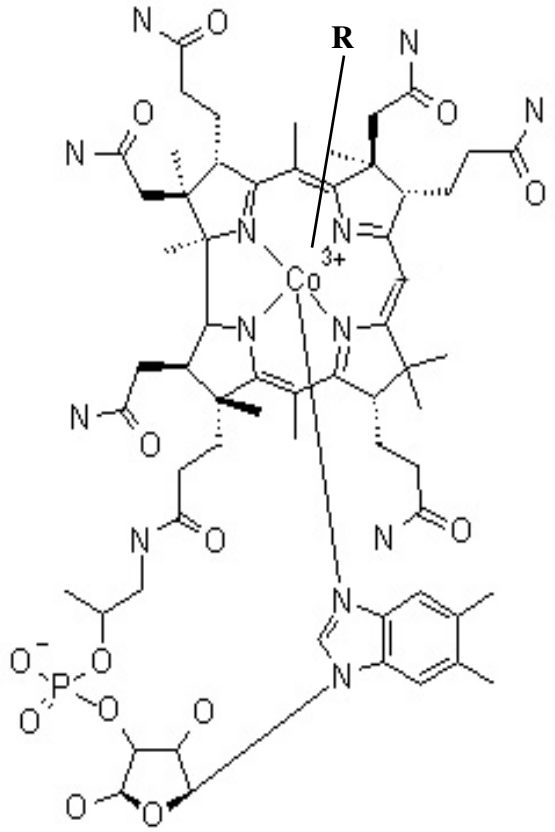

Where R =	$-CH_3$	methylcobalamin
	-CN	cyanocobalamin (Vitamin B_{12})
	$-H_20$	aquocobalamin
	-adenosyl	adenosylcobalamin

Figure 1.4: The catalytic cycle and reductive activation of methionine synthase. The methionine synthase system showing the modulation of the reactions dependent on the redox state of the cobalamin-binding domain of methionine synthase. The dotted line indicates the binding on the lower ligand, 5,6-dimethylbenzimidazole.

Figure 1.4

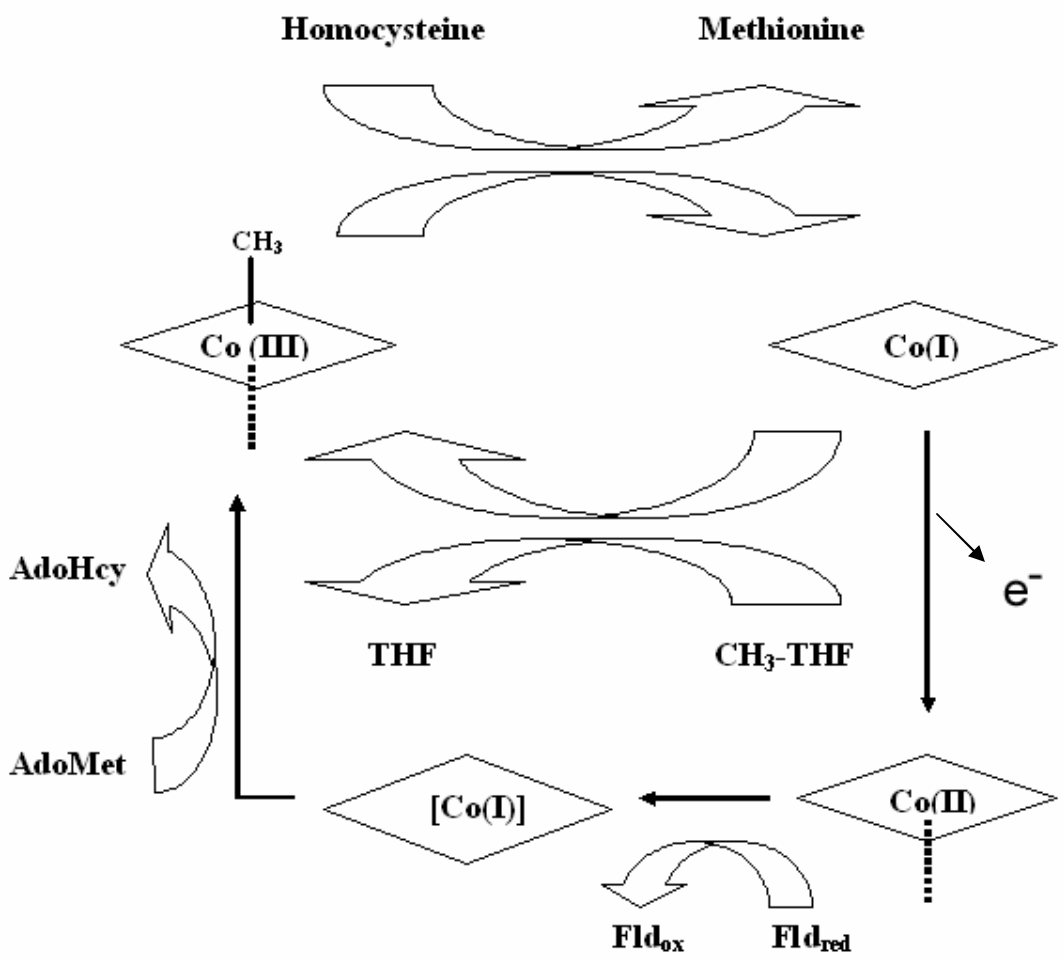
Homocysteine
Methionine
CH3
Co (III)
Co(I)
e-
AdoHcy
AdoMet
THF
CH3-THF
[Co(I)]
Co(II)
Fldox
Fldred

domain may function (Drennan *et. al.* 1994). One feature was the lower axial ligand, i.e., the 5,6-dimethylbenzimidazole base being displaced from the tetrapyrrole ring and is buried within a domain consisting of a Rossman fold. This feature is different from that of the free cofactor which has the dimethylbenzimidazole base coordinated to the lower ligand of the cobalt atom. However, instead of this base is replaced by a conserved histidine residue, which is part of a consensus sequence motif, DxHxxG, which is involved in coordinating the lower ligand.

1.7 Reductive activation of corrinoid proteins

The corrinoid prosthetic group, being nucleophilic in nature, is elegantly designed to transfer methyl groups (Stupperich, 1993). However, the cobalt cofactor can only accomplish the displacement of methyl groups when in the superreduced Co(I) redox state. Due to the very low redox potential for the Co(II)/Co(I) couple, the corrinoid cofactor is prone to oxidation to the Co(II) form and thereby the inactivation of the enzyme. The reactivation of the corrinoid cofactor from the Co(II) to the Co(I) state is unfavorable with typical electron carriers due to the low Co(II)/Co(I) redox couple which has been estimated as being below -500 mV (Harder *et. al.* 1989, Banerjee *et. al.* 1990(a)). It has been estimated that the oxidative inactivation of methionine synthase occurs once every 2000 turnovers (Drummond *et. al.* 1993 (b)). Organisms that utilize corrinoid proteins as part of their metabolism include reactivation systems that

are able to push the unfavorable reduction from Co(II) to Co(I) over a thermodynamic barrier (Matthews *et. al.* 1990). Reductive activation is necessary for these inactive corrinoid proteins to reenter the catalytic cycle. A number of different activation systems have been elucidated that accomplish this unfavorable reaction.

In the case of methionine synthase, reductive activation of the corrinoid cofactor is coupled with the highly exergonic demethylation of AdoMet to form methylcobalamin (Banerjee *et. al.* 1990(a), Jarrett *et. al.* 1998). In *E. coli*, the low potential electrons are provided by flavodoxin towards this reductive activation as shown in Figure 4. However, in humans, the flavodoxin is replaced by methionine synthase reductase (Olteanu *et. al.* 2001). Apart from the requirement of low potential electrons, the cobalt cofactor has to adopt a base-off conformation to facilitate this reduction. In methionine synthase, the cobalamin-binding domain shows the presence of a catalytic triad consisting of the H759, D757 and S810 residues. The histidine residue coordinates the lower ligand of the cobalt cofactor to keep this cofactor in the 5-coordinate Co(II) form. However, on protonation, this histidine base is removed from the lower ligand promoting the conversion of the cofactor from the 5-coordinate to the 4-coordinate Co(II) form. (Hoover *et. al.* 1997(a), (b)).

The adoption of the base-off 4-coordinate Co(II) form of the cofactor is an important aspect of reactivation. In the acetogenic system, the Co(II) form of the corrinoid iron-sulfur protein (CFeSP) is isolated in the base-off Co(II) state. The redox potential of the Co(II)/Co(I) couple is higher than that of the MetH system.

Reductive activation takes place by the transfer of electrons from a low-potential ferredoxin to an iron-sulfur cluster in CFeSP. These electrons are in turn transferred to the inactive corrinoid cofactor (Ragsdale *et. al.* 1987, Menon S *et. al.* 1999).

The methylotrophic methyltransferases of *Methanosarcina spp.* also possess an activation system which can convert corrinoid proteins to the active Co(I) state. This represents a third method of activation apart from the previously described systems, and it is dependent on a source of reducing power and ATP. The methanol methyltransferase corrinoid protein was shown to be activated by a methanol activating protein (MAP) in the presence of ATP, and crude preparations of hydrogenase and ferredoxin. It was proposed that MAP coupled with ATP hydrolysis converted the Co(II) base-on form of the cofactor to the base-off state. This was proposed to be followed by the reduction of the cofactor by a low potential ferredoxin (Daas *et. al.* 1996(a), (b)). In *Acetobacterium dehalogenans*, the reduction of a cognate corrinoid protein of the veratrol *O*-demethylase was shown to be achieved by the presence of an activating enzyme and ATP in extracts and is as yet, uncharacterized. (Kaufmann F *et. al.* 1998, Siebert *et. al.* 2005).

A functionally similar enzyme, RAM (reductive activation of methylamines) has been shown to be involved in the ATP-dependent activation of methylamines: CoM methyl transfer (Tsuneo Ferguson, personal communication). RAM has been shown to be an oxygen-sensitive redox active protein, which is required in catalytic amounts to stimulate methylamine: CoM

methyl transfer in the MMA, DMA and TMA systems. It has been shown to possess 2 iron-sulfur clusters in the C-terminus, and a putative ATP-binding domain in the N-terminus.

1.8 Electrophilic catalysis by enzymes

Substrate activation by enzymes involving the action of electrophilic groups is a rare occurrence. This is mostly owing to the fact that the side chains of amino acids contain only nucleophilic groups. As a result, enzyme-based electrophilic catalysis is achieved by the utilization of cofactors or post-translationally modified side chains of amino acids. The role of the electrophilic cofactor pyridoxal phosphate in the synthesis of amino acids has been well characterized (Christen *et. al.* 2001). The post-translational modification of nucleophilic groups of amino acid side chains to electrophilic groups have been discovered more recently.

In the case of histidine decarboxylase, the OH group of a serine residue is transformed to the electrophilic pyruvyl group (Snell *et. al.* 1986). This enzyme, as a result of this modification can catalyze a similar reaction to which pyridoxal phosphate could be used. Another modification to an electrophilic group is the conversion of serine or cysteine residues to a formylglycine residue in aryl sulfatases (Lukatela *et. al.* 1998). One more example of such modifications is the oxidation of aromatic residues such as tyrosine or tryptophan to quinones (Dove *et. al.* 2001, Firbank *et. al.* 2001).

Figure 1.5: The hypothesized role of *L*-pyrrolysine in catalysis. The mechanism by which *L*-pyrrolysine on MtmB bind MMA and methylates the cobalt cofactor of MtmC and generating ammonia. (Figure modified from Krzycki 2004)

Figure 1.5

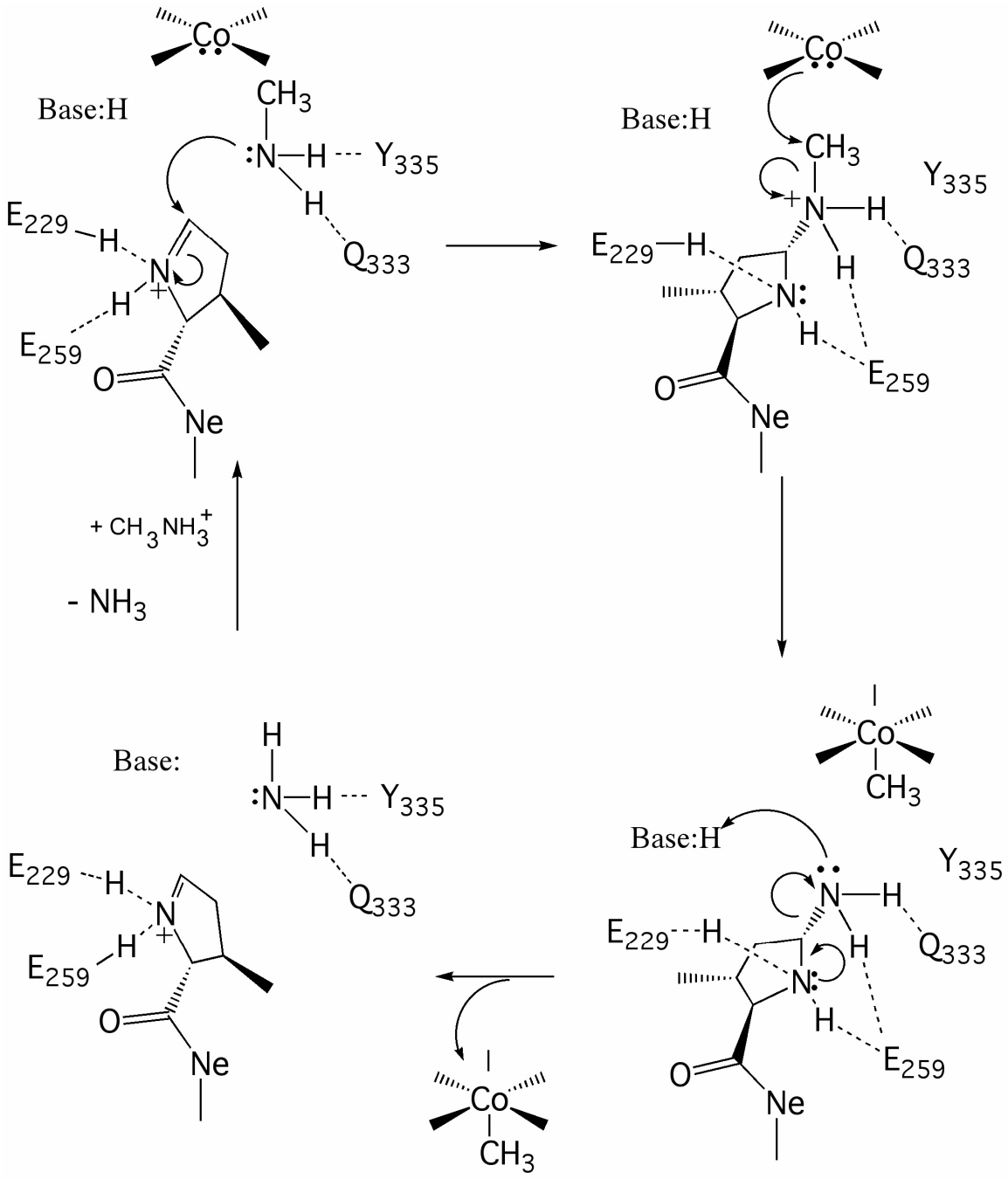
Co
Base:H
CH3
:N—H --- Y335
H
Q333
E229
H
N
H
E259
O
Ne
+ CH3NH3+
- NH3
Base:H
CH3
Y335
N—H
E229—H
H
Q333
N:
H
E259
O
Ne
Co
CH3
Base:H
Y335
N—H
E229---H
H
Q333
N:
H
E259
O
Ne
Co
CH3
Base:
H
:N—H --- Y335
H
Q333
E229
H
N
H
E259
O
Ne

Enzymes, histidine ammonia-lyase (HAL), phenylalanine ammonia-lyase and tyrosine 2,3-aminomutase show the presence of a post-translational modification of an internal tripeptide, Ala-Ser-Gly into the strongly electrophilic 5-methylene-3,5-dihydroimidazol-4-one (MIO) (Poppe *et. al.* 2005, Christenson *et. al.* 2003(a), (b)) . The first evidence for the presence of an electrophilic group in HAL that was involved in catalysis came from studies involving the use of a nucleophile, $NaBH_4$ (Wickner, 1969).

Based on x-ray crystallographic data, *L*-pyrrolysine has been shown to bind nucleophiles such as hydroxylamine and sulfite in the C2 position of pyrrolysine demonstrating the presence on an electrophilic property. The hypothesized role of pyrrolysine in catalysis is shown in Figure 1.5. According to this model, in the case of MtmB, MMA is deprotonated by a base, and the methylamine nucleophile bonds to the electrophilic C2 position of pyrrolysine. The pyrrolysyl ring in this form is proposed to rotate approximately 90°, presenting the methyl group of the methylammonium to the supernucleophile Co(I) of the cognate corrinoid protein, MtmC. Following a nucleophilic attack of the cobalt center on the methylammonium ion, a methyl group is transferred to the cognate corrinoid protein, with pyrrolysine releasing the end product, ammonia (Hao *et. al.* 2002).

1.9 Overview of this work

The discovery of *L*-pyrrolysine was a major step towards understanding the mechanism by which methane is generated from methylamines. X-ray crystallography had identified the residue as being a lysine with $^{\varepsilon}N$ in amide linkage with (4R, 5R)-4-substituted-pyrroline-5-carboxylate. The C4-substituent could not be accurately identified. Also, the presence of this amino acid was shown in MtmB alone. My first goal was to identify this residue in MtmB, MtbB and MttB using a technique other than x-ray crystallography. In doing so, it was important to identify the functional group at the C4-position of pyrrolysine, and complete the structure of *L*-pyrrolysine. My aim was to isolate MtmB, MtbB and MttB and using mass spectrometry, determine the mass of the residue encoded for by the in-frame UAG-codons in these three methylamine methyltransferases.

Secondly, evidence based on x-ray crystallographic data suggested that this amino acid may play a role in catalysis by coordinating methylamine substrate. MtmB crystallized in the presence of nucleophiles such as hydroxylamines and dithionite demonstrated the electrophilic character of the N1-C2 imine bond in pyrrolysine. My aim was to study the function of *L*-pyrrolysine using a chemical inhibitor $NaBH_4$, and studying its effect on MtmB and MtbB catalysis.

Thirdly, Tsuneo Ferguson had isolated RAM and shown this enzyme to be involved in methylamine: CoM methyl transfer with the requirement of ATP. It was shown to be redox active and was hypothesized to play a role in the

reductive activation of methylamine methyltransferase corrinoid proteins. My goal was to study the function of RAM in the ATP-dependent reductive activation of these corrinoid proteins. In chapter 4, RAM is demonstrated to mediate the direct reduction of corrinoid protein in an ATP-dependent manner.

CHAPTER 2

THE RESIDUE MASS OF *L*-PYRROLYSINE IN THREE DISTINCT METHYLAMINE METHYLTRANSFERASES

2.1 Introduction

The genes of methylamine methyltransferases (*mtmB, mtbB* and *mttB*) in *Methanosarcina barkeri* all show the presence of in-frame amber (UAG) codons (Burke, *et al*. 1997, Burke *et. al.* 1998, Paul *et. al.* 2000) . These methyltransferases are key enzymes in the formation of methane from monomethylamine (MMA), dimethylamine (DMA) and trimethylamine (TMA) respectively (Ferguson *et al.* 1997, Ferguson *et. al.* 2000). The methylamine methyltransferases were suggested to bind their respective methylamine substrates and catalyze the methylation of cognate corrinoid proteins MtmC, MtbC and MttC respectively. Upon methylation, the corrinoid proteins initiate the methylation of CoM through the catalysis of a CoM methylase, MtbA. Methylated

CoM is the substrate of Methyl-CoM reductase, which generates methane (Krzycki, 2004).

James *et. al.* showed that on expressing *mtmB1* in *E. coli*, followed by Western Blot analysis, the UAG codon functioned as a stop codon. An accumulation of a truncated product of approximately 23 kDa was observed which corresponded to the positioning of the in-frame amber codon in *mtmB1*. Anti-MtmB Western Blot analysis of *M. barkeri* MS extracts showed that MtmB was synthesized as a full-length protein, and pointed to read-through of this UAG codon (James *et. al.* 2001). Edman degradation and tandem MS of purified tryptic fragments identified the residue to be lysine in the position of the in-frame UAG codon. The harshly acidic conditions used in the isolation of the peptide may have resulted in the hydrolysis of the pyrroline ring of pyrrolysine.

L-pyrrolysine, the 22nd genetically-encoded amino acid was first found to exist when Hao *et. al.* determined the x-ray crystal structure of MtmB to a resolution of 1.55 A^{o}. The structure was proposed to be a lysine residue with the epsilon-nitrogen in amide linkage to a (4R, 5R)-4-substituted pyrrolyine-5-carboxylate ring (Hao *et. al.* 2002, Srinivasan *et. al.* 2002) (Figure 2.1). The C4 substituent could not be accurately identified, and was hypothesized as being a methyl, amine or hydroxyl group. The structure of MtmB determined to 2 A^{o} in the presence of the nucleophile, hydroxylamine, was shown to form an adduct with *L*-pyrrolysine. The structure of this derivative allowed for Hao *et. al.* to propose that the methyl group was the most likely substituent at the C4 position on the pyrroline ring of *L*-pyrrolysine (Hao *et. al.* 2004). Electrospray ionization mass

spectrometry was used to detect the mass of pyrrolysine by a technique other than crystallography. It was shown that the mass of MtmB was 107 +/- 2 Da larger than the predicted mass of MtmB with a lysine residue present at the UAG position. However, this data was not accurate enough to decipher the substituent at the C4 position.

Multiple copies of genes encoding methylamine methyltransferases are present in *Methanosarcina* species and contain in-frame amber codons (Paul *et. al.* 2000, Galagan et al. 2003, Deppenmeier *et al.* 2002). In *M. barkeri* MS, two nearly identical copies (95% identity) of genes encoding for MtmB are present. The two genes have been annotated as *mtmB1* and *mtmB2* respectively. In the case of MtbB, there are three copies present, *mtbB1*, *mtbB2* and *mtbB3*. The TMA methyltransferase, MttB is expressed by a single gene, *mttB* (Figure 2.2) (Paul *et. al.* 2000). The DMA and TMA methylamine methyltransferases genes, *mtbB* and *mttB* have also been demonstrated to express full-length proteins, as observed by the size of the isolated proteins. Thus, it can be concluded that the in-frame amber codons in the *mtbB* and *mttB* genes are read through. Although it seems very likely, it has not been demonstrated that *L*-pyrrolysine is the residue inserted at the position of the UAG codon.

In this chapter, using mass spectrometry in collaboration with Dr. K.B. Green-Church, the first demonstration for the presence of *L*-pyrrolysine, the 22nd genetically-encoded amino acid by a technique other than x-ray crystallography is shown. The study provides strong evidence for the existence, location and structure of the novel amino acid in all three methylamine methyltransferases.

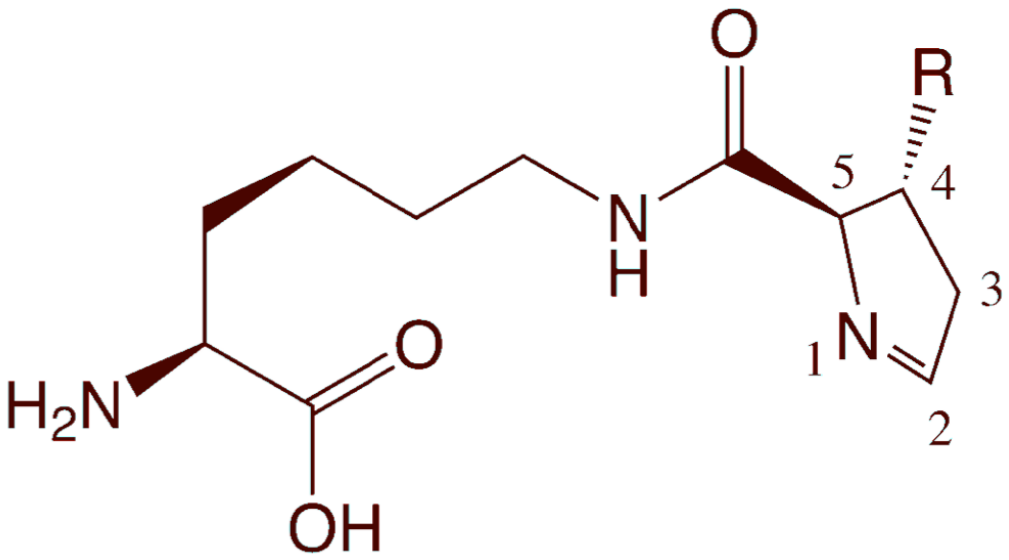

Figure 2.1: The structure of *L*-pyrrolysine. Crystallographic studies on MtmB revealed the presence of *L*-pyrrolysine. The structure consists of a lysine residue with the epsilon-nitrogen in amide linkage to a (4R, 5R)-4-substitued pyrrolyine-5-carboxylate ring. The C4-substituent (-R) could not be accurately determined, but was hypothesized as being either a methyl, amine or hydroxyl group. This study shows that the C4-substituent (-R) corresponds to a methyl- group.

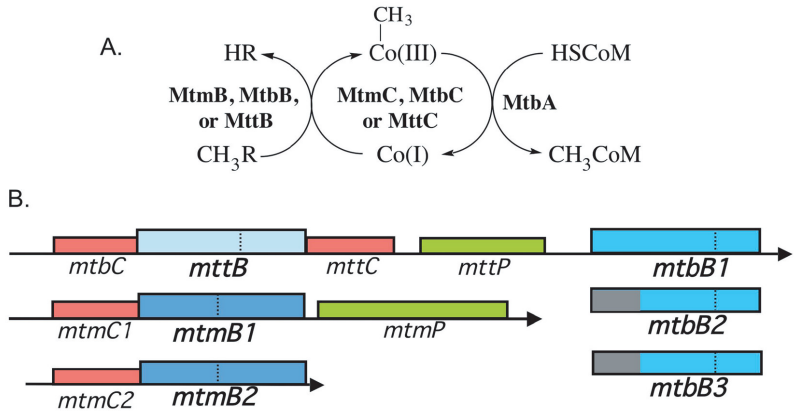

Figure 2.2: A. Scheme showing the methylation of CoM by analogous methylamine methyltransferase systems in *Methanosarcina spp*. Each methylamine methyltransferase (MtmB, MtbB, and MttB), binds substrate (MMA, DMA, and TMA respectively), and methylates its cognate corrinoid protein (MtmC, MtbC, and MttC respectively). These methylated corrinoid proteins are then substrates for MtbA, which catalyzes the methylation of CoM.

B. The genes present in *M. barkeri* MS of the three methylamine methyltransferase systems, and indicating the presence of in-frame amber codons (by dotted lines) in the genes substrate binding methylamine methyltransferases. The grey area on *mtbB2* and *mtbB3* indicate the 5' regions of these genes that have not been sequenced in *M. barkeri* MS.

2.2 MATERIALS AND METHODS

2.2.1 Cell cultivation and extracts

M. barkeri MS (DSM800) cells were grown on 80 mM TMA or MMA in a phosphate buffered medium (Krzycki *et. al.* 1989) in 15 to 40 l glass carboys with a nitrogen gas phase, and harvested seven days after inoculation. Cell extracts were anaerobically prepared with lysis using a French pressure cell, and frozen at –70°C prior to use.

2.2.2 Isolation of methylamine methyltransferases

MtmB was purified as the MtmBC complex (50 mgs) from 200 gms cell extracts of *M. barkeri* MS grown on MMA as previously described for the co-purification of MtbA and MtmC (Burke *et. al.* 1995) with the exception that all steps were performed aerobically. In order to separate MtmB from the MtmBC complex, MtmBC was flush/evacuated under hydrogen then reduced with 5 mM titanium (III)-citrate. The reduced MtmBC complex (25 mgs) was then loaded onto an anoxic Sephacryl-S100 (Amersham Biosciences, Piscataway, NJ) gel filtration column (80 by 2.5 cm) operated in an anoxic chamber (Coy Laboratories, Grass Lake, MI). The Secpahcryl-S100 column was pre-equlibrated in 50 mM MOPS (pH 7.0) and 100 mM NaCl. MtmB with trace amounts of MtmC eluted near the void volume under these conditions, while most of MtmC (5 mgs) eluted later in the profile. The procedure was repeated to remove traces of MtmC from MtmB. The MtmB used in these experiments yielded only a single 50-kDa

band when subjected to denaturing 12.5% polyacrylamide gel electrophoresis with detection by Coomassie staining. The yield of MtmB was 15 mgs.

The DMA methyltransferase, MtbB, was isolated entirely in the anoxic chamber. The dimethylamine:CoM methyltransferase assay was performed as described previously (Ferguson *et. al.* 2000). The buffers and column matrices were made anaerobic before use by repeated cycles of flush/evacuation using N_2. The purification was initiated by absorbing 1.5 liter (20 mg protein/ml) of soluble extract prepared from cells grown on TMA (approximately 500 gms of cells extracted in 1 liter 50 mM Tris, pH 8.0) onto a 40 x 5 cm DE-52 (Whatman Inc., Fairfield NJ) column equilibrated with 50 mM NaCl in 50 mM Tris, pH 8.0. A gradient (2.4 l) of 50-500 mM NaCl in the same buffer, was applied to the column at 2 ml/min. MtbB eluted in 250 mM NaCl and the pooled fractions (120 ml) of MtbB were concentrated 10 fold by ultrafiltration with a YM-10 membrane (Amicon, Inc., Beverly, MA). The sample was then diluted about 10 fold with 50 mM MOPS, pH 6.5. An aliquot (35 ml) was then chromatographed with a Mono-Q HR 10/10 column (Amersham Biosciences) equilibrated with 50 mM NaCl in 50 mM MOPS, pH 6.5. A 160 ml gradient of 50-500 mM NaCl in the same buffer was applied to the column at a flow rate of 2 ml/min. The MtbB activity eluted with approximately 300 mM NaCl in a total volume of 12 ml. The procedure was repeated with the remaining DE-52 aliquots, and MtbB fractions pooled and concentrated 10-fold using a YM-10 membrane. The concentrated sample was rediluted 10 fold with 50 mM TrisHCl, pH 8.0 and the pooled active fractions chromatographed on two UNO-Q1 columns (Bio-Rad Laboratories, Hercules,

Calif.) that were connected in series and pre-equilibrated with 50 mM Tris, pH 8.0. A 160 ml gradient of 150-350 mM NaCl in 50 mM Tris, pH 8.0 was applied to the column at a flow rate of 0.5 ml/min. The MtbB activity eluted at 220 mM NaCl in a volume of 24 ml. The pooled active MtbB fractions from the UNO-Q column were concentrated with a YM-10 membrane, and adjusted to 700 mM $(NH_4)_2SO_4$ with a saturated solution. The sample was then loaded onto a phenyl-Sepharose HP cartridge (Amersham-Pharmacia) equilibrated with 500 mM $(NH_4)_2SO_4$ in 50 mM MOPS, pH 7.0. A gradient (80 mls) of 500 to 0 mM $(NH_4)_2SO_4$ in 50 mM MOPS, pH 7.0 was applied to the column at 0.5 ml/min. The active MtbB eluted at approximately 420 mM $(NH_4)_2SO_4$ in 6 mls. The purified MtbB (35 mgs) was concentrated in three Amicon Centricon 10 concentrators to a volume of 1 ml and adjusted to a volume of 4 ml with 50 mM MOPS, pH 7.0. The sample was homogeneous when 3 µg protein was analyzed on a denaturing polyacrylamide gel electrophoresis and stained with Coomassie.

The TMA methyltransferase, MttB, was isolated as described previously as the MttB:MttC complex (Ferguson *et. al.* 1997). Repeated gel permeation chromatography was used to separate MttB from MttC, as described above for MtmB, but using 10 mM dithiothreitol as the reducing agent rather than titanium citrate.

2.2.3 Proteolysis by Chymotrypsin

Intact protein was first reduced with dithiothreitol then carbamidomethylated with iodoacetamide prior to proteolytic digestion using chymotrypsin (Roche Diagnostic GmbH, Indianapolis, IN). The final buffer conditions for digestion of desalted samples were 25 mM ammonium bicarbonate and 5% acetonitrile. The final ratio of methyltransferase to chymotrypsin was 25:1 (w/w) in a total volume of 80 µl. The digestion was carried out at 37℃ for 4 hours and stopped by acidification with 1 µl trifluoroacetic acid.

2.2.4 Proteolysis of MtmB by ArgC

750 µg MtmB was initially denatured in a 8M Urea, 14.2 mM dithiothreitol, 7.1 mM Tris-HCl, pH 7.6 solution in a total volume of 560 µL and incubated at 80°C for 1 hour. To 425 µL of the above mix, 425 µL of 200 mM TRIS-HCl, 20 mM calcium chloride, pH 7.6 was added. The digestion of MtmB was then initiated by adding 100 µL of the Arg-C activation solution, and 5 µg Arg-C. The reaction was incubated at 37°C for 18 hours.

Proteolysis products of MtmB, using Arg-C, were studied by 15% SDS-polyacrylamide gel electrophoresis against standard low molecular weight markers (Bio-Rad) and Coomassie staining. For higher sensitivity for the detection of peptides, silver staining was carried out.

2.2.5 Matrix-assisted laser desorption/ionization (MALDI) mass spectrometry

MALDI-MS of the chymotryptic peptides was performed on a Bruker Reflex III (Bruker, Breman, Germany) mass spectrometer operated in reflectron positive ion mode with an N2 laser using alpha- cyano-4-hydroxy cinnamic acid as the matrix prepared as a saturated solution in 50% acetonitrile/ 0.1% trifluoroacetic acid (in water). Allotments of 5 µL of matrix and 1 µL of sample were thoroughly mixed together; then 0.5 µL of this mixture spotted on the target plate and allowed to dry. Surfactant assisted-MALDI was performed on the digestion products to further increase the number of peptides detected as previously described (Breaux *et al.* 2000).

2.2.6 Liquid chromatography-tandem mass spectrometry

In order to obtain sequence of individual peptide ions, a Micromass Q-TOF II (Micromass, Wythenshawe, UK) equipped with an orthogonal nanospray source (New Objective, Inc., Woburn, MA) was operated in positive ion mode in conjunction with a Dionex Capillary LC-System (LC Packings-A Dionex Co., Sunnyvale, CA). The experiments were carried out in the Campus Chemical Instrumentation Center at The Ohio State University by Dr. K.B. Green-Church. Samples (2.5 µl) were first injected onto a trapping column (Michrom BioResources, Auburn, CA), then washed with 50 mM acetic acid, then injected onto a 5 cm long, 75 mm internal diameter ProteoPep II C18 column (New Objective, Inc.) packed directly in the nanospray tip. The column was then eluted with mobile phase A as 50 mM acetic acid and mobile phase B as acetonitrile.

Peptides were eluted directly off the column into the Q-TOF system using a gradient of 2 to 80% B over 45 minutes with a flow rate of 0.3 µl/min. The total run time was 58 minutes. The nanospray capillary voltage was set at 3.0 kV and the cone voltage at 55 V. The source temperature was maintained at 1000 ^{o}C. Mass spectra were recorded using MassLynx 4.0 with automatic switching functions. Mass spectra were acquired from mass 400- 2,000 Daltons every 1 second with a resolution of 8,000 (full-width, half-maximum). When the desired peak (using include tables) was detected at a minimum of 15 ion counts, the mass spectrometer automatically switched to acquire a collision induced dissociation (CID) MS/MS spectrum of the individual peptide. Collision energy was set dependent on charge state recognition properties. The PEAKS program from Bioinformatics Solutions was used for MS/MS data processing. Sequence information from the MS/MS data was processed using Mascot Distiller to form a peaklist file. Data was minimally processed with application of a 3 point smoothing function and with the centroid calculated from the top 80% of the peak height. The charge state of each ion selected for MS/MS was calculated, however, the peaks were not deisotoped. Assigned peaks were judged valid only if they had a minimum of 5 counts (S/N of 3) and displayed the corresponding C13 ion. The mass accuracy of the precursor ions were set to 1.2 Da to accommodate accidental selection of the C13 ion and the fragment mass accuracy was set to 0.3 Da. Considered modifications were methionine oxidation and carbamidomethyl cysteine. Pyrrolysine was also programmed into PEAKS as a modification. The data was acquired several times to ensure reproducibility.

2.2.7 MALDI-Fourier Transform Ion Cyclotron Resonance (MALDI-FTICR)

Chymotryptic digests of MtmB were also studied by MALDI-FTICR at Dr. J. Amster's laboratory at the University of Georgia. The chymotryptic digestion products of MtmB were mixed 1:1 with 1.3 M 2,5-dihydroxybenzoic acid and air-dried on a MALDI target plate. Ions from 15 laser shots from a Scout intermediate pressure MALDI source were accumulated into an external hexapole ion trap, and then transferred into the analyzer cell of a Bruker BioApex 7 Tesla FTICR mass spectrometer. Twelve repetitions of this cycle were co-added for each mass spectrum. The mass spectra were externally calibrated using a bovine serum albumin tryptic digest, then internally calibrated on 7 different MtmB chymotryptic peptides, achieving a final mass accuracy of 1.5 ppm.

2.3 RESULTS

2.3.1 Sequence coverage achieved for monomethylamine methyltransferase, MtmB

Initially, proteolytic digests of MtmB in the aqueous solution phase were attempted using ArgC in the presence of urea as denaturant. This was further extended by a dual digestion with ArgC and GluC. Adequate sequence coverage was achieved using these digestion protocols for the N-terminal and C-terminal portions of MtmB, but did not yield any peptides with the 202 position

corresponding with the location of pyrrolysine in the protein. Initial attempts in the aqueous phase were also attempted with chymotrypsin, but were unsuccessful. As a result, alternate digestion protocols were developed in acetonitrile, a denaturant, which is an organic solvent compatible with mass spectrometry (Russell *et. al.* 2001). ArgC/GluC digests of MtmB were inhibited in the presence of acetonitrile, however, chymotrypsin digests enhanced sequence coverage significantly, allowing for the detection of peptides covering the location of the amber codon. The detected *m/z* of peptides by a variety of mass spectrometric techniques such as, MALDI-FTICR, MALDI-TOF, and LC-MS/MS was as much as 83.4% sequence coverage for MtmB (Figure 2.3). The digestion of MtmB was carried out in 5% acetonitrile for 18 hours and allowed for the detection of pyrrolysine at the UAG position by all three mass spectrometric techniques mentioned. This was the first time the presence of pyrrolysine was detected by a technique other than mass spectrometry. The predicted mass of pyrrolysine was determined to be 237.1477 Da (C12H19N3O2), 238.1429 Da (C11H18N4O2) or 239.1269 (C11H17N3O3), depending on the identity of the C4-substituent as a methyl, amine, or hydroxyl group respectively. Using these predicted masses and the predicted gene product, the 194-208 chymotryptic fragment of MtmB was detected as a singly charged (M+H) ion using MALDI (Table 2.1). This peptide was also observed utilizing Electrospray ionization mass spectrometry as a doubly charged ion (M+2H).

2.3.2 Determination of the mass of the UAG-encoded residue in MtmB

Peptides generated by chymotryptic digestion were analyzed by LC-MS/MS, and detected by matching the masses of statistically significant peptides observed to their theoretical masses. The acidic conditions used for electrospray, allowed for the detection of the peptide containing pyrrolysine as a doubly charged peptide. The reason for the double charge is likely the protonation of basic sites such as arginine and the N-terminal amine in the pyrrolysine-containing peptide ^{194}AGRPGM$_{OX}$GVOGPETSL^{208}. An *m/z* of 791.6^{2+} was detected for this peptide as compared with the theoretical *m/z* of 791.4^{2+} for this peptide if pyrrolysine was present and C4-substituent of pyrrolysine was a methyl group. The *m/z* = 791.6^{2+} peptide was subjected to collision-induced dissociation (CID) and the spectrum generated confirmed the identity of the sequence of the peptide (Figure 2.4). The y and b ions detected allowed for the first determination of the complete residue mass of pyrrolysine. As listed in (Table 2.2), the mass difference calculated by the b9/b8 or y7/y6 ion pairs indicated that the residue encoded by the amber codon at position 202 of MtmB has a residue mass of 237.3 Da, with a statistical error of approximately 0.2 Da. This was consistent with the mass of the 4-substituent of pyrrolysine being a methyl group.

A more accurate method of determining the residue mass of pyrrolysine was sought. MALDI-FTICR was used to identify a chymotryptic fragment of MtmB

1 M**TFRKSFDCYDFYDRAKVGEKCTQDDWDLMKIPMKAMEL**KQKY**GLDFKGE**
51 **FIPTDKDMMEKLFKAGFEMLLECGIYCTDTHRIVKYTEDEIWDAINNVQK**
101**EFVLGTGRDAVNVRKRSVGDKAKPIVQGGPTGSPISEDVFMPVHM**SY**ALE**
151 **KEVDTIVNGVMTSVRGKSPIPKSPYEVLAAKTETRLIKNACAMAGRPGMG**
200 **VOGPETSL**SAQGNISADCTGGMTCTDSHEVSQLNEL**KIDLDAISVIAHYK**
251 **GNSDIIMDEQMPIFGGYAGGIEETTIVDVATHINAVL**MSSASW**HLDGPVH**
301 **IRWGSTNTRETLMIAGWACATISEFTDILSGNQYYPCAGPCTEMCLLEAS**
351 **AQSITDTASGREILSGVASAKGVVTDKTTGM**EARMMGEVARATAGVEISE
400 VNVILDKLVSLYEKNY**ASAPAGKTFQECYDVKTVTPTEEYMQVYDGARKK**
451 **LEDLGLVF**

Figure 2.3: Enzymatic map of the sequence coverage achieved by the digestion of MtmB with chymotrypsin. Sequence marked in blue are the residues that were detected. The ‘O’ denotes the position of the UAG codon at position of 202.

Table 2.1: A comparison of the predicted and observed peptide masses of MtmB digested with chymotrypsin. The data was generated by LC-MS/MS on a Q-TOF II mass spectrophotometer. The peptide marked in bold is the pyrrolysine-containing peptide at position 202 of the polypeptide.

Table 2.1

Observed *m/z*	**Predicted *m/z***	**Observed Sequence from b/y Ion Analysis**
410.69^{+3}	410.56^{+3}	$_{294}$HLDGPVHIRW$_{303}$
489.91^{+2}	489.75^{+2}	$_{304}$GSTNTRETL$_{312}$
501.44^{+2}	501.27^{+2}	$_{103}$VLGTGRDAVN$_{112}$
506.45^{+3}	506.29^{+3}	$_{162}$TSVRGKSPIPKSPY$_{175}$
521.13^{+3}	520.96^{+3}	$_{445}$DGARKKLEDLGLVF$_{458}$
530.96^{+2}	530.80^{+2}	$_{31}$KIPMKAMEL$_{39}$
538.97^{+2}	538.80^{+2}	$_{31}$ KIPM$_{ox}$KAMEL $_{39}$
615.53^{+2}	615.33^{+2}	$_{294}$HLDGPVHIRW$_{303}$
620.22^{+3}	620.02^{+3}	$_{162}$TSVRGKSPIPKSPYEVL$_{178}$
629.06^{+2}	628.85^{+2}	$_{103}$VLGTGRDAVNVR$_{114}$
632.04^{+2}	631.83^{+2}	$_{353}$SITDTASGREIL$_{364}$
641.52^{+2}	641.31^{+2}	$_{430}$DVKTVTPTEEY$_{440}$

Table 2.1 continued

Observed *m/z*	Predicted *m/z*	Observed Sequence from b/y Ion Analysis
671.05^{+2}	670.82^{+2}	$_{318}AC_{cam}ATISEFTDIL_{329}$
715.56^{+2}	715.32^{+2}	$_{417}ASAPAGKTFQEC_{cam}Y_{429}$
729.64^{+2}	729.40^{+2}	$_{237}KIDLDAISVIAHY_{249}$
757.13^{+2}	756.88^{+2}	$_{268}AGGIEETTIVDVATH_{282}$
759.17^{+2}	758.93^{+2}	$_{162}TSVRGKSPIPKSPY_{175}$
759.64^{+2}	759.40^{+2}	$_{148}ALEKEVDTIVNGVM_{161}$
766.12^{+2}	765.87^{+2}	$_{64}KAGFEMLLEC_{cam}GIY_{76}$
767.63^{+2}	767.40^{+2}	$_{148}ALEKEVDTIVNGVM_{OX}X_{161}$
774.13^{+2}	773.88^{+2}	$_{64}KAGFEM_{ox}LLEC_{cam}GIY_{76}$
781.19^{+2}	780.94^{+2}	$_{445}DGARKKLEDLGLVF_{458}$
787.97^{+3}	787.72^{+3}	$_{44}GLDFKGEFIPTDKDMMEKLF_{63}$
791.67^{+2}	**791.41^{+2}**	**$_{194}AGRPGM_{ox}GVOGPETSL_{208}$**
793.63^{+3}	793.72^{+3}	$_{44}GLDFKGEFIPTDKDMM_{ox}EKLF_{63}$

Table 2.1 continued

Observed *m/z*	**Predicted *m/z***	**Observed Sequence from b/y Ion Analysis**
805.17^{+2}	804.92^{+2}	$_{365}$SGVASAKGVVTDKTTGM$_{381}$
813.18^{+2}	812.91^{+2}	$_{365}$SGVASAKGVVTDKTTGM$_{ox}$$_{381}$
819.00^{+3}	818.74^{+3}	$_{83}$IVKYTEDEIWDAINNVQKEF$_{102}$
839.71^{+2}	839.44^{+2}	$_{179}$AAKTETRLIKNAC$_{cam}$AM$_{193}$
847.72^{+2}	847.44^{+2}	$_{179}$AAKTETRLIKNAC$_{cam}$AM$_{OX}$ $_{193}$
871.05^{+3}	870.78^{+3}	$_{82}$RIVKYTEDEIWDAINNVQKEF$_{102}$
875.22^{+2}	874.94^{+2}	$_{348}$EASAQSITDTASGREIL$_{364}$
902.22^{+2}	901.93^{+2}	$_{430}$DVKTVTPTEEYMQVY$_{444}$
910.22^{+2}	909.93^{+2}	$_{430}$DVKTVTPTEEYM$_{ox}$QVY$_{444}$
929.82^{+2}	929.53^{+2}	$_{162}$TSVRGKSPIPKSPYEVL$_{178}$
945.73^{+2}	945.43^{+2}	$_{318}$AC$_{cam}$ATISEFTDILSGNQY$_{334}$
976.26^{+2}	975.96^{+2}	$_{87}$TEDEIWDAINNVQKEF$_{102}$
994.47^{+3}	994.17^{+3}	$_{117}$SVGDKAKPIVQGGPTGSPISEDVFMP VHM$_{145}$
1008.28^{+2}	1007.97^{+2}	$_{250}$KGNSDIIMDEQMPIFGGY$_{267}$
1016.28^{+2}	1015.97^{+2}	$_{250}$KGNSDIIMDEQM$_{ox}$PIFGGY$_{267}$

Table 2.1 continued

Observed *m/z*	**Predicted *m/z***	**Observed Sequence from b/y Ion Analysis**
1019.75^{+3}	1019.43^{+3}	$_{318}$AC$_{cam}$ATISEFTDILSGNQYY PC$_{cam}$AGPC$_{cam}$TM$_{344}$
1025.07^{+3}	1025.76^{+3}	$_{318}$AC$_{cam}$ATISEFTDILSGNQYYPC$_{cam}$A GPC$_{cam}$TEM$_{ox344}$
1034.29^{+2}	1033.97^{+2}	$_{14}$DRAKVGEKC$_{cam}$TQDDWDLM$_{30}$
1042.30^{+2}	1041.97^{+2}	$_{14}$DRAKVGEKC$_{cam}$TQDDWDLM$_{ox30}$
1068.37^{+2}	1068.04^{+2}	$_{345}$C$_{cam}$LLEASAQSITDTASGREIL$_{364}$
1075.85^{+3}	1075.52^{+3}	$_{77}$C$_{cam}$TDTHRIVKYTEDEIWDAI NNVQKEF$_{102}$
1181.45^{+2}	1181.07^{+2}	$_{44}$GLDFKGEFIPTDKDMMEKLF$_{63}$
1189.45^{+2}	1189.07^{+2}	$_{44}$GLDFKGEFIPTDKDMM$_{ox}$EKLF$_{63}$
1192.97^{+2}	1193.11^{+2}	$_{117}$SVGDKAKPIVQGGPTGSPISEDVF$_{140}$
1306.08^{+2}	1305.66^{+2}	$_{82}$RIVKYTEDEIWDAINNVQKEF$_{102}$
1529.16^{+2}	1528.64^{+2}	$_{318}$AC$_{cam}$ATISEFTDILSGNQYY PC$_{cam}$AGPC$_{cam}$TEM$_{344}$

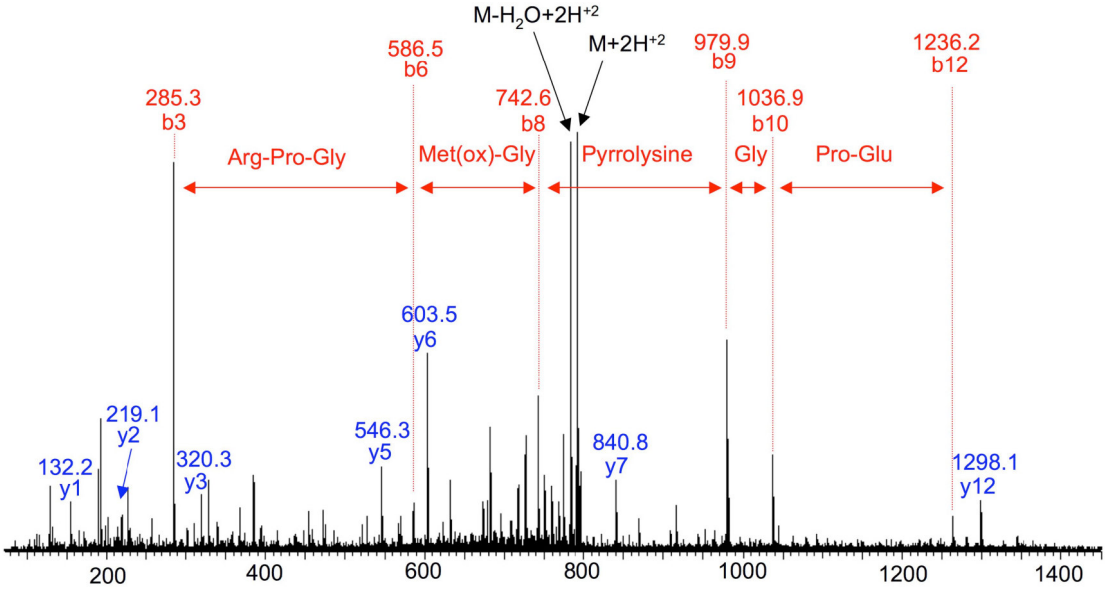

Figure 2.4: Collision-Induced Dissociation spectra for peptide ^{194}AGRPGM$_{OX}$GVOGPETSL^{208} generated by chymotryptic digest of MtmB, showing the presence of peptides corresponding to the mass of pyrrolysine with a methyl group at the C4-substituent.

y- Ion Type	Observed m/z (M+H)	Sequence	Observed m/z (M+H)	b-Ion Type
		Ala		
		Gly	129.1	b-2
		Arg	285.3	b-3
y-12	1298.2	Pro		
		Gly	439.4	b-5
		Mox	586.5	b-6
		Gly		
		Val	742.6	
y-7	840.8	Pyrrolysine	979.9	b-9
y-6	603.5	Gly	1036.9	b-10
y-5	546.3	Pro		
y-3	320.3	Thr		
y-2	219.1	Ser		
y-1	132.2	Leu		

Table 2.2: The b/y ions generated following Collision-Induced Dissociation of the ^{194}AGRPGM$_{OX}$GVOGPETSL^{208} peptide of MtmB.

Table 2.3: Predicted and observed m/z from MALDI-TOF data of MtmB digested with chymotrypsin acquired on a Bruker Reflex III. All mass errors are within 0.3 Da.

Table 2.3

Observed M+H	Predicted M+H	Sequence
975.41	975.44	^{4}RKSFDCCAMY^{10}
1070.52	1070.57	^{59}MEKLFKAGF^{67}
1400.54	1400.59	^{4}RKSFDCYDFY^{13}
1457.70	1457.80	^{237}KIDLDAISVIAHY^{249}
1516.81	1516.85	^{162}TSVRGKSPIPKSPY^{175}
1552.67	1552.74	^{304}GSTNTRETLMoxIAGW^{317}
1560.82	1560.87	^{445}DGARKKLEDLGLVF^{458}

Table 2.3 continued

Observed M+H	Predicted M+H	Sequence
1677.85	1677.88	^{179}AAKTETRLIKNACcamAM^{193}
1802.80	1802.85	^{430}DVKTVTPTEEYMQVY^{444}
1857.99	1858.04	^{162}TSVRGKSPIPKSPYEVL^{178}
2014.87	2014.93	^{250}KGNSDIIMDEQMPIFGGY^{267}
2022.96	2023.07	^{268}AGGIEETTIVDVATHINAVL^{287}
2134.99	2135.07	^{345}CcamLLEASAQSITDTASGREIL^{364}
2361.08	2361.05	^{11}DFYDRAKVGEKCcamTQDDWDL^{29}

Table 2.4: A comparison of the peptide masses observed for MtmB generated by chymotryptic digests detected by Fourier Transform Ion Cyclotron Resonance mass spectrometry versus predicted masses.

Table 2.4

Observed M + H	Predicted M + H	Δ(predicted - observed)	Sequence
1223.548	1223.551	0.003	^{2}TFRKSFDC$_{cam}$Y^{10}
1229.653	1229.654	0.001	^{294}HLDGPVHIRW^{303}
1261.647	1261.653	0.006	^{80}THRIVKYTED^{89}
1445.851	1445.847	–0.004	^{446}GARKKLEDLGLVF^{458}
1457.805	1457.800	–0.005	^{237}KIDLDAISVIAHY^{249}
1516.849	1516.848	–0.001	^{162}TSVRGKSPIPKSPY^{175}
1530.738	1530.733	–0.005	^{64}KAGFEMLLEC$_{cam}$GIY^{76}
1560.868	1560.874	0.006	^{445}DGARKKLEDLGLVF^{458}
1581.805	1581.805	0.000	^{193}AGRPGM$_{ox}$GVO GPETSL^{208}
1648.714	1648.710	–0.004	^{2}TFRKSFDC$_{cam}$YDFY^{13}
1802.855	1802.852	–0.003	^{430}DVKTVTPTEEYM QVY^{444}
1858.039	1858.043	0.004	^{162}TSVRGKSPIPKS PYEVL^{178}

as an M+H ion with an *m/z* = 1581.8036 (n=6, S.D.=0.0009) (Table 2.4). The mass of this ion matched up with the theoretical mass of an M+H ion of the ^{194}AGRPGM$_{OX}$GVOGPETSL^{208} peptide of *m/z* 1581.8059 Da for a pyrrolysine residue at the "O" position with a methyl group as the 4-substituent. The data also eliminated the other possibilities for the 4-substituent, namely, an amine group (1583.7852 Da) or a hydroxyl group (1582.8012 Da) for a singly protonated state of the peptide containing pyrrolysine. The theoretical mass for the 194-208 peptide without the pyrrolysine residue is 1344.6582 Da, which leads to the calculation of the residue mass of pyrrolysine as being 237.1456 Da. The deduced empirical formula for pyrrolysine, the 22nd genetically encoded amino acid is $C_{12}H_{19}N_3O_2$.

2.3.3 Determination of the mass of the UAG-encoded residue in MtbB1

Similar to the methodology used to resolve the mass of pyrrolysine in MtmB, the residue mass of the amino acid encoded by a UAG in MtbB was determined by chymotryptic digests in the presence of acetonitrile as denaturant. The aforementioned treatment was followed by the determination of the masses of peptides by LC-MS/MS. Keeping in mind the presence of three copies of *mtbB* in *M. barkeri* MS, eight peptides with predicted masses for peptides unique for protein arising from the *mtbB1* gene were observed. No peptides were detected that could have arisen from the gene products of either *mtbB2* or *mtbB3* (Paul *et. al.* 2000). Thus, it was concluded that MtbB1 was the major component found in the DMA methyltransferase preparation isolated for this study.

The chymotryptic digest of MtbB1 yielded 86% sequence coverage (Figure 2.5) which included the ^{341}RASKAMVEIAGVDGIOIGVGDPL^{363} and ^{347}VEIAGVDGIOIGVGDPLGMPIAHIM^{371} peptides, both covering the residue encoded by the in-frame UAG (Table 2.5) . The peptide predicted to be that of ^{341}RASKAMVEIAGVDGIOIGVGDPL^{363} was found to be in the triply charged state, *m/z* = 802.523^{3+}, whereas two different ionic states were found for the ^{347}VEIAGVDGIOIGVGDPLGMPIAHIM^{371} peptide, *m/z* = 871.21^{3+} and *m/z* = 1306.32^{2+}. The CID spectra for both peptides were studied, and confirmed the identity of the sequence assignments (Figure 2.6). In Table 2.6 is listed the b and y ion series for the data obtained from the CID of *m/z* = 871.21^{3+}. The mass difference between both the b10/b9 ion pair and that of y16/y15 were found to be 237.22 Da, which coincided with the predicted mass of pyrrolysine with a methyl group as the 4-substituent. As a result, MtbB1 can be included in the list of proteins containing the 22nd genetically-encoded amino acid.

2.3.4 Determination of the mass of the UAG-encoded residue in MttB

Chymotryptic digests were used for the determination of the residue mass of the amino acid residue encoded by the in-frame UAG in the TMA methyltransferase, *mttB* using mass spectrometry. Unlike *Methanosarcina acetivorans* and *Methanosarcina mazeii*, *M. barkeri* possesses a single copy of the TMA methyltransferase gene, *mttB*. LC-MS/MS carried out on the peptides generated by chymotrypsin allowed for 85% sequence coverage of MttB (Figure

1 MATEY**ALRMG DGKRVYLTKE KIVSEIEAGT ADAADLGEIP ALSANEMDKL**
51 AEILMMPGKT VSVEQGMEIP VTH**DIGTIRL DGDQGNSGVG IPSSRLVGCM**
101 THERAFGADT MELGHIDYSF KPVKPVVSNE CQAMEVCQQN MVIPLFYGAM
151 PNMGLY**YTPD GPFENPGDLM KAFKIQEAWE SMEHAAEHLT RDTVW**VMQKL
201 F**ASGADGVNF DTTGAAGDGD MYGTLHAIEA LRKEFPDMYI EAGMAGECVL**
251 GMHGNLQYDG VTLAGLWPHQ QAPLVAKAGA NVFGPVCNTN TSKTSAWNLA
301 RAVTFMKAAV EASPIPCHVD MGMGVGGIPM LETPPIDAVT **RASKAMVEIA**
351 GVDGIOIGVG DPLGMPIAHI MASGMTGM**RA AGDLVARMEF SKNMRIGEAK**
401 EYVAKKLGVD KMDLVDEHVM RELREELDIG IITSVPGAAK GIAAKMNIEK
451 LLDIKINSCN LFRKQIA

Figure 2.5: Enzymatic map of the sequence coverage achieved by the digestion of MtbB1 with chymotrypsin. Sequence marked in blue are the residues that were detected. The ‘O’ denotes the position of the UAG codon at position of 356.

Table 2.5: A comparison of the predicted and observed peptide masses of MtbB1 digested with chymotrypsin. The data was generated by LC-MS/MS on a Q-TOF II mass spectrophotometer. The peptides marked in bold, is the pyrrolysine-containing peptide at position 356 of the polypeptide. The peptides that corresponded to *mtbB1* only, are marked with a single asterisk, whereas peptides unique to *mtbB1* and *mtbB2* are marked with double asterisks.

Table 2.5

Observed *m/z*	Predicted Mass	Observed Sequence from b/y Ion Analysis
422.60^{+3}	1265.66	$_{6}$ALRMGDGKRVY$_{16}$
423.74^{+2}	846.38	$_{112}$ELGHIDY$_{118}$
435.27^{+2}	869.42	$_{364}$GMPIAHIM$_{371}$ *
438.79^{+2}	876.48	$_{275}$VAKAGANVF$_{283}$
446.30^{+2}	891.49	$_{298}$NLARAVTF$_{305}$
460.25^{+2}	919.39	$_{251}$GMHGNLQY$_{258}$ **
462.81^{+2}	924.50	$_{223}$GTLHAIEAL$_{231}$ **
475.95^{+3}	1425.70	$_{391}$SKNMRIGEAKEY$_{402}$
514.31^{+2}	1027.51	$_{188}$HLTRDTVW$_{195}$
529.65^{+3}	1586.79	$_{121}$KPVKPVVSNE$_{Cca}$mQAM$_{134}$
543.30^{+2}	1085.49	$_{232}$RKEFPDMY$_{239}$ **
548.82^{+2}	1096.53	$_{394}$MRIGEAKEY$_{402}$

Table 2.5 continued

Observed *m/z*	Predicted Mass	Observed Sequence from b/y Ion Analysis
577.31^{+2}	1153.48	$_{180}$ESMEHAAEHL$_{189}$
600.89^{+2}	1200.66	$_{434}$SVPGAAKGIAAKM$_{446}$
604.32^{+2}	1207.52	$_{97}$VG$_{Cca}$mMTHERAF$_{106}$
609.36^{+2}	1217.62	$_{264}$AGLWPHQQAPL$_{274}$ **
612.36^{+2}	1223.59	$_{453}$DIKINS$_{Cca}$mNLF$_{462}$ *
623.87^{+2}	1246.62	$_{44}$ANEMDKLAEIL$_{54}$
629.36^{+3}	1885.90	$_{408}$GVDKMDLVDEHVMREL$_{423}$
633.40^{+2}	1265.66	$_{6}$ALRMGDGKRVY$_{16}$
638.01^{+3}	1911.85	$_{180}$ESMEHAAEHLTRDTVW$_{195}$
657.36^{+3}	1970.90	$_{132}$QAMEV$_{Cca}$mQQNMVIPLFY$_{147}$
661.34^{+2}	1321.56	$_{107}$GADTMELGHIDY$_{118}$
667.40^{+2}	1333.65	$_{43}$SANEMDKLAEIL$_{54}$
668.40^{+2}	1335.67	$_{379}$RAAGDLVARMEF$_{390}$
678.39^{+2}	1355.64	$_{413}$DLVDEHVMREL$_{423}$
702.87^{+2}	1404.64	$_{251}$GMHGNLQYDGVTL$_{263}$ **

Table 2.5 continued

Observed *m/z*	Predicted Mass	Observed Sequence from b/y Ion Analysis
713.42^{+2}	1425.70	$_{391}$SKNMRIGEAKEY$_{402}$
744.41^{+2}	1487.67	$_{408}$GVDKMDLVDEHVM$_{420}$
761.92^{+2}	1522.68	$_{284}$GPVCNTNTSKTSAW$_{297}$
776.47^{+3}	2327.18	$_{74}$DIGTIRLDGDQGNSGVGIPSSRL$_{96}$
776.89^{+2}	1552.64	$_{157}$YTPDGPFENPGDLM$_{170}$
779.94^{+2}	1558.73	$_{81}$DGDQGNSGVGIPSSRL$_{96}$
793.94^{+2}	1586.72	$_{232}$RKEFPDMYIEAGM$_{244}$ **
793.97^{+2}	1586.79	$_{121}$KPVKPVVSNE$_{Cca}$mQAM$_{134}$
802.52^{+3}	**2405.30**	**$_{341}$RASKAMVEIAGVDGIOIGVGDPL$_{363}$** *
808.98^{+2}	1616.79	$_{249}$VLGMHGNLQYDGVTL$_{263}$
852.47^{+3}	2555.18	$_{306}$MKAAVEASPIP$_{Cca}$mHVDMGMGVGGIPM$_{330}$
871.21^{+3}	**2611.38**	**$_{347}$VEIAGVDGIOIGVGDPLGMPIAHIM$_{371}$** *
889.83^{+3}	2667.24	$_{174}$KIQEAWESMEHAAEHLTRDTVW$_{195}$ **
911.03^{+2}	1820.89	$_{119}$SFKPVKPVVSNE$_{Cca}$mQAM$_{134}$
943.54^{+2}	1885.90	$_{408}$GVDKMDLVDEHVMREL$_{423}$

Table 2.5 continued

Observed *m/z*	Predicted Mass	Observed Sequence from b/y Ion Analysis
950.02^{+2}	1898.85	$_{157}$YTPDGPFENPGDLMKAF$_{173}$ **
956.51^{+2}	1911.85	$_{180}$ESMEHAAEHLTRDTVW$_{195}$
963.52^{+2}	1925.86	$_{312}$ASPIP$_{Cca}$mHVDMGMGVGGIPM$_{330}$ *
967.61^{+2}	1934.02	$_{447}$NIEKLLDIKINS$_{Cca}$mNLF$_{462}$ *
996.48^{+2}	1991.77	$_{202}$ASGADGVNFDTTGAAGDGDMY$_{222}$
1062.96^{+3}	3186.59	$_{17}$LTKEKIVSEIEAGTADAADLGEIPALSANEM$_{47}$
1108.61^{+2}	2216.00	$_{232}$RKEFPDMYIEAGMAGE$_{Cca}$mVL$_{250}$ **
1123.99^{+3}	3369.68	$_{22}$IVSEIEAGTADAADLGEIPALSANEMDKLAEIL$_{54}$
1132.08^{+2}	2262.93	$_{202}$ASGADGVNFDTTGAAGDGDMYGTL$_{225}$
1148.33^{+3}	3442.65	$_{119}$SFKPVKPVVSNE$_{Cca}$mQAMEV$_{Cca}$mQQNMVIPLFY$_{147}$
1164.20^{+2}	2327.18	$_{74}$DIGTIRLDGDQGNSGVGIPSSRL$_{96}$
1170.75^{+2}	2340.28	$_{424}$REELDIGIITSVPGAAKGIAAKM$_{446}$
1181.71^{+3}	3542.80	$_{17}$LTKEKIVSEIEAGTADAADLGEIPALSANEMDKL$_{50}$
1286.12^{+3}	3855.96	$_{18}$TKEKIVSEIEAGTADAADLGEIPALSANEMDKLAEIL$_{54}$
1306.32^{+2}	**2611.38**	**$_{347}$VEIAGVDGIOIGVGDPLGMPIAHIM$_{371}$** *
1323.80^{+3}	3969.04	$_{17}$LTKEKIVSEIEAGTADAADLGEIPALSANEMDKLAEIL$_{54}$
1334.25^{+2}	2667.24	$_{174}$KIQEAWESMEHAAEHLTRDTVW$_{195}$ **

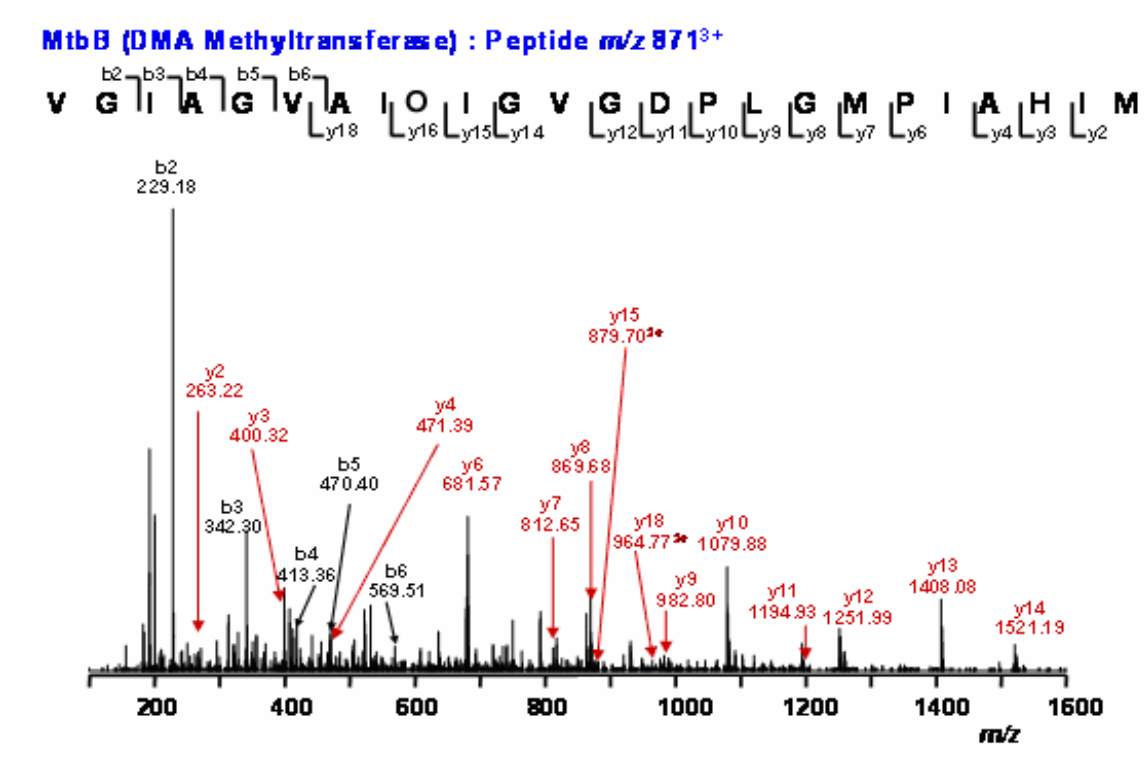

Figure 2.6: Collision-Induced Dissociation spectra for peptide ^{347}VEIAGVDGIOIGVGDPLGMPIAHIM^{371} generated by chymotryptic digest of MtbB1, showing the presence of pyrrolysine at residue position 356.

Table 2.6: The b/y ions generated following collision-induced dissociation of the ^{347}VEIAGVDGIOIGVGDPLGMPIAHIM^{371} peptide of MtbB1.

Table 2.6

y-ion type	**Observed *m/z* (M + H)**	**Sequence**	**Observed *m/z* (M + H)**	**b-ion type**
		Val		
		Glu	229.18	b-2
		Ile	342.30	b-3
		Ala	413.34	b-4
		Gly	470.38	b-5
		Val	569.46	b-6
		Asp		
y-18	964.74^{2+}	Gly	741.60	b-8
		Ile	854.74	b-9
y-16	879.70^{2+}	Pyrrolysine	1091.96	b-10
y-15	1521.16	Ile		
y-14	1408.05	Gly	1262.03	b-12

Table 2.6 continued

y-ion type	**Observed *m/z* (M + H)**	**Sequence**	**Observed *m/z* (M + H)**	**b-ion type**
		Val		
y-12	1251.90	Gly		
y-11	1194.95	Asp		
y-10	1079.87	Pro		
y-9	982.77	Leu		
y-8	869.63	Gly		
y-7	812.62	Met		
y-6	681.56	Pro		
y-5	584.51	Ile		
y-4	471.37	Ala		
y-3	400.31	His		
y-2	263.22	Ile		
		Met		

1 MAKNNAVAGF **NALNGVELNL FTTDELKAIH YATMEVLMDP GIQVSDPEAR**
51 QIFKENGCEV NEKTNVVKIP EYLVRKAL**QL APSRFV**LWGR DKKF**NTVQEC**
101 GGKVHWTCFG TGVKVCKY**QD GKYVTVDSVE KDIADIAKLC DWAENIDYFS**
151 LPVSARDIAG QGAQDVHETL TPLANTAKHF **HHIDPVGENV EYYRDIVKAY**
201 YGGDEEEARK KPIFSMLLCP TSPLELSVNA CQVIIKGARF GIPVNVL**SMA**
251 MSGGSSPVYL AGTLVTHNAE VLSGIVL**AQL TVPGAKVWY**G SSTTTFD**LKK**
301 GTAPVGSPEL GLISAAVAKL AQFY**GLPSYV AGSOSDAKVP DDQAGHEKTM**
351 TTLLPALAGA NTIYGAGMLE LGMTFSMEQL VIDNDIFSMV K**KAMQGIPVS**
401 EETLAVESIQ KVGIGNNFLA LKQTRQLVDY PSNPMLLDRH MFGDWAAAGS
451 KDLATVAHEK VEDVLKNHQV TPIDADIFKD MQAIVDKADK AFRGM

Figure 2.7: Sequence coverage map achieved by the digestion of MttB with chymotrypsin. Sequences marked in blue are the residues that were detected. The ‘O’ denotes the position of the UAG codon at position of 334.

Table 2.7: A comparison of the predicted and observed peptide masses of MttB digested with chymotrypsin. The data was generated by LC-MS/MS on a Q-TOF II mass spectrophotometer. The peptide marked in bold, is the pyrrolysine-containing peptide at position 334 of the polypeptide.

Table 2.7

Observed *m/z*	Predicted Mass	Observed Sequence from b/y Ion Analysis
409.58^{+2}	818.43	$_{79}$QLAPSRF$_{85}$
421.42^{+3}	1262.69	$_{230}$AC$_{Cam}$QVIIKGARF$_{240}$
466.07^{+2}	931.46	$_{436}$LLDRHMF$_{442}$
472.06^{+3}	1414.64	$_{95}$NTVQECGGKVHW$_{106}$
514.10^{+2}	1027.54	$_{193}$YRDIVKAY$_{200}$
515.08^{+2}	1029.51	$_{218}$LCPTSPLEL$_{226}$
527.08^{+3}	1579.80	$_{479}$KDMQAIVDKADKAF$_{492}$
532.07^{+3}	1595.79	$_{479}$KDM$_{ox}$QAIVDKADKAF$_{492}$
546.75^{+3}	1638.79	$_{201}$YGGDEEEARKKPIF$_{214}$
559.42^{+3}	1676.82	$_{422}$KQTRQLVDYPSNPM$_{435}$
563.57^{+2}	1126.51	$_{365}$GAGMLELGMTF$_{375}$
572.44^{+3}	1715.92	$_{124}$VTVDSVEKDIADIAKL$_{139}$
585.13^{+2}	1169.65	$_{278}$AQLTVPGAKVW$_{288}$
595.59^{+2}	1190.59	$_{22}$TTDELKAIHY$_{31}$
602.11^{+2}	1203.62	$_{11}$NALNGVELNLF$_{21}$
612.62^{+2}	1224.64	$_{261}$AGTLVTHNAEVL$_{272}$

Table 2.7 continued

Observed *m/z*	Predicted Mass	Observed Sequence from b/y Ion Analysis
631.63^{+2}	1262.69	$_{230}$AC$_{Cam}$QVIIKGARF$_{240}$
645.07^{+2}	1289.59	$_{436}$LLDRHMFGDW$_{445}$
653.08^{+2}	1303.77	$_{208}$ARKKPIFSMLL$_{218}$
657.09^{+3}	1969.95	$_{201}$YGGDEEEARKKPIFSML$_{217}$
666.52^{+2}	1332.50	$_{140}$C$_{Cam}$DWAENIDYF$_{149}$
669.14^{+2}	1337.72	$_{260}$LAGTLVTHNAEVL$_{272}$
675.11^{+3}	2024.05	$_{446}$AAAGSKDLATVAHEKVEDVL$_{465}$
688.10^{+2}	1376.73	$_{229}$NAC$_{Cam}$QVIIKGARF$_{240}$
704.57^{+2}	1408.63	$_{181}$HHIDPVGENVEY$_{192}$
707.58^{+2}	1414.64	$_{95}$NTVQECGGKVHW$_{106}$
709.64^{+2}	1418.77	$_{351}$TTLLPALAGANTIY$_{364}$
712.09^{+2}	1423.66	$_{376}$SMEQLVIDNDIF$_{387}$
749.11^{+2}	1497.75	$_{466}$KNHQVTPIDADIF$_{478}$
766.09^{+3}	**2296.07**	**$_{330}$VAGSOSDAKVPDDQAGHEKTM$_{0x}$$_{350}$**
769.46^{+3}	2307.19	$_{119}$QDGKYVTVDSVEKDIADIAKL$_{139}$
778.84^{+3}	2335.34	$_{297}$DLKKGTAPVGSPELGLISAAVAKL$_{320}$
781.65^{+2}	1562.83	$_{227}$SVNAC$_{Cam}$QVIIKGARF$_{240}$

Table 2.7 continued

Observed *m/z*	Predicted Mass	Observed Sequence from b/y Ion Analysis
782.63^{+2}	1564.78	$_{19}$NLFTTDELKAIHY$_{31}$
786.08^{+2}	1571.69	$_{181}$HHIDPVGENVEYY$_{193}$
788.11^{+3}	2363.17	$_{54}$KENGC$_{Cam}$EVNEKTNVVKIPEYL$_{73}$
790.13^{+2}	1579.80	$_{479}$KDMQAIVDKADKAF$_{492}$
794.44^{+3}	2382.18	$_{443}$GDWAAAGSKDLATVAHEKVEDVL$_{465}$
798.13^{+2}	1595.79	$_{479}$KDM$_{ox}$QAIVDKADKAF$_{492}$
816.11^{+3}	2447.18	$_{32}$ATMEVLMDPGIQVSDPEARQIF$_{53}$
819.62^{+2}	1638.79	$_{201}$YGGDEEEARKKPIF$_{214}$
825.46^{+3}	2475.27	$_{150}$SLPVSARDIAGQGAQDVHETLTPL$_{173}$
838.62^{+2}	1676.82	$_{422}$KQTRQLVDYPSNPM$_{435}$
843.47^{+3}	2529.30	$_{395}$QGIPVSEETLAVESIQKVGIGNNF$_{418}$
858.16^{+2}	1715.92	$_{124}$VTVDSVEKDIADIAKL$_{139}$
876.10^{+3}	2627.33	$_{457}$AHEKVEDVLKNHQVTPIDADIF$_{478}$
882.61^{+2}	1764.86	$_{157}$DIAGQGAQDVHETLTPL$_{173}$
901.61^{+2}	1802.86	$_{38}$MDPGIQVSDPEARQIF$_{53}$
932.78^{+3}	**2797.33**	**$_{325}$GLPSYVAGSOSDAKVPDDQAGHEKTM$_{350}$**
938.44^{+3}	**2813.32**	**$_{325}$GLPSYVAGSOSDAKVPDDQAGHEKTM$_{ox}$$_{350}$**

Table 2.7 continued

Observed *m/z*	Predicted Mass	Observed Sequence from b/y Ion Analysis
942.50^{+3}	2826.51	$_{395}$QGIPVSEETLAVESIQKVGIGNNFLAL$_{421}$
951.67^{+2}	1902.99	$_{422}$KQTRQLVDYPSNPMLL$_{437}$
953.48^{+3}	2859.47	$_{392}$KAMQGIPVSEETLAVESIQKVGIGNNF$_{418}$
985.13^{+2}	1969.95	$_{201}$YGGDEEEARKKPIFSML$_{217}$
993.13^{+2}	1985.95	$_{201}$YGGDEEEARKKPIFSM$_{ox}$L$_{217}$
1010.12^{+3}	3029.43	$_{124}$VTVDSVEKDIADIAKL$_{CCam}$mDWAENIDYF$_{149}$
1012.17^{+2}	2024.05	$_{446}$AAAGSKDLATVAHEKVEDVL$_{465}$
1036.16^{+2}	2072.05	$_{252}$SGGSSPVYLAGTLVTHNAEVL$_{272}$
1072.15^{+2}	2144.05	$_{35}$EVLMDPGIQVSDPEARQIF$_{53}$
1153.70^{+2}	2307.19	$_{119}$QDGKYVTVDSVEKDIADIAKL$_{139}$
1167.77^{+2}	2335.34	$_{297}$DLKKGTAPVGSPELGLISAAVAKL$_{320}$
1181.67^{+2}	2363.17	$_{54}$KENGC$_{Cam}$EVNEKTNVVKIPEYL$_{73}$
1206.79^{+3}	3620.69	$_{119}$QDGKYVTVDSVEKDIADIAKLC$_{Cam}$ DWAENIDYF$_{149}$
1223.68^{+2}	2447.18	$_{32}$ATMEVLMDPGIQVSDPEARQIF$_{53}$
1237.70^{+2}	2475.27	$_{150}$SLPVSARDIAGQGAQDVHETLTPL$_{173}$
1246.17^{+2}	2492.20	$_{248}$SMAMSGGSSPVYLAGTLVTHNAEVL$_{272}$
1264.71^{+2}	2529.30	$_{395}$QGIPVSEETLAVESIQKVGIGNNF$_{418}$
1398.68^{+2}	**2797.33**	**$_{325}$GLPSYVAGSOSDAKVPDDQAGHEKTM$_{350}$**

Table 2.8: The b/y ions generated following collision-induced dissociation of the ^{325}GLPSYVAGSOSDAKVPDDQAGHEKTM^{350} peptide of MttB.

Table 2.8

y-ion type	Observed *m/z* (M + H)	Sequence	Observed *m/z* (M + H)	b-ion type
		Gly		
		Leu	171.08	b-2
y-24	1313.89^{2+}	Pro		
y-23	1265.37^{2+}	Ser	355.13	b-4
y-22	1221.83^{2+}	Tyr	518.17	b-5
y-21	1140.33^{2+}	Val	617.21	b-6
y-20	1090.81^{2+}	Ala	688.23	b-7
y-19	1055.30^{2+}	Gly	745.26	b-8
y-18	1026.77^{2+}	Ser		
y-17	983.30^{2+}	Pyrrolysine		
y-16	1728.52	Ser		
		Asp		
y-14	1526.47	Ala		

Table 2.8 continued

y-ion type	Observed *m/z* (M + H)	Sequence	Observed *m/z* (M + H)	b-ion type
y-13	1455.46	Lys		
y-12	1327.34	Val		
		Pro		
		Asp		
y-9	1016.27	Asp		
y-8	901.26	Gln		
y-7	773.23	Ala		
y-6	702.18	Gly		
y-5	645.17	His		
y-4	508.16	Glu		
y-3	379.12	Lys		
y-2	251.06	Thr		
y-1	150.03	Met		

2.7). The sequence coverage included ions coinciding with those of peptide masses generated by pyrrolysine-containing peptides at the 334 position. Ions with a triple and double charge were detected for the ^{325}GLPSYVAGSOSDAKVPDDQAGHEKTM^{350} peptide, and their respective masses were found to be *m/z* = 932.78^{3+} and *m/z* = 1398.68^{2+}. This peptide was also detected in the oxidized methionine (residue, 350) form as the triply protonated *m/z* = 938.44^{3+} (Table 2.7). Another peptide containing the UAG-encoded residue, ^{330}VAGSOSDAKVPDDQAGHEKTMox^{350} was identified with a mass of *m/z* = 766.09^{3+}. CID spectra for all the aforementioned peptides for the TMA methyltransferase confirmed the sequence identity of the ions. Table 2.8, shows the b and y ions series for the ions observed when CID was performed on the ^{325}GLPSYVAGSOSDAKVPDDQAGHEKTM^{350}, *m/z* = 932.78^{3+} ion. The mass of the UAG-encoded residue could not be determined by the b-ion series, however, the difference in the y17/y16 ions yielded the mass as being 237.1 Da. The mass of the UAG-encoded residue in the TMA methyltransferase, MttB also coincided with the calculated mass of pyrrolysine with a methyl group present at the 4-substituent.

2.4 DISCUSSION

This chapter describes the first detection of L-pyrrolysine by a technique other than crystallography. Initial attempts to observe the presence of the residue by mass spectroscopy of tryptic digests of MtmB by James *et. al.* may have been

unsuccessful owing to the harsh digestion conditions. Hao *et. al*. have shown that synthetic pyrrolysine is unstable and prone to hydrolysis under prolonged exposure to acidic or basic conditions (James *et. al.* 2001, Hao *et. al.* 2004). Earlier conditions used for the tryptic digests of MtmB included carboxymethylation with iodoacetic acid and following tryptic digestion, separation by reverse-phase HPLC in the presence trifluoroacetic acid. These conditions may have caused pyrrolysine to be hydrolyzed at the amide linkage, and resulting in the determination of a lysine residue being detected at the position encoded by the in-frame UAG. Chymotryptic digests of iodoacetamide-treated MtmB in the presence of acetonitrile as denaturant, coupled with LC-MS reduced the exposure time of pyrrolysine to harsh conditions, and resulted in the first detection of the amino acid by mass spectrometry. No peptides containing lysine were observed during the duration of this study, and only masses corresponding with an unmodified pyrrolysine were observed.

The crystal structure of MtmB as resolved by Hao *et. al.* deduced the structure of pyrrolysine as a lysine residue with the epsilon-nitrogen in amide linkage with a (4R,5R)-4-substituted-pyrrolyine-5-carboxylate. The 4-substituent could not be definitely assigned, but a methyl, amine, or hydroxyl groups were suggested as distinct possibilities. Crystal structures of MtmB with pyrrolysine derivatized with hydroxylamine, led to further refinement of the structure, and best matched the 4-substituent as being a methyl group. However, the presence of an amine group was an admitted possibility in this study, ruling out the occurrence of a hydroxyl group at that position (Hao *et. al*. 2004). In this study,

the mass of the pyrrolysine residue has been determined by mass spectrometry, and assigned to be a methyl group at the 4-substituent position. This has significant implications when formulating biosynthetic pathways for the amino acid. It has importance when designing labeling when studying the pathway for the biosynthesis of pyrrolysine. The precise mass of the residue will also be useful when using proteomic approaches to observe the presence of this novel residue in other proteins.

A key aspect of this study points to the presence of pyrrolysine in all three methylamine methyltransferases strongly suggesting that this residue may play a role in catalysis. Hao *et al.* have shown that this residue possesses electrophilic properties, given the demonstrated reactivity of this residue with nucleophiles such as hydroxylamine, sulfite and ammonia. The x-ray crystal structures of the derivatized pyrrolysine with the aforementioned chemicals suggest the presence of a reactive imine (Hao *et. al.* 2002, Hao *et. al.* 2004). The methyltetrahydrofolate:corrinoid methyltransferase domain of methionine synthase (Evans *et. al.* 2004) is a close structural homolog of MtmB, and the active sites of the two proteins have been shown to be super imposable (Krzycki *et. al.* 2004). The C2 position of pyrrolysine and the methyl group to be transferred in methyltetrahydrofolate occupy similar positions relative to the active site of the protein. Accordingly, the pyrrolysyl residue is ideally situated at the bottom of a catalytic cleft to bind substrate and orient a methyl group which is transferred to a cognate corrinoid protein, MtmC. The same should be true for the other two methylamine methyltransferases, MtbB and MttB in transferring

methyl groups to MtbC and MttC respectively. This also brings to light an alternative hypothesis by which pyrrolysine could function. Pyrrolysine could bind the demethylation product of the methylamine substrates. Ammonia is the end product of the transfer of the methyl group from MMA to MtmC via MtmB. It has already been shown that ammonia can interact with the pyrrolysyl residue. Thus, this alternative hypothesis remains a distinct possibility.

The presence of in-frame UAG codons, and their translation as pyrrolysine in *mtmB*, *mtbB* and *mttB* brings to light some interesting questions with respect to the mechanism of amber codon suppression. In the case of selenocysteine, selenocysteinyl-tRNA^{Sec}, is synthesized from a tRNA^{Sec} charged with a serine residue by a seryl-tRNA synthetase. Selenocysteine residues are encoded by specific UGA codons. A *cis*-acting selenocysteine insertion sequence (SECIS) is found within the 3' untranslated region (UTR) in Archaea and Eucarya, whereas this element is present just 3' of the UGA codon to be suppressed in Bacteria. The SECIS element plays an essential role in the incorporation of selenocysteine at the appropriate UGA codons (Small-Howard *et. al.* 2005, Copeland *et. al.* 2001). Bioinformatic approaches have suggested the presence of a stem loop structure just downstream of the in-frame UAG codon in *mtmB* called the pyrrolysine insertion element (PYLIS) (Namy *et. al.* 2004, Paul, 2000, Zhang *et. al.* 2005). Theobald-Dietrich *et. al.* have shown that the PYLIS element does exist in solution using structure-probing studies *in vitro*(Theobald-Dietrich *et al.* 2005). Thus it was suggested that the PYLIS element may play a role similar to that of SECIS in the insertion of pyrrolysine at the UAG codon. Longstaff *et. al.*

have shown that the UTRs flanking *mtmB* were not required for translation of the UAG codon. However, the loss of the PYLIS element resulted in a decrease in the UAG-translated product, with a corresponding increase in the UAG-terminated product (Longstaff *et. al.* 2007). The demonstration that MtbB and MttB possess pyrrolysine at the UAG encoded positions raises interesting questions about the role of the PYLIS element. Variations of the PYLIS element are observed in *mtmB1* and *mttB* transcripts, but are completely lacking in *mtbB* (Namy *et. al.* 2004). The lack of the presence of a putative PYLIS element in *mtbB* transcripts raises the possibility that if any cis-acting element were present and required for the insertion of pyrrolysine, the element would have limited or no sequence similarity.

Pyrrolysine is inserted into proteins by a mechanism similar to the other 20 canonical amino acids (Blight *et. al.* 2004, Polycarpo *et. al.* 2004). Chemically synthesized pyrrolysine with the R-substituent being a methyl group was shown to be the substrate for charging $tRNA^{Pyl}$ with the pyrrolysyl-tRNA synthetase PylS. *E.coli* was shown to incorporate this amino acid at the UAG position of *mtmB* while expressing the pyrrolysyl-tRNA synthetase and $tRNA^{Pyl}$ in the presence of exogenously supplied pyrrolysine. Mass spectrometric data confirmed the incorporation of this residue at the position of the UAG codon in MtmB, and was shown to be 237.2 Da in mass. This suggests that the synthesized chemical used in the charging experiments, both *in vitro* and *in vivo* were chemically equivalent to the pyrrolysine residue present in *M. barkeri* MS.

CHAPTER 3

THE 22ND AMINO ACID AS THE SITE OF BOROHYDRIDE INHIBITION OF METHYLAMINE METHYLTRANSFERASE ACTIVITY

3.1 INTRODUCTION

Methanosarcina species are more versatile than other methanogenic archaea with respect to the catabolism of various substrates. They can metabolize carbon dioxide (CO_2) and hydrogen (H_2) as well as a variety of methylotrophic compounds such as acetate, methylated thiols, methanol, monomethylamine (MMA), dimethylamine (DMA) and trimethylamine (TMA) (Deppenmeier 2002, Ferry 1999). Methanogenesis from the three classes of methylamines has been characterized and shown to occur by similar pathways. These pathways converge to form methyl-CoM, a central intermediate in the generation of methane. Methanogenesis from MMA is initiated by the methyltransferase, MtmB, which catalyzes the methylation of a cognate corrinoid protein, MtmC. Similarly, the methyltransferases corresponding to DMA, MtbB,

and TMA, MttB, methylate cognate corrinoid proteins MtbC and MttC, respectively, only in the presence of their specific substrates (Ferguson *et. al.* 1997, Ferguson *et. al.* 2000) Methyl-CoM is generated by a methylcobamide:coenzyme M methyltransferase, MtbA, which transfers the methyl group from the corrinoid protein to CoM (2-mecaptoethanesulfonate) (Burke *et. al.* 1998). The F_{430}-dependent methyl-CoM reductase reduces methyl-CoM to generate methane (Ermler *et. al.* 1997, Shima *et. al.* 1997, Kunz *et. al.* 2006).

The unique feature of the non-homologous methylamine methyltransferases, MtmB, MtbB and MttB, is that the genes encoding these polypeptides all contain in-frame amber (UAG) codons which are translated (Krzycki 2005, Paul *et. al.* 2000, James *et. al.* 2001). Initially, mass spectrometric experiments using tryptic digests of MtmB identified the residue that corresponded to this UAG codon in *mtmB* as lysine (James *et. al.* 2001). The first evidence for the presence of a novel amino acid in the form of a 4-substituted-pyrroline-5-carboxylate in amide linkage with a lysine at this position came from the x-ray crystal structure of MtmB (Hao *et. al.* 2002, Srinivasan *et. al.* 2002). Recently, it has been demonstrated that the structure of the 22nd genetically encoded amino acid is a 4-methyl-pyrroline-5-carboxylate, and was shown to be present in MtmB, MtbB and MttB by mass spectrometry using chymotryptic digests of the polypeptides (Soares *et. al.* 2005). In the crystal structure of MtmB, the overall conformation was an αβ TIM barrel with pyrrolysine found at the center of a negatively-charged, solvent exposed cleft. This would allow for the

approach of a monomethylamine substrate to the putative catalytic cleft, followed by binding to pyrrolysine. This may result in the orienting of MMA on pyrrolysine to interact with the cobalt atom in the corrin ring of the cognate corrinoid protein MtmC (Hao *et al.* 2002, Krzycki 2004).

Two MtmB crystal structures had been determined by Hao *et al.* One structure, determined at a resolution of 1.55 angstrom, showed the presence of pyrrolysine in a single orientation when crystallized in the presence of NaCl. A second structure, resolved to 1.75 angstrom when MtmB crystals grown in $(NH_4)_2SO_4$, showed the presence of pyrrolysine with 60% occupancy of an amine added at the C2 position of the pyrroline ring. This difference between the two structures suggested that the C2 carbon was sp^2 hybridized and implied the presence of an imine bond between the N1 and C2 atoms in the pyrroline ring (Hao *et. al.* 2002). This crystal structure suggested that the imine bond may play a role in coordinating the methylamine substrate and orienting the methyl group of the substrate to the cobalt of the cognate corrinoid protein. The addition of the amine to the C2 position of the pyrroline ring was also accompanied by a 90° rotation of the ring, which positioned the Glu229 and Glu259 residues to act as proton donors to the N1 atom on the pyrroline ring. The protonation of the N1 atom would be predicted to make it more electron-withdrawing resulting in the activation of the C-2 carbon for a nucleophilic attack by deprotonated methylamines.

Hao *et al.* also determined the structures of MtmB treated with nucleophiles such as hydroxylamine, methylhydroxylamine and dithionite (Hao

et. al. 2004). The crystal structure of hydroxylamine-treated MtmB showed the predicted addition of hydroxylamine to the C2 carbon bonded through the nitrogen of hydroxylamine. On treatment with dithionite, an addition of sulfite to the C2 carbon was observed via the sulfur atom based on an MtmB structure resolved to 1.8 angstroms. Together, the data suggest the involvement of the imine bond in binding methylamines due to the presence of an electrophilic C2 carbon. Thus, it was proposed that *L*-pyrrolysine may play a role in catalysis.

The methyltetrahydrofolate binding domain of methionine synthase and the structure of MtmB with the addition of a methylamine ion at the C2 position of pyrrolysine are superimposable. On superimposition of the two structures, the methylamino-pyrrolysyl transient intermediate was found to be approximately 3 angstroms away from the positioning of the methyl- group of the methyltetrahydrofolate in the CH_3THF-binding domain structure (Krzycki 2004). The methyl-group of methyltetrahydrofolate is taken up by the cobalt of the cobalamin-binding domain of methionine synthase, a domain of high sequence similarity to MtmC. Since the two superimposed proteins interact with corrinoid proteins of high sequence similarity and therefore likely high structural similarity, it is reasonable to predict that pyrrolysine from MtmB can orient the methyl-group from the substrate MMA to the cobalt center of MtmC.

The use of $NaBH_4$ as a reductant of electrophilic imine bonds has been well documented (Schuster *et. al.* 1995, Lu-Chang 2006, Morris et. al. 1996). Given the aforementioned electrophilic character of the imine bond of pyrrolysine, we tested the role of this imine bond in catalysis by reduction with $NaBD_4$. In this

work we show the importance of the imine bond in the functioning of two of the methylamine methyltransferases, MtmB and MtbB, using low concentrations of $NaBD_4$. The reduction of the N1-C2 bond using this imine-specific reductant led to a chemical change found in either methyltransferase using mass spectrometry and supports the hypothesis that *L*-pyrrolysine plays an essential role in the catalysis of methylamine methyltransferases.

3.2 MATERIALS AND METHODS

3.2.1 Cell cultivation and extraction

M. barkeri MS (DSM 800) cells were grown in the presence of either 80 mM TMA or MMA in 40 liter carboys with a nitrogen gas phase. The cells were harvested 7 days after inoculation and incubation at 37°C. Cells were then washed twice in 50 mM MOPS (pH 7.0) and stored at -70°C until they were aerobically extracted by lysis using a French pressure cell.

3.2.2 Isolation of methylamine methyltransferases

MtmB was purified as described in Soares *et al.* 2005, from cell-free extracts of *M. barkeri* cells grown on MMA. The MtmB used in the experiments were shown to yield a single polypeptide band following analysis using denaturing 12.5% polyacrylamide gel electrophoresis and detection using Coomassie staining. The DMA methyltransferase, MtbB, was isolated as

described by Soares *et al.* 2005, from cell-free extracts of *M. barkeri* MS cells grown on TMA. The isolation was carried out entirely under anoxic conditions in an anaerobic glove compartment (Coy laboratories, Grass Lakes, MI).

3.2.3 Isolation of MtmC

Crude cell extracts of *M. barkeri* MS grown on MMA and harvested 7 days after inoculation were loaded onto a 38 x 2.5 cm DE-52 column (Whatman Inc., Fairfield N.J.) equilibrated with 50 mM NaCl in 50 mM Tris, pH 8.0. A 2.5 liter gradient of 50 to 500 mM NaCl in 50 mM Tris, pH 8.0 was used to elute the contents of the column at a flow rate of 2 ml/min. MtmC co-eluted with MtmB as described previously (Burke *et al.* 1995) at approximately 300 mM NaCl. This fraction was pooled and diluted 10-fold with 50 mM 3-[N-morpholino]propanesulfonic acid (MOPS), pH 6.5 and loaded onto a 30 x 2.5 cm Q-Sepharose column equilibrated with 100 mM NaCl in 50 mM MOPS, pH 6.5. A 2.5 liter gradient of 100 to 500 mM NaCl in the same buffer was applied to the column at a rate of 2 ml/min. MtmC complexed with MtmB eluted with activity centered around 250 mM NaCl. This fraction was pooled and concentrated 5-fold by ultracentrifugation using a YM-10 membrane (Amicon, Inc., Beverly, M.A.). The sample was diluted with 50 mM MOPS, pH 6.5 and loaded onto a Mono-Q HR 10/10 column (Amersham Biosciences, Piscataway, N.J.) equilibrated with 50 mM NaCl in 50 mM MOPS, pH 6.5. On running a 160 ml 50 to 500 mM NaCl gradient in 50 mM MOPS, pH 6.5 at 1 ml/min, the MtmB/MtmC complex eluted around 200 mM NaCl. This fraction was diluted 3-fold with 50 mM MOPS, pH 7.0

and loaded onto a 2.5 x 11 cm hydroxyapatite column (Bio-Rad Laboratories, Inc., Hercules, C.A.) equilibrated with 50 mM MOPS, pH 7.0. A gradient of 0 mM to 250 mM potassium phosphate over 240 ml was applied to the column at 1 ml/min. MtmB/MtmC complex eluted at around 170 mM potassium phosphate and was found to be apparently homogenous as detected by denaturing 12.5% polyacrylamine gel electrophoresis followed by Coomassie staining. For the purification of MtmC, the MtmB/MtmC complex was made anaerobic with alternate cycles of flush/evacuation in the presence of H_2 after it had been concentrated to approximately 2 ml by ultrafiltration with a YM-10 centricon (Amicon, Inc., Beverly, M.A.). This sample was treated with 5 mM Ti(III)-citrate and was loaded onto an anaerobic 80 x 2.5 cm Sephacryl S-100 column (Amersham Biosciences, Piscataway, N.J.) gel filtration column. This procedure was carried out under strict anaerobic conditions in an anaerobic glove bag. The column was run isocratically with 400 ml 50 mM MOPS containing 50 mM NaCl, pH 7.0 at a flow rate of 0.5 ml/min. MtmC eluted around 250 ml into the column run and was found apparently homogeneous when run on a denaturing 12.5% polyacrylamide gel followed by detection with Coomassie staining.

3.2.4 Isolation of MtbA

MtbA co-eluted with MtmB/MtmC complex after the initial DE-52 column as described above for the purification of MtmC. On running the subsequent Q-sepharose column, MtbA eluted with activity centered around 200 mM NaCl. Following this column, spectrophotometric assays for MtbA activity

were carried out as described below. The MtbA fraction was concentrated 5-fold using ultracentrifugation using a YM-10 membrane (Amicon, Inc., Beverly, M.A.). This fraction was then diluted using 50 mM MOPS, pH 7.0, and loaded onto a Mono-Q HR 10/10 column (Amersham Biosciences, Piscataway, N.J.) equilibrated with 50 mM MOPS, pH 7.0, containing 50 mM NaCl. On running a 160 ml 50 to 500 mM NaCl gradient in 50 mM MOPS, pH 7.0 at 0.5 ml/min, MtbA eluted around 150 mM NaCl. The MtbA active fraction was concentrated 5-fold using a YM-10 membrane and diluted with 50 mM MOPS, pH 7.0. The fraction was run on a 2.5 x 11 cm hydroxyapatite column (Bio-Rad Laboratories, Inc., Hercules, C.A.) equilibrated with 50 mM MOPS, pH 7.0. A gradient of 0 mM to 250 mM potassium phosphate (pH 7.0) over 240 ml was applied to the column at 1 ml/min. MtbA eluted with activity centered around 180 mM potassium phosphate and was found to be apparently homogeneous when electrophoresed through a denaturing 12.5% polyacrylamide gel followed by Coomassie staining.

3.2.5 Isolation of *M. barkeri* MS hexahistidine-tagged MtbB1 and *M. acetivorans* MtbC

MtbC was isolated during the isolation of hexa-histidine tagged MtbB1 from *M. barkeri* MS expressed in *M. acetivorans* (extracts were a gift from Jodie Y. Lee). A culture of *M. acetivorans* over-expressing C-terminal hexa-histidine tagged MtbB1 from *M. barkeri* MS grown on TMA were harvested at 5 days post-inoculation at log phase. These cells were extracted by French Press in 50 mM MOPS, pH 7.0, and loaded onto a 5 ml Ni-NTA column (Pharmacia). On running

a 160 ml, 0 to 500 mM imidazole gradient, at a flow rate 1 ml/min., MtbC from *M. acetivorans* bound to the hexa-histidine tagged, MtbB1, eluted separately at approximately 20 mM imidazole. The MtbC fractions were pooled and exchanged into a 50 mM MOPS, pH 7.0 buffer by ultracentrifugation using a YM-10 membrane (Amicon, Inc., Piscataway, N.J.). The MtbC fraction was then loaded onto a 1 x 5 ml hydroxyapatite column (Bio-Rad Laboratories, Inc., Hercules, C.A.) equilibrated with 50 mM MOPS, pH 7.0. A gradient of 0 mM to 250 mM potassium phosphate (pH 7.0) over 160 ml was applied to the column at 2 ml/min. The MtbC fraction eluted at approximately 25 mM potassium phosphate. This fraction was pooled and exchanged into a 50 mM MOPS, pH 7.0, buffer by ultracentrifugation using a YM-10 membrane and then loaded onto a Mono-Q HR 10/10 column (Amersham Biosciences, Piscataway, N.J.) equilibrated with 50 mM NaCl in 50 mM MOPS, pH 7.0. A 160 ml, 500 mM NaCl gradient in 50 mM MOPS, pH 7.0, was run at a rate of 1 ml/min. MtbC eluted at approximately 250 mM NaCl of the gradient. The protein preparation was found to be apparently homogenous as detected by denaturing 12.5% polyacrylamide gel electrophoresis followed by Coomassie staining. The activity of MtbC was confirmed by a CoM methylation assay.

3.2.6 Isolation of RAM

RAM was isolated from extracts prepared by the method described above from 1 kg of *M. barkeri* MS cells in 50 mM Tris, pH 8.0. The protein content of the

extract was quantitated as 27 gms of total soluble protein as determined by the BCA assay.

The entire isolation procedure for RAM was conducted in a Coy anaerobic chamber flushed with 98% nitrogen and 2% hydrogen. All the column matrices, prepacked columns and buffers used in the isolation were made anaerobic by multiple cycles of flushing with nitrogen and evacuating under vacuum.

The entire protein extract was loaded onto a 65 x 5 cm DE-52 column (Whatman Inc., Fairfield, NJ). A 4 liter linear gradient of 50 mM NaCl to 500 mM NaCl in 50 mM Tris, pH 8.0 was used to separate proteins on this column at a flow rate of 4 ml/min. The CoM methylation assay (described below) was used to detect fractions containing RAM. A RAM fraction was detected in a 480 ml range centered at approximately 420 mM NaCl. The active fraction were pooled, concentrated and diluted five-fold in 50 mM MOPS, pH 6.5 by ultrafiltration with a YM-10 membrane (Amicon, Inc., Beverly, MA). The extract was loaded onto a 65 x 5 cm Q-Sepharose column (Sigma, St. Louis, Missouri) equilibrated with 50 mM NaCl in 50 mM MOPS, pH 6.5. A 2.4 liter linear gradient from 50 mM to 500 mM NaCl in 50 mM MOPS, pH 6.5 was applied to the column at a flowrate of 2 ml/min. RAM eluted in a 112 ml range centered at 360 mM NaCl. The RAM fractions were pooled, concentrated and diluted five-fold in 50 mM MOPS, pH 7.5 by ultrafiltration with a YM-10 membrane. The concentrated fraction of RAM was loaded onto a 40 x 5 cm DEAE-Sepharose column (Sigma, St. Louis, Missouri) equilibrated with 50 mM NaCl in 50 mM MOPS, pH 7.5. A 2400 ml linear gradient from 50 mM NaCl to 500 mM NaCl in 50 mM MOPS, pH 7.5 was applied to the

column at a flowrate of 2 ml/min. A peak of RAM activity was detected at approximately 250 mM NaCl. The RAM fraction was pooled and concentrated and diluted five-fold in 50 mM MOPS, pH 7.0 by ultrafiltration with a YM-10 membrane. This fraction was split into three equal portions, and each loaded onto a Mono-Q HR 10/10 column (Amersham Biosciences). Each sample was chromatographed separately by running a 160 ml, 50 mM to 500 mM NaCl gradient in 50 mM MOPS, pH 7.0 over the Mono-Q column at a flowrate of 1 ml/min. RAM activity was detected at approximately 280 mM NaCl in all three runs, and these fractions were pooled, concentrated and diluted ten-fold in 50 mM MOPS, pH 7.0 by ultrafiltration with a YM-10 membrane. The fractions were split into three equal portions and loaded onto a BioRad CH2-I hydroxyapatite column equilibrated with 50 mM MOPS, pH 7.0. Each portion was chromatographed separately by applying a 80 ml 0 mM to 250 mM potassium phosphate gradient over the hydroxyapatite column at a flowrate of 2 ml/min. The active RAM fraction was found to elute at approximately 50 mM potassium phosphate in all three runs. These fractions were pooled, concentrated and diluted ten-fold in 50 mM Tris, pH 8.0 by ultrafiltration with a YM-10 membrane. The RAM fraction was loaded onto two Bio-Rad Uno Q-1 (3.3 ml each) equilibrated with 50 mM Tris, pH 8.0. A 160 ml linear gradient of 50 mM NaCl to 500 ml NaCl in 50 mM Tris, pH 8 was applied to the column at a flowrate of 1 ml/min. A RAM-active fraction was found to elute at 200 mM NaCl. This fraction was pooled, concentrated by ultrafiltration with a YM-10 membrane. This fraction was further concentrated to approximately 2 ml using an Amicon Centricon 10

concentrator fitted with a 10 kDa cut-off membrane. The sample was loaded onto a 80 x 2.5 cm Sephacryl S-200 HR column (Amersham Pharmacia) which was equilibrated with 50 mM NaCl in 50 mM MOPS, pH 7.0. The column was run isocratically with 400 ml of 50 mM NaCl in 50 mM MOPS, pH 7.0 being applied to the column at a flowrate of 1 ml/min. RAM eluted at approximately 260 ml of the isocratic run. This fraction was pooled, concentrated and diluted ten-fold in 50 mM MOPS, pH 7.0 by ultrafiltration with a YM-10 membrane. The RAM sample was divided into three equal portions. Each fraction was adjusted to 600 mM $(NH_4)_2SO_4$ and loaded onto a 1 ml pre-packed Phenyl-Speharose HP column (Pharmacia) which was pre-equilibrated with 600 mM $(NH_4)_2SO_4$. A 40 ml gradient from 600 mM $(NH_4)_2SO_4$ to 0 mM $(NH_4)_2SO_4$ was applied to the column at a flowrate of 0.5 ml/min. RAM eluted at approximately 450 mM $(NH_4)_2SO_4$. The final yield of RAM was 2 mgs.

3.2.7 CoM methylation Activity Assay

Activity assays were performed under strict anaerobic conditions in 2 ml rubber capped serum vials flushed with N_2. The reaction mixture was comprised of 50 mM MOPS at pH 7.0, 4 mM titanium citrate, 10 mM ATP, 20 mM $MgCl_2$, 3.2 mM 2-bromoethanesulfonic acid (BES), 2 mM CoM; 100 mM MMA, MtbA and the activation protein, RAM in a total volume of 125 µl. MtmB was added to the assay for testing for MtmC activity in fractions eluting of the Sephacryl S-100 column. For the initial DE-52 column to test for MtbA activity, MtbA was excluded from the reaction mix and MtmB and MtmC were

supplemented in the reaction. Activity assays for MtbB (9 µg) were carried out in the presence of MtbC (9 µg) rather than MtmC and MtbA (10 µg) in a total reaction volume of 125 µl. The assay was carried out at 37°C and 3.5 µl aliquots were periodically removed and added to 250 µl of 5,5'-dithio-bis(2-nitrobenzoic acid) (DTNB). The methylation of the free thiol was monitored by a loss of absorbance at 410 nm.

3.2.8 Spectrophotometric assay for MtbA activity

Column fractions were tested for MtbA activity by adding 20 µl fraction aliquots to 200 µl 1 mM CoM and 0.5 mM methylcobalamin in 50 mM Tris-HCl, pH 8.0 in a cuvette. MtbA activity was followed by an increase in absorbance at 620 nm over time.

3.2.9 $NaBD_4$ treatment of MtmB and MtbB

MtmB and MtbB were treated with varying concentration of $NaBD_4$ (Sigma-Aldrich, St. Louis, MO) in 100 mM HEPES and 20 mM $NaHCO_3$, pH 8.0 and incubated at 37°C for 1 hour. Excess $NaBD_4$ was removed by passing the treated protein samples through 1 ml Sephadex G-25 (Sigma-Aldrich, St. Louis, MO) spin columns pre-equilibrated with 100 mM HEPES, pH 8.0. The protein concentrations were quantitated using the bicinchoninic acid protein assay, and activity assays were carried out as described above.

For the substrate protection studies, the MtmB was initially pre-incubated for 30 min. in the presence of up to 1 M MMA, followed by reduction with $NaBD_4$.

Similarly, the end product inhibition study was carried out by incubating the enzyme with 100 mM NH_4Cl for 30 min, followed by reduction with $NaBD_4$ for 2 mins. When carrying out the substrate protection or end product protection study, the pre-treated enzymes were then reduced with 500 µM $NaBD_4$.

3.2.10 Cobalamin methylation assay

The direct methylation of cobalamin by MtbB treated with varying concentrations of $NaBD_4$ was carried out under strict anaerobic conditions in an atmosphere of H_2 gas in 2 mm cuvettes as previously developed (Ferguson *et. al.* 2000). The assay was conducted in the presence of 0.5 M DMA, 2.5 mM hydroxocobalamin and 15 mM Ti(III)-citrate in 50 mM MOPS, pH 7.0 in a total volume of 400 µl. The blank included a solution of 0.5 M DMA, 2.5 mM hydroxocobalamin and 100 µg MtbB in 50 mM MOPS, pH 7.0, buffer. Methylation of cobalamin was followed at 540 nm. The specific activities were determined based on the $\Delta\varepsilon$ previously determined to be 4.4 mM^{-1} cm^{-1} for the CH_3-Co(III) form of cobalamin.

3.2.11 Proteolysis by chymotrypsin

Intact protein was first reduced with dithiothreitol then carbamidomethylated with iodoacetamide prior to proteolytic digestion using chymotrypsin (Roche Diagnostic GmbH, Indianapolis, IN). The final buffer conditions for digestion of desalted samples were 25 mM ammonium bicarbonate and 5% acetonitrile. The final ratio of methyltransferase to chymotrypsin was 25:1 (w/w) in a total volume

of 80 µl. The digestion was carried out at 37℃ for 4 hours and stopped by acidification with 1 µl trifluoroacetic acid.

3.2.12 Matrix-assisted laser desorption/ionization (MALDI) mass spectrometry

MALDI-MS of the chymotryptic peptides was performed on a Bruker Reflex III (Bruker, Breman, Germany) mass spectrometer operated in reflectron positive ion mode with an N_2 laser using alpha-cyano-4-hydroxy cinnamic acid as the matrix prepared as a saturated solution in 50% acetonitrile/ 0.1% trifluoroacetic acid (in water). Allotments of 5 µL of matrix and 1 µL of sample were thoroughly mixed together; then 0.5 µL of this mixture was spotted on the target plate and was allowed to dry. Surfactant assisted-MALDI was performed on the digestion products to further increase the number of peptides detected as previously described (Breaux *et. al.* 2000).

3.2.13 Liquid chromatography-tandem mass spectrometry

In order to obtain sequence of individual peptide ions, a Micromass Q-TOF II (Micromass, Wythenshawe, UK) equipped with an orthogonal nanospray source (New Objective, Inc., Woburn, MA) was operated in positive ion mode in conjunction with a Dionex Capillary LC-System (LC Packings-A Dionex Co., Sunnyvale, CA). Samples (2.5 µl) were first injected onto a trapping column (Michrom BioResources, Auburn, CA), were washed with 50 mM acetic acid, then were injected onto a 5 cm long, 75 mm internal diameter ProteoPep II C18 column (New Objective, Inc.) packed directly in the nanospray tip. The column

was then eluted with mobile phase A as 50 mM acetic acid and mobile phase B as acetonitrile. Peptides were eluted directly off the column into the Q-TOF system using a gradient of 2 to 80% B over 45 minutes with a flow rate of 0.3 µl/min. The total run time was 58 minutes. The nanospray capillary voltage was set at 3.0 kV and the cone voltage at 55 V. The source temperature was maintained at 1000°C. Mass spectra were recorded using MassLynx 4.0 with automatic switching functions. Mass spectra were acquired from mass 400 to 2,000 Daltons every 1 second with a resolution of 8,000 (full-width, half-maximum). When the desired peak (using include tables) was detected at a minimum of 15 ion counts, the mass spectrometer automatically switched to acquire a collision induced dissociation (CID) MS/MS spectrum of the individual peptide. Collision energy was set dependent on charge state recognition properties. The PEAKS program from Bioinformatics Solutions was used for MS/MS data processing. Sequence information from the MS/MS data was processed using Mascot Distiller to form a peaklist file. Data was minimally processed with application of a 3 point smoothing function and with the centroid calculated from the top 80% of the peak height. The charge state of each ion selected for MS/MS was calculated, however, the peaks were not deisotoped. Assigned peaks were judged valid only if they had a minimum of 5 counts (S/N of 3) and displayed the corresponding C13 ion. The mass accuracy of the precursor ions were set to 1.2 Da to accommodate accidental selection of the C13 ion and the fragment mass accuracy was set to 0.3 Da. Considered modifications were methionine oxidation and carbamidomethyl cysteine. Pyrrolysine was also

programmed into PEAKS as a modification. The data was acquired several times to ensure reproducibility.

3.3 RESULTS

3.3.1 Effect of $NaBD_4$-treated MtmB and MtbB on CoM methylation

MtmB was treated with $NaBD_4$, an imine bond reductant, at concentrations varying from 200 µM to 20 mM. To maintain consistent concentrations of $NaBD_4$, the solution of $NaBD_4$ was prepared in HEPES buffer (pH 8.0) as $NaBD_4$ is unstable under acidic conditions. The specific activity of MtmB after reduction was then tested by following the loss of the free sulfhydryl of CoM as methyl-CoM was produced. As shown in Table 3.1, the specific activities decreased with increasing concentrations of $NaBD_4$ with activity no longer being detected at a minimum concentration of 2 mM $NaBD_4$. Intermediate concentrations of, 200 µM to 500 µM $NaBD_4$, caused a decrease of approximately 69% and 87% MMA:CoM methyl transfer activity. MtmB supplementation assays were carried out by adding untreated MtmB to the assay vials containing $NaBD_4$-treated MtmB. The specific activities of these samples were observed to be comparable with those of the untreated MtmB sample, approximately 1.6 µmol. min^{-1}. mg^{-1}, which shows that the assay was not affected by $NaBD_4$ in the reaction. The specific activity of the untreated sample was similar to that observed previously (Burke *et. al.* 1997).

Condition	MtmB-dependent CoM methylation Activity (µmol/min.mg)
Untreated MtmB	1.6
MtmB + 0.2 mM $NaBD_4$	0.5
MtmB + 0.5 mM $NaBD_4$	0.2
MtmB + 2 mM $NaBD_4$	N.D.

Table 3.1: Specific activities for CoM methylation of MtmB samples treated with varying concentrations of $NaBD_4$. N.D. in this table and the following tables indicated no detectable activity. The assay vials contained 2.9 µM MtmB, 4 µM MtmC, 5 µM MtbA, and 0.4 µM RAM.

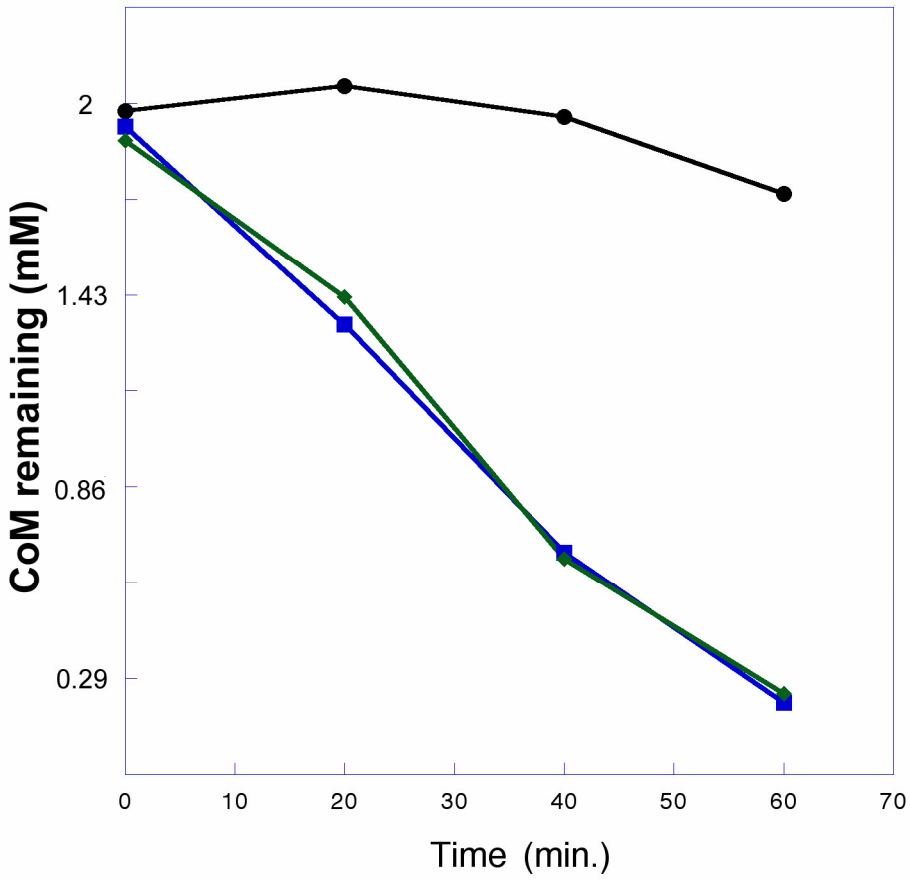

Figure 3.1: CoM methylation assay of MtmB sample treated with 100 mM DTT (diamond) has a specific activity similar to that of the untreated MtmB control (square). A negative control (circle) without MtmB was run.

Sample	MtbB-dependent CoM methylation Activity (µmol/min.mg)
MtbB (untreated)	3.1
MtbB (2 mM $NaBD_4$)	1.68
MtbB (10 mM $NaBD_4$)	N.D.
MtbB (10 mM $NaBD_4$) + MtbB (untreated)	4.1

Table 3.2: Specific activities for CoM methylation of MtmB samples treated with varying concentrations of $NaBD_4$. The assay vials contained 1.4 µM MtmB, 2.5 µM MtbC, 2.0 µM MtbA, and 0.4 µM RAM.

Cobalamin methylation with MtbB samples reduced with 2 mM and 10 mM $NaBD_4$ were also studied. The results corroborated those observed for CoM. $NaBD_4$ is known to reduce disulfide bonds. To test if disulfide bond reduction may play a role in the loss of activity, MtmB was treated with 100 mM DTT. There was no change in specific activity of the enzyme (Figure 3.1).

A similar study was carried out on MtbB. Initially complete inhibition of MtbB treated with 2 mM $NaBD_4$ was observed on DMA:CoM methyl transfer activity. While repeating the experiments, the minimum inhibitory concentration of MtbB with $NaBD_4$ for the complete inhibition of DMA:CoM methyl transfer activity increased to 10 mM $NaBD_4$. This was due to the age of the $NaBD_4$ stock sample used in the experiments. The effect of varying concentrations of $NaBD_4$ on DMA:CoM methyl transfer activity were similar to that on MtmB as shown in Table (Table 3.2). The minimal inhibitory concentration of MtbB activity was found to be approximately 10 mM $NaBD_4$. An intermediate level of activity was observed when MtbB was treated with 2 mM $NaBD_4$ which corresponded with approximately 50% CoM methylation activity as compared to the control.

3.3.2 Effect of $NaBD_4$ on MtbB-dependent direct methylation of cobalamin

Ferguson *et. al.* developed an anaerobic spectrophotometric method for studying the direct methylation of cobalamin by MtbB in the presence of DMA and reductant, Ti(III)-citrate (Ferguson *et. al.* 2000). The direct methylation of cob(I)alamin could be followed spectrophotometrically by an increase in

Sample	Cobalamin Methylation Activity (nmol/min.mg)
MtbB (untreated)	12.2
MtbB (2 mM $NaBD_4$)	4.32
MtbB (10 mM $NaBD_4$)	N.D.
MtbB (10 mM $NaBD_4$) + MtbB (untreated)	10.2

Table 3.3: Specific activities for cob(I)alamin methylation of MtbB samples treated with varying concentrations of $NaBD_4$.

absorbance at 540 nm corresponding to the generation of the CH_3-Co(III)-form of cobalamin. methylation. The specific activity for the control untreated protein on cobalamin methylation was 12.2 nmol.min^{-1}.mg^{-1}. The 2 mM $NaBD_4$-treated MtbB sample showed approximately 50% of the specific activity of the untreated protein, which correlated with the CoM methylation study. As observed in the CoM methylation study for 10 mM $NaBD_4$-treated MtbB, no activity was detectable for the direct methylation of cobalamin. To ensure that the inhibition was not due to the presence of $NaBD_4$ in the cuvette, untreated MtbB was added to a vial containing 10 mM $NaBD_4$-treated MtbB, and activity was restored to the specific activity expected for the amount of untreated MtbB added (Table 3.3).

Once again, the minimum inhibitory concentration of $NaBD_4$ on the cobalamin methylation activity of MtbB increased with the age of the $NaBD_4$ stock sample.

3.3.3 Studying the overall modification of MtmB and MtbB with $NaBD_4$ by electrospray mass spectrometry

To study the overall modification of MtmB with 2 mM $NaBD_4$, the total mass of the protein was measured by electrospray. The molecular mass of untreated MtmB was found to be 50,114 ± 2 Da as compared with 50,117 ± 2 Da for the $NaBD_4$-treated MtmB sample (Figure 3.2 and Figure 3.3). The mass difference of an average of 3 Da is consistent with the specific reduction of the imine bond of pyrrolysine. Similarly, the molecular mass of untreated MtbB was found to be 50,092 ± 2 Da as compared with 50,094 ± 2 Da (Figure 3.4 and

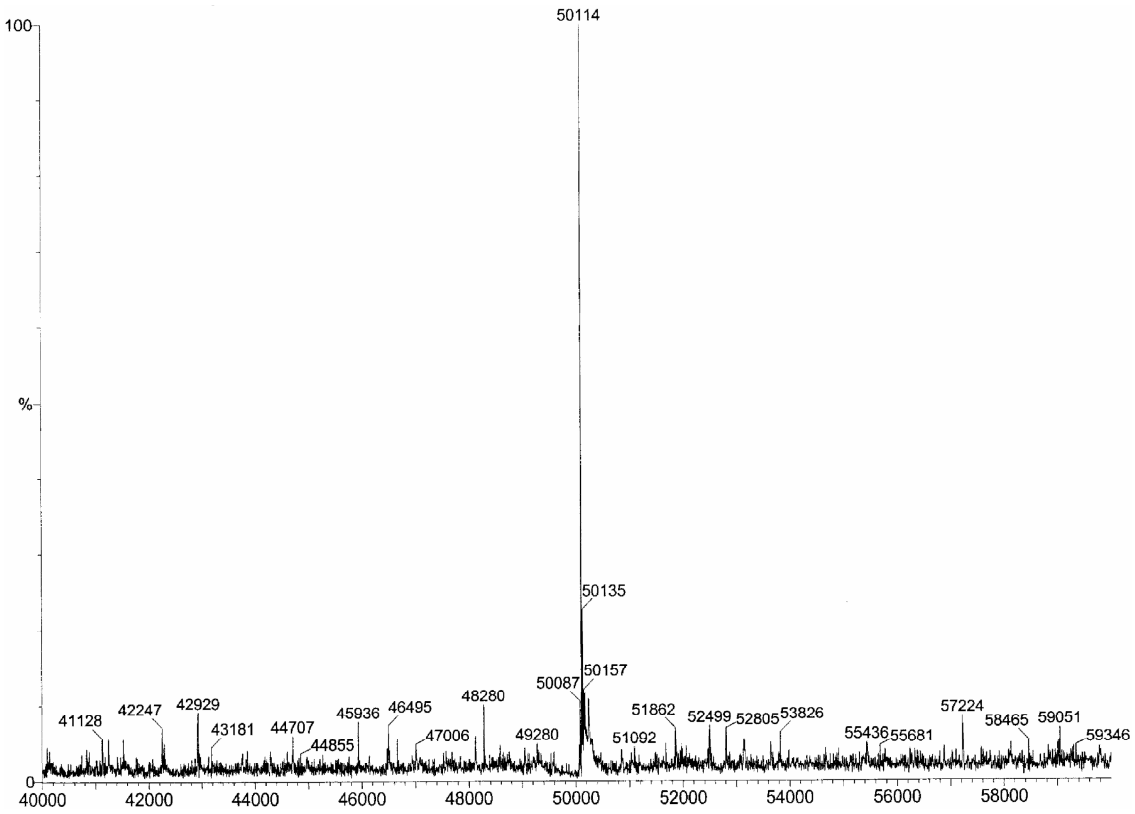

Figure 3.2: The mass of MtmB (untreated) is 50,114 Da as detected by electrospray mass spectrometry. The mass has an experimental error of +/- 2 Da.

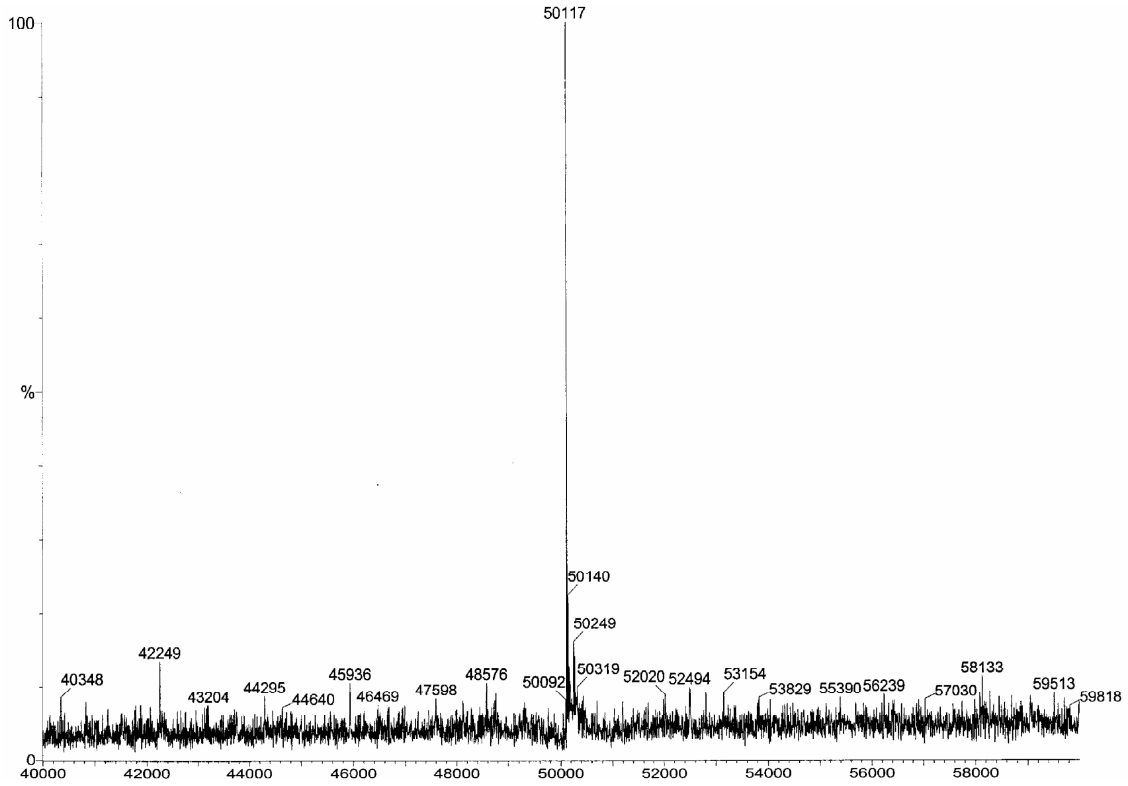

Figure 3.3: The mass of MtmB treated with 2 mM $NaBD_4$ is observed to be 50117 Da as detected by electrospray mass spectrometry. The mass has an experimental error of +/- 2 Da. A mass increase of 3 Da was observed in comparison with the MtmB control.

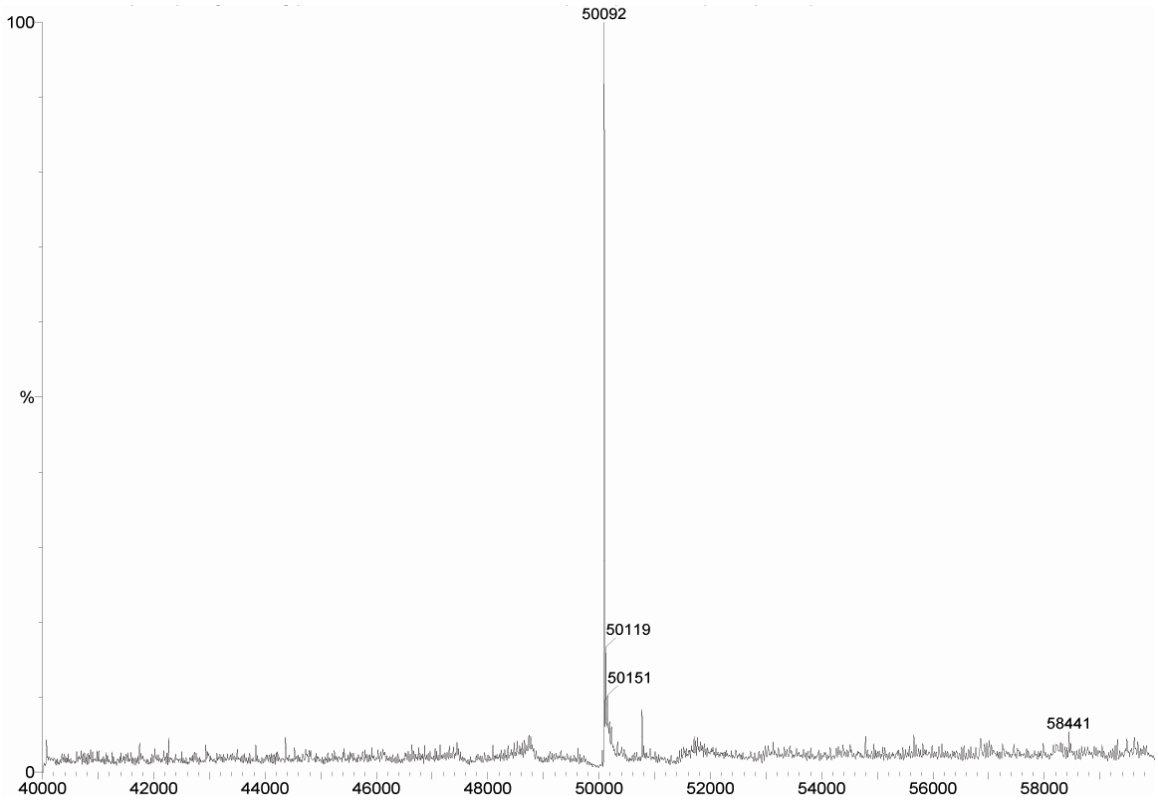

Figure 3.4: The mass of native MtbB (untreated) was observed to be 50,092 Da as detected by electrospray mass spectrometry. The mass has an experimental error of +/- 2 Da.

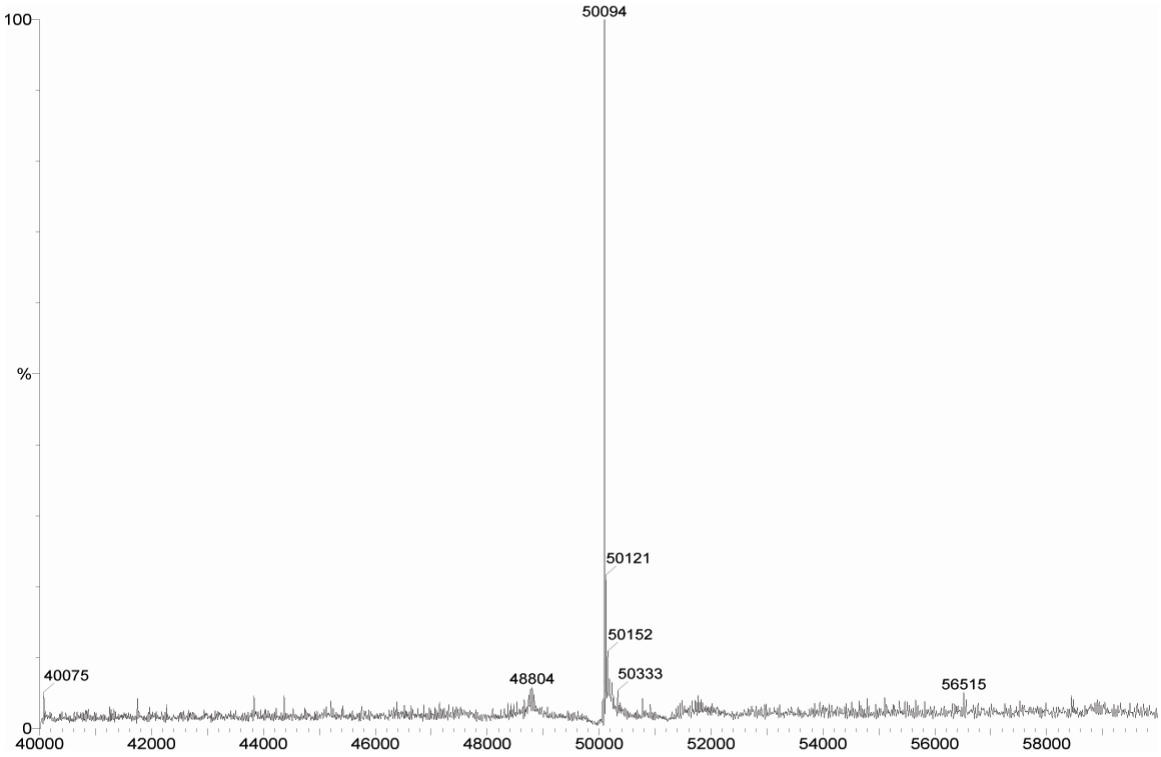

Figure 3.5: The mass of native MtbB treated with 2 mM $NaBD_4$ observed as 50,094 Da as detected by electrospray mass spectrometry. The mass has an experimental error of +/- 2 Da.

Figure 3.6: Enzymatic map of peptides detected by mass spectrometry following chymotryptic digestion of MtmB. The residues whose masses were observed are highlighted in blue. A. Coverage map of the untreated MtmB, B. Coverage map of the 2 mM $NaBD_4$-treated MtmB sample, and C. Coverage map showing the residues detected in both control and 2 mM $NaBD_4$-treated MtmB.

A. MtmB untreated (384/458) = 84%

1 MTFRKSFDCYDFYDRAKVGEKCTQDDWDLMKIPMKAMELKQKYGLDFKGE
51 FIPTDKDMMEKLFKAGFEMLLECGIYCTDTHRIVKYTEDEIWDAINNVQK
101EFVLGTGRDAVNVRKRSVGDKAKPIVQGGPTGSPISEDVFMPVHMSYALE
151 KEVDTIVNGVMTSVRGKSPIPKSPYEVLAAKTETRLIKNACAMAGRPGMG
200 VOGPETSLSAQGNISADCTGGMTCTDSHEVSQLNELKIDLDAISVIAHYK
251 GNSDIIMDEQMPIFGGYAGGIEETTIVDVATHINAVLMSSASWHLDGPVH
301 IRWGSTNTRETLMIAGWACATISEFTDILSGNQYYPCAGPCTEMCLLEAS
351 AQSITDTASGREILSGVASAKGVVTDKTTGMEARMMGEVARATAGVEISE
400 VNVILDKLVSLYEKNYASAPAGKTFQECYDVKTVTPTEEYMQVYDGARKK
451 LEDLGLVF

B. MtmB treated with $NaBD_4$ (375/458) = 82%

1 MTFRKSFDCYDFYDRAKVGEKCTQDDWDLMKIPMKAMELKQKYGLDFKGE
51 FIPTDKDMMEKLFKAGFEMLLECGIYCTDTHRIVKYTEDEIWDAINNVQK
101EFVLGTGRDAVNVRKRSVGDKAKPIVQGGPTGSPISEDVFMPVHMSYALE
151 KEVDTIVNGVMTSVRGKSPIPKSPYEVLAAKTETRLIKNACAMAGRPGMG
200 VOGPETSLSAQGNISADCTGGMTCTDSHEVSQLNELKIDLDAISVIAHYK
251 GNSDIIMDEQMPIFGGYAGGIEETTIVDVATHINAVLMSSASWHLDGPVH
301 IRWGSTNTRETLMIAGWACATISEFTDILSGNQYYPCAGPCTEMCLLEAS
351 AQSITDTASGREILSGVASAKGVVTDKTTGMEARMMGEVARATAGVEISE
400 VNVILDKLVSLYEKNYASAPAGKTFQECYDVKTVTPTEEYMQVYDGARKK
451 LEDLGLVF

C. Peptides covered by Control and $NaBD_4$-treated MtmB (364/458) = 79.5%

1 MTFRKSFDCYDFYDRAKVGEKCTQDDWDLMKIPMKAMELKQKYGLDFKGE
51 FIPTDKDMMEKLFKAGFEMLLECGIYCTDTHRIVKYTEDEIWDAINNVQK
101EFVLGTGRDAVNVRKRSVGDKAKPIVQGGPTGSPISEDVFMPVHMSYALE
151 KEVDTIVNGVMTSVRGKSPIPKSPYEVLAAKTETRLIKNACAMAGRPGMG
200 VOGPETSLSAQGNISADCTGGMTCTDSHEVSQLNELKIDLDAISVIAHYK
251 GNSDIIMDEQMPIFGGYAGGIEETTIVDVATHINAVLMSSASWHLDGPVH
301 IRWGSTNTRETLMIAGWACATISEFTDILSGNQYYPCAGPCTEMCLLEAS
351 AQSITDTASGREILSGVASAKGVVTDKTTGMEARMMGEVARATAGVEISE
400 VNVILDKLVSLYEKNYASAPAGKTFQECYDVKTVTPTEEYMQVYDGARKK
451 LEDLGLVF

Figure 3.5). The data was within the range of specific reduction of the imine bond of pyrrolysine. The overall molecular mass of the samples are comparable with the theoretical molecular mass of MtbB1 which is 50,094 Da as calculated by PeptideMass on the ExPAsy website. The mass was calculated with the C-4 substituent of pyrrolysine being a methyl group as previously determined (Soares *et al.* 2005). The electrospray data is consistent with the presence of pyrrolysine in MtbB.

3.3.4 Reduction of the imine bond of pyrrolysine by $NaBD_4$ in MtmB is specific as detected by mass spectrometry

In order to determine the site of modification of the $NaBD_4$-treated MtmB, the samples were digested with chymotrypsin in 5% acetonitrile using a previously determined protocol. The masses of the peptides generated were determined by LC-MS/MS. Sequence coverage of untreated MtmB was 84% and that of the $NaBD_4$- treated MtmB was 82% as shown in Figure. 3.6. Overlapping sequence coverage of these two samples allowed for the comparison of 79.5% of the residues of MtmB. Importantly, the ^{194}AGRPGMGVOGPETSL^{208} peptide masses were determined in both the untreated as well as $NaBD_4$-treated samples. A peptide *m/z* 783.58^{2+} was observed for the untreated MtmB whereas a *m/z* 785.1^{2+} peptide was observed in the modified sample. Thus, a net mass increase of 3.04 Da was seen to correspond to this peptide (Table 3.4 and Table 3.5). Amongst the peptides observed, no significant mass difference was observed for any other peptide in $NaBD_4$-treated MtmB. In the untreated sample,

Table 3.4: List of predicted and observed *m/z* values of peptides generated by chymotrypsin-digested MtmB and detected by LC-MS/MS. The protein was modified by iodoacetamide before protein digestion, and the carbamidomethylated cysteine residues are indicated (CAM). Methionine residues are prone to oxidation, and therefore, the methionine residues detected as oxidized are indicated (OX). Two ions, m/z = 783.58^{2+} and m/z = 522.72^{3+} were observed for peptide AGRPGMGVOGPETSL covering the pyrrolysyl-residue.

Table 3.4

Measured *m/z*	Measured Mass	Theoretical Mass	Mass difference	Peptide
410.64^{3+}	1229.92	1229.6538	0.266	HLDGPVHIRW
409.83^{2+}	818.66	818.4627	0.197	KIPMKAM
425.32^{2+}	849.64	849.4465	0.194	ASAPAGKTF
432.79^{2+}	864.58	864.37	0.21	MPVHMSY
488.33^{2+}	975.66	975.4353	0.225	RKSFDC(CAM)Y
530.91^{2+}	1060.82	1060.5893	0.231	KIPMKAMEL
555.39^{2+}	1109.78	1109.5255	0.255	GSTNTRETLM
560.09^{3+}	1678.27	1677.8774	0.393	AAKTETRLIKNAC(CAM)AM
615.46^{2+}	1229.92	1229.6538	0.266	HLDGPVHIRW
620.15^{3+}	1858.45	1858.0432	0.407	TSVRGKSPIPKSPYEVL
651.11^{3+}	1951.33	1950.9079	0.422	TEDEIWDAINNVQKEF
670.97^{2+}	1340.94	1340.6402	0.3	AC(CAM)ATISEFTDIL
692.5^{2+}	1384.00	1383.6903	0.31	EKNYASAPAGKTF
699.5^{3+}	2096.5	2096.0474	0.453	SGVASAKGVVTDKTTGMEARM
708.06^{2+}	1415.12	1415.6333	0.513	M(OX)IAGWACATISEF
715.47^{2+}	1429.94	1429.6416	0.298	ASAPAGKTFQEC (CAM)Y
729.55^{2+}	1458.1	1457.7998	0.3	KIDLDAISVIAHY
759.56^{2+}	1518.12	1517.7879	0.332	ALEKEVDTIVNGVM
769.04^{2+}	1537.08	1536.7475	0.333	GSTNTRETLMIAGW
781.1^{2+}	1561.2	1560.8744	0.326	DGARKKLEDLGLVF
783.58^{2+}	1566.16	1565.8096	0.35	**AGRPGMGVOGPETSL**
787.88^{3+}	2361.64	2361.1505	0.49	GLDFKGEFIPTDKDMMEKLF
805.09^{2+}	1609.18	1608.8261	0.354	SGVASAKGVVTDKTTGM
825.03^{2+}	1649.06	1648.7100	0.35	TFRKSFDC(CAM)YDFY
831.54^{3+}	2492.62	2492.0856	0.534	DFYDRAKVGEKC(CAM)TQDDWDLM
839.63^{2+}	1678.26	1677.8774	0.383	AAKTETRLIKNAC(CAM)AM
875.12^{2+}	1749.24	1748.8661	0.374	EASAQSITDTASGREIL
902.1^{2+}	1803.2	1802.8517	0.348	DVKTVTPTEEYMQVY
907.68^{2+}	1814.36	1813.9694	0.391	NELKIDLDAISVIAHY
916.03^{3+}	2746.09	2745.5032	0.587	GEVARATAGVEISEVNVILDKLVSLY
929.72^{2+}	1858.44	1858.0432	0.397	TSVRGKSPIPKSPYEVL
945.64^{2+}	1890.28	1889.8585	0.422	AC(CAM)ATISEFTDILSGNQY
957.17^{2+}	1913.34	1913.9248	0.585	LECGIYCTDTHRIVKY
959.72^{3+}	2877.16	2876.5437	0.616	MGEVARATAGVEISEVNVILDKLVSLY

Table 3.4 continued

Measured *m/z*	Measured Mass	Theoretical Mass	Mass change	Peptide
976.16^{2+}	1951.32	1950.9079	0.412	TEDEIWDAINNVQKEF
994.96^{3+}	2982.88	2982.2510	0.629	SAQGNISADC(CAM)TGGMTC(CAM)TD SHEVSQLNEL
1012.25^{2+}	2023.5	2023.0705	0.43	AGGIEETTIVDVATHINAVL
1019.64^{3+}	3056.92	3056.2780	0.642	AC(CAM)ATISEFTDILSGNQYYPC(CAM) AGPC(CAM)TEM
1031.29^{2+}	2061.58	2062.8555	1.276	TDILSGNQYYPCAGPCTEM
1034.18^{2+}	2067.36	2066.9270	0.433	DRAKVGEKC(CAM)TQDDWDLM
1068.26^{2+}	2135.52	2135.0648	0.455	C(CAM)LLEASAQSITDTASGREIL
1072.05^{3+}	3214.15	3213.4754	0.675	ASAPAGKTFQEC(CAM)YDVKTVTPTEE YMQVY
1075.73^{3+}	3225.19	3224.5316	0.659	C(CAM)TDTHRIVKYTEDEIWDAINNVQK EF
1077.76^{3+}	3231.28	3230.3859	0.894	ACATISEFTDILSGNQYYPC AGPCTEM(OX)CLL
1181.32^{2+}	2361.64	2361.1505	0.49	GLDFKGEFIPTDKDMMEKLF
1192.28^{2+}	2383.56	2383.0468	0.513	QEC(CAM)YDVKTVTPTEEYMQVY
1246.81^{2+}	2492.62	2492.0856	0.534	DFYDRAKVGEKC(CAM)TQDDWDLM
1373.55^{2+}	2746.1	2745.5032	0.597	GEVARATAGVEISEVNVILDKLVSLY
1491.97^{2+}	2982.94	2982.2510	0.689	SAQGNISADC(CAM)TGGMTC(CAM)TD SHEVSQLNEL
521.07^{3+}	1561.21	1560.8744	0.336	DGARKKLEDLGLVF
522.72^{3+}	1566.16	1565.8096	0.350	**AGRPGMGVOGPETSL**
538.92^{2+}	1076.84	1076.5791	0.261	KIPMKAM(OX)EL

TABLE 3.5: List of predicted and observed m/z values of peptides generated by chymotrypsin-digested MtmB treated with 2 mM $NaBD_4$ and detected by LC-MS/MS. The protein was modified by iodoacetamide before protein digestion, and the carbamidomethylated cysteine residues are indicated (CAM). Methionine residues are prone to oxidation, and therefore, the methionine residues detected as oxidized are indicated (OX). One peptide m/z = 785.1^{2+} was observed for peptide AGRPGMGVOGPETSL covering the pyrrolysyl-residue. No peptide corresponding to the mass of unmodified AGRPGMGVOGPETSL was observed.

Table 3.5

Measured *m/z*	Observed Mass (Da)	Predicted Mass (Da)	Mass Difference (Da)	Peptide
410.63^{3+}	1229.89	1229.6538	0.236	HLDGPVHIRW
425.32^{2+}	849.64	849.4465	0.194	ASAPAGKTF
432.79^{2+}	864.58	864.37	0.21	MPVHMSY
472.71^{3+}	1416.13	1416.5666	0.437	YPCAGPCTEM(OX)CLL
486.7^{3+}	1459.1	1459.7579	0.658	KQKYGLDFKGEF
488.33^{2+}	975.66	975.4353	0.225	RKSFDC(CAM)Y
530.92^{2+}	1060.84	1060.5893	0.251	KIPMKAMEL
555.37^{2+}	1109.74	1109.5255	0.215	GSTNTRETLM
560.07^{3+}	1678.21	1677.8774	0.333	AAKTETRLIKNAC(CAM)AM
612.42^{2+}	1223.84	1223.5513	0.289	TFRKSFDC(CAM)Y
615.45^{2+}	1229.9	1229.6538	0.246	HLDGPVHIRW
620.13^{3+}	1858.39	1858.0432	0.347	TSVRGKSPIPKSPYEVL
651.13^{3+}	1951.39	1950.9079	0.482	TEDEIWDAINNVQKEF
670.98^{2+}	1340.96	1340.6402	0.32	AC(CAM)ATISEFTDIL
690.11^{3+}	2068.33	2066.9270	1.423	DRAKVGEKC(CAM)TQDDWDLM
708.54^{2+}	1416.08	1415.6333	0.447	M(OX)IAGWACATISEF
715.45^{2+}	1429.9	1429.6416	0.258	ASAPAGKTFQEC(CAM)Y
729.54^{2+}	1458.08	1457.7998	0.28	KIDLDAISVIAHY
759.52^{2+}	1518.04	1517.7879	0.252	ALEKEVDTIVNGVM
769.03^{2+}	1537.06	1536.7475	0.313	GSTNTRETLMIAGW
781.1^{2+}	1561.2	1560.8744	0.326	DGARKKLEDLGLVF
785.1^{2+}	1569.2	1565.8096	3.39	**AGRPGMGVOGPETSL**
788.21^{3+}	2362.63	2363.1443	0.514	MPVHMSYALEKEVDTIVNGVM
805.08^{2+}	1609.16	1608.8261	0.334	SGVASAKGVVTDKTTGM
839.62^{2+}	1678.24	1677.8774	0.363	AAKTETRLIKNAC(CAM)AM
875.13^{2+}	1749.26	1748.8661	0.394	EASAQSITDTASGREIL
902.12^{2+}	1803.24	1802.8517	0.388	DVKTVTPTEEYMQVY
916.34^{3+}	2747.02	2747.3834	0.363	HLDGPVHIRWGSTNTRETLM IAGW
930.22^{2+}	1859.44	1858.0432	1.397	TSVRGKSPIPKSPYEVL

Table 3.5 continued

Measured *m/z*	Observed Mass (Da)	Predicted Mass (Da)	Mass Difference (Da)	Peptide
960.04^{3+}	2878.12	2876.5437	1.576	MGEVARATAGVEISEVN VILDKLVSLY
976.71^{2+}	1952.42	1951.0647	1.355	QVYDGARKKLEDLGLVF
995.05^{3+}	2983.15	2982.2510	0.899	SAQGNISADC(CAM)TGG MTC(CAM)TDSHE VSQLNEL
1010.72^{2+}	2020.44	2019.0725	1.368	EVLAAKTETRLIKNAC(CA M)AM
1012.76^{2+}	2024.52	2023.0705	1.45	AGGIEETTIVDVATHINAV L
1019.97^{3+}	3057.91	3058.5958	0.686	AAKTETRLIKNACAMAG RPG MGVKGPETSL
1031.79^{2+}	2062.58	2062.8555	0.276	TDILSGNQYYPCAGPCT EM
1034.7^{2+}	2068.4	2066.9270	1.473	DRAKVGEKC(CAM)TQD DWDLM
1068.74^{2+}	2136.48	2135.0648	1.415	C(CAM)LLEASAQSITDTA SGREIL
1078.23^{3+}	3232.69	3232.6915	0.001	EARMMGEVARATAGVEI SEV NVILDKLVSL
1078.23^{2+}	2155.46	2154.1110	1.389	AGGIEETTIVDVATHINAV LM
1089.68^{2+}	2178.36	2179.0119	0.652	IPTDKDM(OX)M(OX)EKL FKAGFEM(OX)
1181.84^{2+}	2362.68	2363.1443	0.464	MPVHMSYALEKEVDTIV NGVM
1192.77^{2+}	2384.54	2383.0468	1.493	QEC(CAM)YDVKTVTPTE EYMQVY
1374.08^{2+}	2747.16	2747.3834	0.223	HLDGPVHIRWGSTNTRE TLMIAGW
700.94^{2+}	1400.88	1400.5939	0.286	RKSFDC(CAM)YDFY
729.54^{2+}	1458.08	1457.7998	0.28	KIDLDAISVIAHY
743.52^{3+}	2228.56	2227.0879	1.472	SGVASAKGVVTDKTTGM EARMM
891.63^{2+}	1782.26	1781.8812	0.379	KGEFIPTDKDMMEKL
931.61^{2+}	1863.22	1861.8160	1.404	QEC(CAM)YDVKTVTPTE EY
1114.28^{2+}	2228.56	2227.0879	1.472	SGVASAKGVVTDKTTGM EARMM
1439.59^{2+}	2878.18	2876.5437	1.636	MGEVARATAGVEISEVN VILDKLVSLY

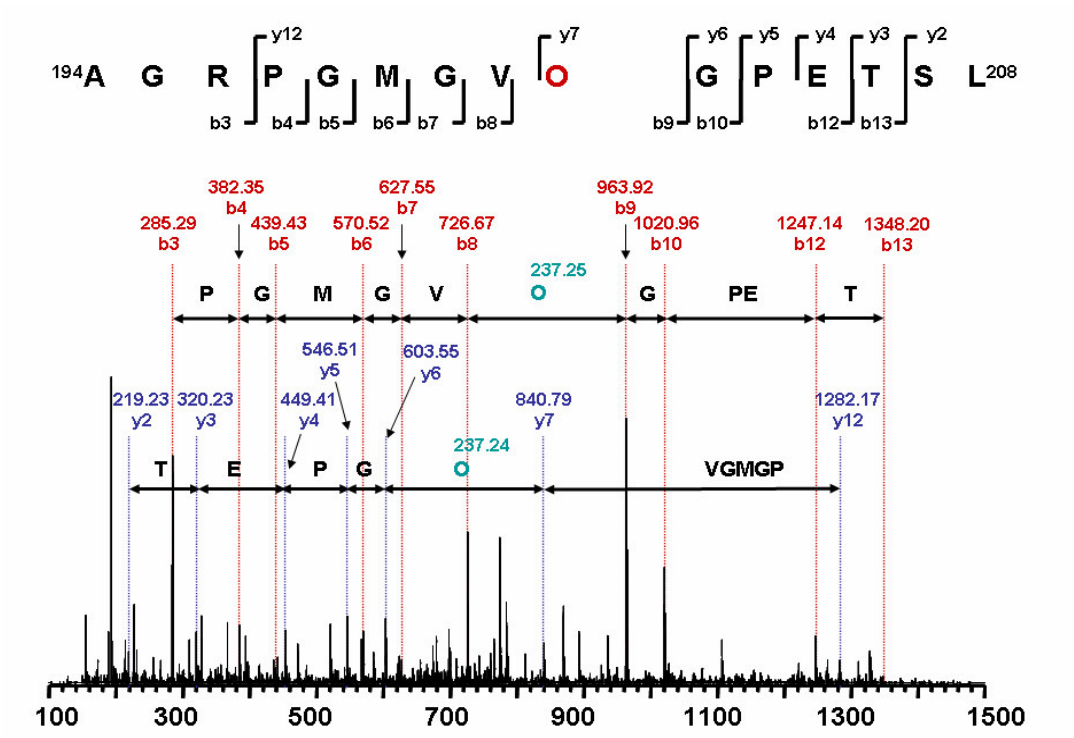

Figure 3.7: Collision-Induced Dissociation Spectrum of *m/z* = 783.58^{2+} of MtmB (untreated) sample.

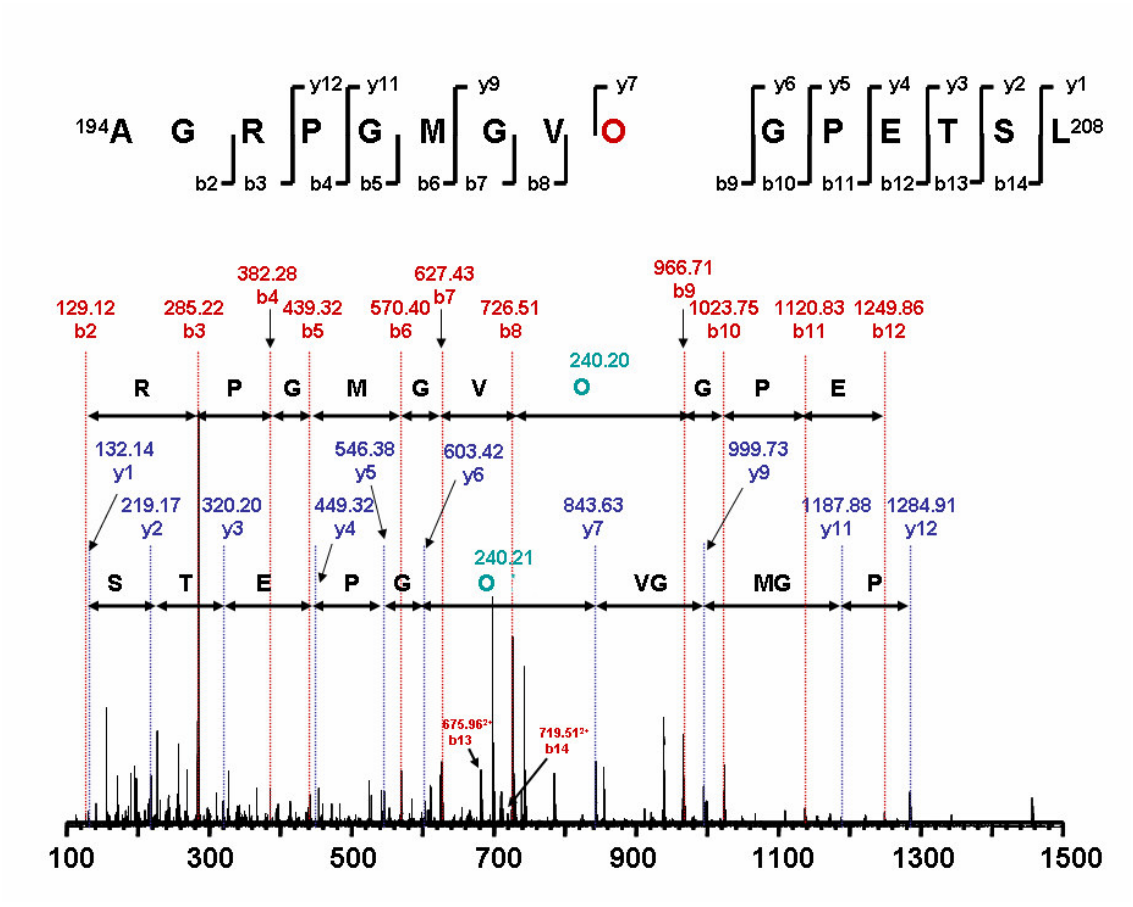

Figure 3.8: Collision-Induced Dissociation Spectrum of *m/z* = 785.1^{2+} of the MtmB sample treated with 2 mM $NaBD_4$

y-ion type	Observed *m/z* (M+H)	Sequence	Observed *m/z* (M+H)	b-ion type
		Ala		
		Gly		
		Arg	285.29	b-3
y-12	1282.17	Pro	382.35	b-4
		Gly	439.43	b-5
		Met	570.52	b-6
		Gly	627.55	b-7
		Val	726.67	b-8
y-7	840.79	Pyrrolysine	963.92	b-9
y-6	603.55	Gly	1020.96	b-10
y-5	546.51	Pro		
y-4	449.41	Glu	1247.14	b-12
y-3	320.23	Thr	1348.20	b-13
y-2	219.23	Ser		
		Leu		

Table 3.6: A list of b- and y-ions detected upon Collision Induced Dissociation of the chymotryptic peptide *m/z* = 783.58^{2+} of the MtmB.

y-ion type	Observed *m/z* (M+H)	Sequence	Observed *m/z* (M+H)	b- ion type
		Ala		
		Gly	129.12	b-2
		Arg	285.22	b-3
y-12	1284.91	Pro	382.28	b-4
y-11	1187.88	Gly	439.32	b-5
		Met	570.40	b-6
y-9	999.73	Gly	627.43	b-7
		Val	726.51	b-8
y-7	843.63	Pyrrolysine	966.71	b-9
y-6	603.42	Gly	1023.75	b-10
y-5	546.38	Pro	1120.83	b-11
y-4	449.32	Glu	1249.86	b-12
y-3	320.20	Thr	(1350.92) 675.96^{2+}	b-13
y-2	219.17	Ser	(1438.02) 719.51^{2+}	b-14
y-1	132.14	Leu		

Table 3.7: A list of b- and y-ions detected by Collision Induced Dissociation mass spectrometry of the chymotryptic peptide *m/z* 785.1^{2+} obtained from the MtmB treated with 2 mM $NaBD_4$.

a second peptide in $NaBD_4$-treated MtmB. In the untreated sample, a second peptide *m/z* 522.72^{3+} was observed consistent with the theoretical mass of the peptide containing unmodified pyrrolysine. The collision-induced dissociation spectra of both *m/z* 783.58^{2+} and *m/z* 785.1^{2+} were studied to determine the site of modification (Figure 3.7 and Figure 3.8). The data confirmed the identity of the peptide being studied as that of the ^{194}AGRPGMGVOGPETSL^{208} peptide fragment. The b- and y- ions of both peptides are listed in Table 3.6. The difference in the b8/b9 ions allowed for the measurement of the pyrrolysine residue in the control sample as 237.25 Da, which is consistent with the previously determined mass of pyrrolysine. Also on studying the y-ion series of this sample, a mass of 237.24 Da was deduced for pyrrolysine. This was done by calculating the difference between the y7 and y12 ion, and accounting for the masses of the other residues in between, i.e., a valine, two glycine residues and a methionine. The difference in mass of the b8/b9 pair of the m/z 785.1^{2+} peptide allowed for the measurement of pyrrolysine as being 240.20 Da (Table 3.7), a mass difference of 2.95 Da as compared with the control. The y-ion series allowed for a second determination of this residue mass. Utilizing the masses of the y7 and y9 ions, the mass of pyrrolysine was determined to be 240.21 Da after accounting for the mass of valine. This showed a modification of 2.97 Da on pyrrolysine in the modified sample. No other residue was found to have any significant mass difference from the predicted mass, thus showing that pyrrolysine was the only detectable site of modification in the peptide map.

An MtmB sample was prepared such that it contained a 1:1 mixture of MtmB that had been treated with 20 mM $NaBD_4$ and untreated MtmB. This mixture was subjected to digestion with chymotrypsin, and relative intensities of the peaks corresponding to the ^{194}AGRPGMGVOGPETSL^{208} peptide were studied (Figure 3.9). Two peaks, *m/z* 783.58^{2+} and *m/z* 785.09^{2+} of approximately the same intensity were observed. The collision-induced dissociation spectra of the *m/z* 783.58^{2+} ion showed the presence of unmodified pyrrolysine with a mass of 237.21 Da using the y-ion series for measurement, and 237.16 Da when utilizing the difference in the masses of the b8/b9 ion pair (Figure 3.10). The determination of the mass of pyrrolysine using the y-ion series was accomplished by theoretical calculation accounting for the mass of a valine and a glycine residue as a control experiment as the difference in the y7 and y10 ions were used to determine the mass of pyrrolysine. The difference in the masses of the b8/b9 ion pair of the *m/z* 785.09^{2+} peptide was found to be 240.19 Da, and the y-ion series measured the mass of pyrrolysine as 240.22 Da. For the determination of the mass of pyrrolysine from the y-ion series of the *m/z* 785.09^{2+} peptide, the difference in mass between the y7 and y9 ions was measured and the mass of a valine residue was accounted for in the measurement. Thus both reduced and unreduced peptides were detected in an experiment when the two samples were mixed. This experiment demonstrates that only one species of pyrrolysine-containing peptide was truly detected, i.e., only modified pyrrolysine-containing peptide in the $NaBD_4$-treated sample, and only the unmodified pyrrolysine-containing peptide in the untreated sample.

3.3.5 The imine bond of pyrrolysine is the only detectable modification observed following the reduction of MtbB with $NaBD_4$

In order to determine the site of modification of the $NaBD_4$-treated MtbB, the samples were digested with chymotrypsin in 5% acetonitrile using a previously determined protocol in 5% acetonitrile. The masses of the peptides generated were studied by LC-MS/MS. Sequence coverage of untreated MtbB was 87.6% and that of the 10 mM $NaBD_4$-treated MtbB was 90.6% (Figure 3.11). A high percentage of the sequence coverage in both samples overlapped (85.4%), allowing for a direct comparison of peptide masses from the untreated and reduced sample. Importantly, a peptide mass *m/z* 871.42^{3+} corresponding with the peptide ^{347}VEIAGVDGIOIGVGDPLGMPIAHIM^{371} (where "O" is pyrrolysine) which includes pyrrolysine at position 356, was observed for the untreated MtbB sample (Table 3.8). However, this peptide mass was not observed for the 10 mM $NaBD_4$-treated MtbB sample, but was replaced by a peptide mass *m/z* 872.45^{3+} corresponding with the mass of the aforementioned peptide containing pyrrolysine in the reduced form (Table 3.9). A comparison of the data showed a mass increase of precisely 3.09 Da for the ^{347}VEIAGVDGIOIGVGDPLGMPIAHIM^{371} peptide when reduced with 10 mM $NaBD_4$. This corresponded closely to the expected 3 Da mass increase expected for a specific reduction of pyrrolysine with $NaBD_4$. No significant mass difference was observed for any of the other peptides.

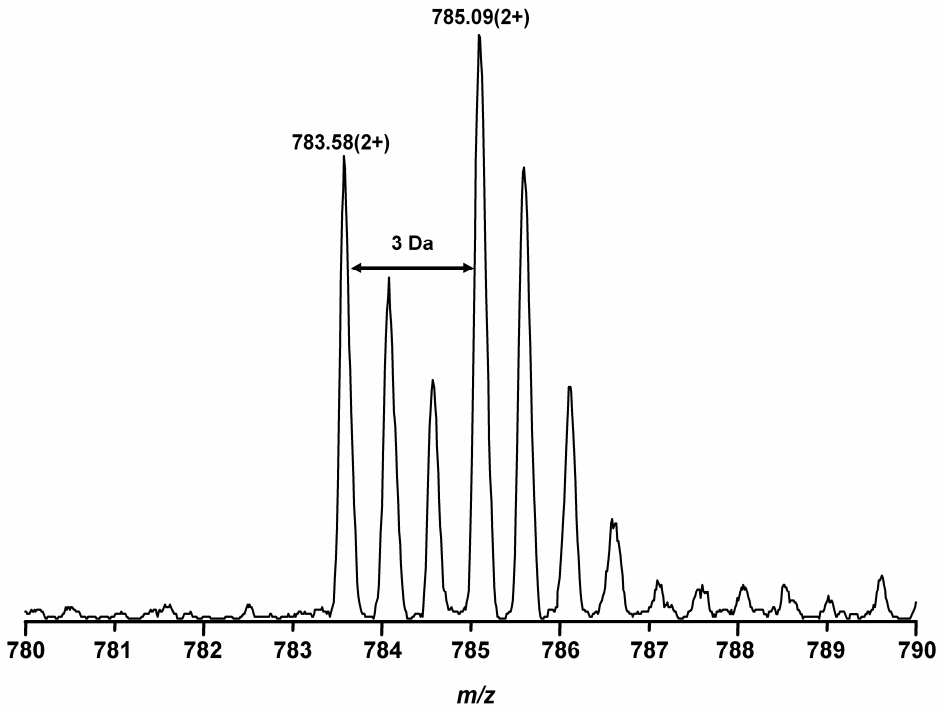

Figure 3.9: Electrospray of chymotrypsin-digested 1:1 mixture of MtmB (untreated) and MtmB (+ 2 mM $NaBD_4$). The peptides indicated are those corresponding to the pyrrolysine-containing peptides (as confirmed by collision-induced dissociation in Figure 3.10).

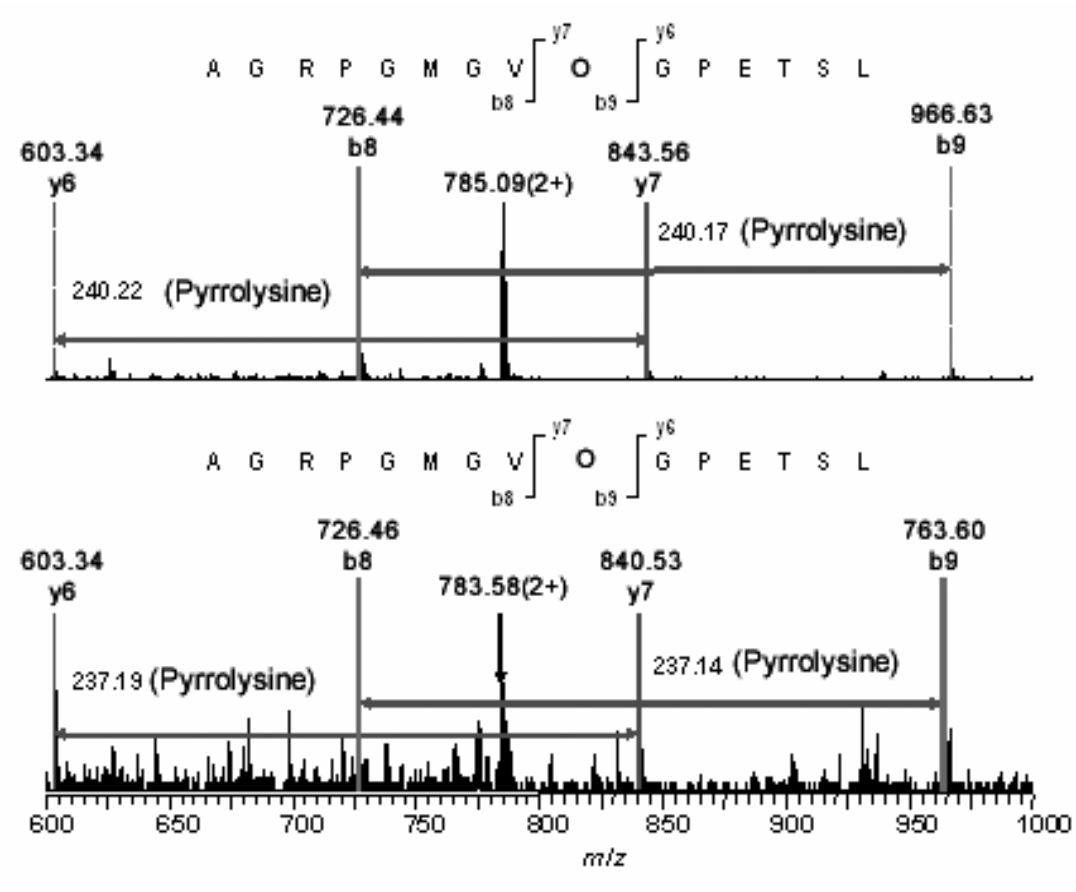

Figure 3.10: The collision-induced dissociation spectra for the pyrrolysine-containing peptides *m/z* 785.09^{2+} and *m/z* 783.58^{2+}, the peptides observed in Figure 3.9. The spectra confirms the identity of the two peptides as being pyrrolysine-containing peptides; one in the reduced form (above) and the other being that of the unreduced form (below).

Figure 3.11: Enzymatic map of peptides detected by mass spectrometry following chymotryptic digestion of MtbB. The residues whose masses were observed are highlighted in blue. A. Coverage map of the untreated MtbB, B. Coverage map of the 10 mM $NaBD_4$-treated MtbB sample, and C. Coverage map showing the peptides covered in both control and 10 mM $NaBD_4$-treated MtbB.

A. MtbB untreated (409/467) = 87.6%

1 MATEYALRMG DGKRVYLTKE KIVSEIEAGT ADAADLGEIP ALSANEMDKL
51 AEILMMPGKT VSVEQGMEIP VTHDIGTIRL DGDQGNSGVG IPSSRLVGCM
101 THERAFGADT MELGHIDYSF KPVKPVVSNE CQAMEVCQQN MVIPLFYGAM
151 PNMGLYYTPD GPFENPGDLM KAFKIQEAWE SMEHAAEHLT RDTVWVMQKL
201 FASGADGVNF DTTGAAGDGD MYGTLHAIEA LRKEFPDMYI EAGMAGECVL
251 GMHGNLQYDG VTLAGLWPHQ QAPLVAKAGA NVFGPVCNTN TSKTSAWNLA
301 RAVTFMKAAV EASPIPCHVD MGMGVGGIPM LETPPIDAVT RASKAMVEIA
351 GVDGIOIGVG DPLGMPIAHI MASGMTGMRA AGDLVARMEF SKNMRIGEAK
401 EYVAKKLGVD KMDLVDEHVM RELREELDIG IITSVPGAAK GIAAKMNIEK
451 LLDIKINSCN LFRKQIA

B. MtbB treated with $NaBD_4$ (423/467) = 90.6%

1 MATEYALRMG DGKRVYLTKE KIVSEIEAGT ADAADLGEIP ALSANEMDKL
51 AEILMMPGKT VSVEQGMEIP VTHDIGTIRL DGDQGNSGVG IPSSRLVGCM
101 THERAFGADT MELGHIDYSF KPVKPVVSNE CQAMEVCQQN MVIPLFYGAM
151 PNMGLYYTPD GPFENPGDLM KAFKIQEAWE SMEHAAEHLT RDTVWVMQKL
201 FASGADGVNF DTTGAAGDGD MYGTLHAIEA LRKEFPDMYI EAGMAGECVL
251 GMHGNLQYDG VTLAGLWPHQ QAPLVAKAGA NVFGPVCNTN TSKTSAWNLA
301 RAVTFMKAAV EASPIPCHVD MGMGVGGIPM LETPPIDAVT RASKAMVEIA
351 GVDGIOIGVG DPLGMPIAHI MASGMTGMRA AGDLVARMEF SKNMRIGEAK
401 EYVAKKLGVD KMDLVDEHVM RELREELDIG IITSVPGAAK GIAAKMNIEK
451 LLDIKINSCN LFRKQIA

C. Peptides covered by untreated and $NaBD_4$-treated MtbB (399/467) = 85.4%

1 MATEYALRMG DGKRVYLTKE KIVSEIEAGT ADAADLGEIP ALSANEMDKL
51 AEILMMPGKT VSVEQGMEIP VTHDIGTIRL DGDQGNSGVG IPSSRLVGCM
101 THERAFGADT MELGHIDYSF KPVKPVVSNE CQAMEVCQQN MVIPLFYGAM
151 PNMGLYYTPD GPFENPGDLM KAFKIQEAWE SMEHAAEHLT RDTVWVMQKL
201 FASGADGVNF DTTGAAGDGD MYGTLHAIEA LRKEFPDMYI EAGMAGECVL
251 GMHGNLQYDG VTLAGLWPHQ QAPLVAKAGA NVFGPVCNTN TSKTSAWNLA
301 RAVTFMKAAV EASPIPCHVD MGMGVGGIPM LETPPIDAVT RASKAMVEIA
351 GVDGIOIGVG DPLGMPIAHI MASGMTGMRA AGDLVARMEF SKNMRIGEAK
401 EYVAKKLGVD KMDLVDEHVM RELREELDIG IITSVPGAAK GIAAKMNIEK
451 LLDIKINSCN LFRKQIA

TABLE 3.8: List of predicted and observed *m/z* values of peptides generated by chymotrypsin-digested MtbB prior to treatment with borodeuteride detected by LC-MS/MS. One peptide *m/z* = 871.42^{3+} was observed for peptide ^{347}VEIAGVDGIOIGVGDPLGMPIAHIM^{371} which includes the pyrrolysyl-residue.

Table 3.8

Observed *m/z*	Observed Mass (Da)	Predicted Mass (Da)	Mass Difference (Da)	Corresponding sequence
1265.54^{1+}	1265.54	1265.68	0.14	^{6}ALRMGDGKRVY^{16}
428.12^{3+}	1282.36	1281.68	0.68	^{6}ALRM$_{(OX)}$GDGKRVY^{16}
541.53^{2+}	1082.06	1081.56	0.5	^{8} RMGDGKRVY^{16}
885.56^{3+}	2654.68	2654.41	0.27	^{17} LTKEKIVSEIEAGTADAADLGEIPAL^{42}
1323.79^{3+}	3969.37	3969.06	0.31	^{17}LTKEKIVSEIEAGTADAADLGEIPALSANEMDKLAEIL^{54}
1329.12^{3+}	3985.36	3985.06	0.3	^{17}LTKEKIVSEIEAGTADAADLGEIPALSANEM$_{(OX)}$DKLAEIL^{54}
1286.04^{3+}	3856.12	3855.98	0.14	^{18}TKEKIVSEIEAGTADAADLGEIPALSANEMDKLAEIL^{54}
1460.02^{3+}	4378.06	4379.18	1.12	^{55}MMPGKTVSVEQGMEIPVTHDIGTIRLDGDQGNSGVGIPSSRL^{96}
780.06^{2+}	1559.12	1558.75	0.37	^{81} DGDQGNSGVGIPSSRL^{96}
604.27^{2+}	1207.54	1207.53	0.01	^{97} VGC$_{(CAM)}$MTHERAF^{106}
403.29^{3+}	1207.87	1207.53	0.34	^{97} VGC$_{(CAM)}$MTHERAF^{106}
612.38^{2+}	1223.76	1223.53	0.23	^{97}VGC$_{(CAM)}$M$_{(OX)}$THERAF^{106}
1255.44^{2+}	2509.88	2510.09	0.21	^{97}VGC$_{(CAM)}$MTHERAFGADTMELGHIDY^{118}
843.10^{3+}	2527.3	2526.09	1.21	^{97}VGC$_{(CAM)}$M$_{(OX)}$THERAFGADTMELGHIDY^{118}
661.38^{2+}	1321.76	1321.57	0.19	^{107}GADTMELGHIDY^{118}
669.49^{2+}	1337.98	1337.57	0.41	^{107}GADTM$_{(OX)}$ELGHIDY^{118}
1044.84^{3+}	3132.52	3132.53	0.01	^{119}SFKPVKPVVSNEC$_{(CAM)}$QAMEVC$_{(CAM)}$QQNMVIPL^{145}
1050.14^{3+}	3148.42	3148.53	0.11	^{119}SFKPVKPVVSNEC$_{(CAM)}$QAM$_{(OX)}$EVC$_{(CAM)}$QQNMVIPL^{145}
1148.18^{3+}	3442.54	3442.67	0.13	^{119}SFKPVKPVVSNEC$_{(CAM)}$QAMEVC$_{(CAM)}$QQNMVIPLFY^{147}
1153.57^{3+}	3458.71	3458.67	0.04	^{119}SFKPVKPVVSNEC$_{(CAM)}$QAM$_{(OX)}$EVC$_{(CAM)}$QQNMVIPLFY^{147}
1070.20^{3+}	3208.6	3208.57	0.03	^{121}KPVKPVVSNEC$_{(CAM)}$QAMEVC$_{(CAM)}$QQNMVIPLFY^{147}
1075.75^{3+}	3225.25	3224.57	0.68	^{121}KPVKPVVSNEC$_{(CAM)}$QAM$_{(OX)}$EVC$_{(CAM)}$QQNMVIPLFY^{147}
953.30^{1+}	953.3	953.42	0.12	^{148} GAMPNMGLY^{156}
969.24^{1+}	969.24	969.42	0.18	^{148} GAM$_{(OX)}$PNMGLY^{156}
1116.29^{1+}	1116.29	1116.49	0.2	^{148} GAMPNMGLYY^{157}
1417.34^{2+}	2833.68	2833.27	0.41	^{148}GAMPNMGLYYTPDGPFENPGDLMKAF^{173}
950.27^{3+}	2848.81	2849.27	0.46	^{148}GAM$_{(OX)}$PNMGLYYTPDGPFENPGDLMKAF^{173}
950.27^{3+}	2848.81	2849.27	0.46	^{148}GAMPNM$_{(OX)}$GLYYTPDGPFENPGDLMKAF^{173}
796.28^{1+}	796.28	796.35	0.07	^{157}YTPDGPF^{163}
949.89^{2+}	1898.78	1898.86	0.08	^{157} YTPDGPFENPGDLMKAF^{173}
958.11^{2+}	1915.22	1914.86	0.36	^{157} YTPDGPFENPGDLM$_{(OX)}$KAF^{173}
868.41^{2+}	1735.82	1735.8	0.02	^{158}TPDGPFENPGDLMKAF^{173}
634.07^{2+}	1267.14	1267.65	0.51	^{170}M$_{(OX)}$KAFKIQEAW ^{179}
774.36^{1+}	774.36	774.41	0.05	^{174} KIQEAW^{179}

Table 3.8 continued

Observed *m/z*	Observed Mass (Da)	Predicted Mass (Da)	Mass Difference (Da)	Corresponding sequence
1334.00^{2+}	2667	2667.26	0.26	^{174}KIQEAWESMEHAAEHLTRDTVW^{195}
889.84^{3+}	2667.52	2667.26	0.26	^{174}KIQEAWESMEHAAEHLTRDTVW^{195}
1342.33^{2+}	2683.66	2683.26	0.40	^{174}KIQEAWESM$_{(OX)}$EHAAEHLTRDTVW^{195}
895.25^{3+}	2683.75	2683.26	0.49	^{174}KIQEAWESM$_{(OX)}$EHAAEHLTRDTVW^{195}
1449.15^{2+}	2897.3	2897.37	0.07	^{174}KIQEAWESMEHAAEHLTRDT VWVM^{197}
766.37^{1+}	766.37	765.43	0.94	^{196}VMQKLF^{201}
984.27^{1+}	984.27	984.44	0.17	^{201}FASGADGVNF^{210}
837.33^{1+}	837.33	837.37	0.04	^{202}ASGADGVNF^{210}
996.40^{2+}	1991.8	1991.79	0.01	^{202}ASGADGVNFDTTGAAGDGDMY^{222}
1005.03^{2+}	2009.06	2007.79	1.27	^{202}ASGADGVNFDTTGAAGDGDM$_{(OX)}$Y^{222}
1131.96^{2+}	2262.92	2262.95	0.03	^{202}ASGADGVNFDTTGAAGDGDMYGTL^{225}
1173.32^{1+}	1173.32	1173.44	0.12	^{211}DTTGAAGDGDMY^{222}
924.41^{1+}	924.41	924.51	0.1	^{223}GTLHAIEAL^{231}
653.53^{1+}	653.53	653.36	0.17	^{226}HAIEAL^{231}
574.01^{3+}	1720.03	1719.85	0.18	^{226}HAIEALRKEFPDMY^{239}
1426.32^{2+}	2851.64	2850.36	1.28	^{226}HAIEALRKEFPDMYIEAGMAGEC$_{(CAM)}$ VL^{250}
543.33^{2+}	1085.66	1085.51	0.15	^{232}RKEFPDMY^{239}
739.36^{3+}	2216.08	2216.02	0.06	^{232}RKEFPDMYIEAGMAGEC$_{(CAM)}$VL^{250}
1201.27^{3+}	3601.81	3601.66	0.15	^{232}RKEFPDMYIEAGMAGEC$_{(CAM)}$VLGMH GNLQYDGVTL^{263}
1404.51^{1+}	1404.51	1404.66	0.15	^{251}GMHGNLQYDGVTL^{263}
702.70^{2+}	1404.4	1404.66	0.26	^{251}GMHGNLQYDGVTL^{263}
852.66^{2+}	1704.32	1702.89	1.43	^{259}DGVTLAGLWPHQQAPL^{274}
1217.56^{1+}	1217.56	1217.64	0.08	^{264}AGLWPHQQAPL^{274}
609.28^{2+}	1217.56	1217.64	0.08	^{264}AGLWPHQQAPL^{274}
876.43^{1+}	876.43	876.49	0.06	^{275}VAKAGANVF^{283}
438.69^{2+}	876.38	876.49	0.11	^{275}VAKAGANVF^{283}
1522.59^{1+}	1522.59	1522.7	0.11	^{284}GPVC$_{(CAM)}$NTNTSKTSAW^{297}
762.01^{2+}	1523.02	1522.7	0.32	^{284}GPVC$_{(CAM)}$NTNTSKTSAW^{297}
891.46^{1+}	891.46	891.5	0.04	^{298}NLARAVTF^{305}
446.50^{2+}	892	891.5	0.50	^{298}NLARAVTF^{305}
664.45^{1+}	664.45	664.38	0.07	^{300}ARAVTF^{305}
1412.64^{3+}	4235.92	4236.08	0.16	^{306}MKAAVEASPIPCHVDMGMGV GGIPMLETPPIDAVTRASKAM^{346}
871.42^{3+}	2612.26	2611.38	0.88	**^{347}VEIAGVDGIOIGVGDPLGMPIAHIM^{371}**
1425.64^{1+}	1425.64	1425.72	0.08	^{391}SKNMRIGEAKEY^{402}
475.95^{3+}	1425.85	1425.72	0.13	^{391}SKNMRIGEAKEY^{402}
481.40^{3+}	1442.2	1441.72	0.48	^{391}SKNM$_{(OX)}$RIGEAKEY^{402}
1140.50^{2+}	2280	2279.24	0.76	^{395}RIGEAKEYVAKKLGVDKM$_{(OX)}$DL^{414}
943.71^{2+}	1886.42	1885.91	0.51	^{408}GVDKMDLVDEHVMREL^{423}
1223.47^{1+}	1223.47	1223.61	0.14	^{453}DIKINSCNLF^{462}
612.25^{2+}	1223.5	1223.61	0.11	^{453}DIKINSCNLF^{462}

TABLE 3.9: List of predicted and observed *m/z* values of peptides generated by chymotrypsin-digested MtbB treated with 10 mM $NaBD_4$ and detected by LC-MS/MS. One peptide *m/z* = 872.45^{3+} was observed for peptide ^{347}VEIAGVDGIOIGVGDPLGMPIAHIM^{371} which includes the pyrrolysyl-residue. No peptide corresponding to the mass of unmodified ^{347}VEIAGVDGIOIGVGDPLGMPIAHIM^{371} was observed.

Table 3.9

Observed *m/z*	Observed Mass (Da)	Predicted Mass (Da)	Mass difference (Da)	Corresponding sequence
1265.63^{1+}	1265.63	1265.68	0.05	^{6}ALRMGDGKRVY^{16}
428.25^{3+}	1282.75	1281.68	1.07	^{6}ALRM$_{(OX)}$GDGKRVY^{16}
460.49^{3+}	1379.47	1378.76	0.71	^{6}ALRMGDGKRVYL^{17}
541.29^{2+}	1081.58	1081.56	0.02	^{8} RMGDGKRVY^{16}
1323.71^{3+}	3969.13	3969.06	0.07	^{17}LTKEKIVSEIEAGTADAADLGEIPALSANE MDKLAEIL^{54}
1329.14^{3+}	3985.42	3985.06	0.36	^{17}LTKEKIVSEIEAGTADAADLGEIPALSANE M$_{(OX)}$DKLAEIL^{54}
1286.07^{3+}	3856.21	3855.98	0.23	^{18}TKEKIVSEIEAGTADAADLGEIPALSANE MDKLAEIL^{54}
957.46^{2+}	1913.92	1913.99	0.07	^{37}GEIPALSANEMDKLAEIL^{54}
1460.56^{3+}	4379.68	4379.18	0.5	^{55}MMPGKTVSVEQGMEIPVTHDIGTIRLDG DQGNSGVGIPSSRL^{96}
780.11^{2+}	1559.22	1558.75	0.47	^{81} DGDQGNSGVGIPSSRL^{96}
1207.42^{1+}	1207.42	1207.53	0.11	^{97} VGC$_{(CAM)}$MTHERAF^{106}
403.02^{3+}	1207.06	1207.53	0.47	^{97} VGC$_{(CAM)}$MTHERAF^{106}
612.25^{2+}	1223.5	1223.53	0.03	^{97}VGC$_{(CAM)}$M$_{(OX)}$THERAF^{106}
1255.45^{2+}	2509.9	2510.09	0.19	^{97} VGC$_{(CAM)}$MTHERAF GADTMELGHIDY^{118}
837.31^{3+}	2509.93	2510.09	0.16	^{97} VGC$_{(CAM)}$MTHERAFG ADTMELGHIDY^{118}
661.36^{2+}	1321.72	1321.57	0.15	^{107}GADTMELGHIDY^{118}
669.45^{2+}	1337.9	1337.57	0.33	^{107}GADTM$_{(OX)}$ELGHIDY^{118}
1050.23^{3+}	3148.69	3148.53	0.16	^{119}SFKPVKPVVSNEC$_{(CAM)}$Q AM$_{(OX)}$EVC$_{(CAM)}$QQNMVIPL^{145}
1148.42^{3+}	3443.26	3442.67	0.59	^{119}SFKPVKPVVSNEC$_{(CAM)}$QAME VC$_{(CAM)}$QQNMVIPLFY^{147}
1153.46^{3+}	3458.38	3458.67	0.29	^{119}SFKPVKPVVSNEC$_{(CAM)}$QA M$_{(OX)}$EVC$_{(CAM)}$QQNMVIPLFY^{147}
967.05^{3+}	2899.15	2898.43	0.72	^{121}KPVKPVVSNEC$_{(CAM)}$QAMEVC$_{(CAM)}$QQN MVIPL^{145}
1206.18^{2+}	2411.36	2412.12	0.76	^{135}EVCQQNMVIPLFYGAMPNMGL^{155}
1263.33^{1+}	1263.33	1263.55	0.22	^{146}FYGAMPNMGLY^{156}
632.23^{2+}	1263.46	1263.55	0.09	^{146}FYGAMPNMGLY^{156}
953.30^{1+}	953.3	953.42	0.12	^{148} GAMPNMGLY^{156}
969.20^{1+}	969.2	969.42	0.22	^{148} GAM$_{(OX)}$PNMGLY^{156}
1116.19^{1+}	1116.19	1116.49	0.3	^{148} GAMPNMGLYY^{157}
1417.29^{2+}	2833.58	2833.27	0.31	^{148}GAMPNMGLYYTPDGPFENPGDLMKAF^{173}
945.14^{3+}	2833.42	2833.27	0.15	^{148}GAMPNMGLYYTPDGPFENPGDLMKAF^{173}
950.36^{3+}	2849.08	2849.27	0.19	^{148}GAM$_{(OX)}$PNMGLYYTPDGPFENPGDLMK AF^{173}
950.36^{3+}	2849.08	2849.27	0.19	^{148}GAMPNM$_{(OX)}$GLYYTPDGPFENPGDLMK AF^{173}
796.12^{1+}	796.12	796.35	0.23	^{157}YTPDGPF^{163}
949.92^{2+}	1898.84	1898.86	0.02	^{157} YTPDGPFENPGDLMKAF^{173}
868.34^{2+}	1735.68	1735.8	0.12	^{158}TPDGPFENPGDLMKAF^{173}
634.08^{2+}	1267.16	1267.65	0.49	^{170}M$_{(OX)}$KAFKIQEAW ^{179}
637.37^{3+}	1910.11	1908.89	1.22	^{174} KIQEAWESMEHAAEHL^{189}

Table 3.9 continued

Observed *m/z*	Observed Mass (Da)	Predicted Mass (Da)	Mass difference (Da)	Corresponding sequence
889.56^{3+}	2666.68	2667.26	0.58	^{174}KIQEAWESMEHAAEHLTRDTVW^{195}
1342.35^{2+}	2683.7	2683.26	0.44	^{174}KIQEAWESM$_{(OX)}$EHAAEHLTRDTVW^{195}
895.23^{3+}	2683.69	2683.26	0.43	^{174}KIQEAWESM$_{(OX)}$EHAAEHLTRDTVW^{195}
1449.25^{2+}	2897.5	2897.37	0.13	^{174}KIQEAWESMEHAAEHLTRDT VWVM^{197}
984.32^{1+}	984.32	984.44	0.12	^{201}FASGADGVNF^{210}
1070.61^{2+}	2140.22	2138.86	1.36	^{201}FASGADGVNFDTTGAAGDGDMY^{222}
837.28^{1+}	837.28	837.37	0.09	^{202}ASGADGVNF^{210}
1992.03^{1+}	1992.03	1991.79	0.24	^{202}ASGADGVNFDTTGAAGDGDMY^{222}
996.53^{2+}	1992.06	1991.79	0.27	^{02}ASGADGVNFDTTGAAGDGDMY^{222}
1005.00^{2+}	2009	2007.79	1.21	^{202}ASGADGVNFDTTGAAGDGDM$_{(OX)}$Y^{222}
1132.03^{2+}	2263.06	2262.95	0.11	^{202}ASGADGVNFDTTGAAGDGDMYGTL^{225}
1139.97^{2+}	2278.94	2278.94	0	^{202}ASGADGVNFDTTGAAGDGDM$_{(OX)}$YGT L^{225}
1173.32^{1+}	1173.32	1173.44	0.12	^{211}DTTGAAGDGDMY^{222}
924.43^{1+}	924.43	924.51	0.08	^{223}GTLHAIEAL^{231}
664.79^{3+}	1992.37	1991	1.37	^{223}GTLHAIEALRKEFPDMY^{239}
1041.10^{3+}	3121.3	3121.52	0.22	^{223}GTLHAIEALRKEFPDMYIEAGMAGE C$_{(CAM)}$VL^{250}
654.30^{1+}	654.3	653.36	0.94	^{226}HAIEAL^{231}
574.35^{3+}	1721.05	1719.85	1.2	^{226}HAIEALRKEFPDMY^{239}
950.93^{3+}	2850.79	2850.36	0.43	^{226}HAIEALRKEFPDMYIEAGMAGEC$_{(CAM)}$VL ^{250}
543.44^{2+}	1085.88	1085.51	0.37	^{232}RKEFPDMY^{239}
739.30^{3+}	2215.9	2216.02	0.12	^{232}RKEFPDMYIEAGMAGEC$_{(CAM)}$VL^{250}
1201.19^{3+}	3601.57	3601.66	0.09	^{232}RKEFPDMYIEAGMAGEC$_{(CAM)}$VLGMHGN LQYDGVTL^{263}
1078.54^{2+}	2156.08	2155.96	0.12	^{239}YIEAGMAGECVLGMHGNLQY^{258}
1404.49^{1+}	1404.49	1404.66	0.17	^{251}GMHGNLQYDGVTL^{263}
702.98^{2+}	1404.96	1404.66	0.30	^{251}GMHGNLQYDGVTL^{263}
710.74^{2+}	1420.48	1420.65	0.17	^{251}GM$_{(OX)}$HGNLQYDGVTL^{263}
852.24^{2+}	1703.48	1702.89	0.59	^{259}DGVTLAGLWPHQQAPL^{274}
1217.36^{1+}	1217.36	1217.64	0.28	^{264}AGLWPHQQAPL^{274}
609.32^{2+}	1217.64	1217.64	0.00	^{264}AGLWPHQQAPL^{274}
876.41^{1+}	876.41	876.49	0.08	^{275}VAKAGANVF^{283}
1190.79^{2+}	2380.58	2380.17	0.41	^{275}VAKAGANVFGPVC$_{(CAM)}$NTNTSKTSA W^{297}
1522.50^{1+}	1522.5	1522.7	0.2	^{284}GPVC$_{(CAM)}$NTNTSKTSAW^{297}
761.78^{2+}	1522.56	1522.7	0.14	^{284}GPVC$_{(CAM)}$NTNTSKTSAW^{297}
891.44^{1+}	891.44	891.5	0.06	^{298}NLARAVTF^{305}
446.52^{2+}	892.04	891.5	0.54	^{298}NLARAVTF^{305}
664.37^{1+}	664.37	664.38	0.01	^{300}ARAVTF^{305}
1412.92^{3+}	4236.76	4236.08	0.68	^{306}MKAAVEASPIPCHVDMGMGV GGIPMLETPPIDAVTRASKAM^{346}
872.45^{3+}	2615.35	2611.38	3.97	**^{347}VEIAGVDGIOIGVGDPLGMPIAHIM^{371}**
1425.60^{1+}	1425.6	1425.72	0.12	^{391}SKNMRIGEAKEY^{402}
713.63^{2+}	1426.26	1425.72	0.54	^{391}SKNMRIGEAKEY^{402}
721.54^{2+}	1442.08	1441.72	0.36	^{391}SKNM$_{(OX)}$RIGEAKEY^{402}
943.43^{2+}	1885.86	1885.91	0.05	^{408}GVDKMDLVDEHVMREL^{423}
809.58^{3+}	2426.74	2426.37	0.37	^{428}DIGIITSVPGAAKGIAAKMN IEKL^{451}
612.29^{2+}	1223.58	1223.61	0.03	^{453}DIKINSCNLF^{462}

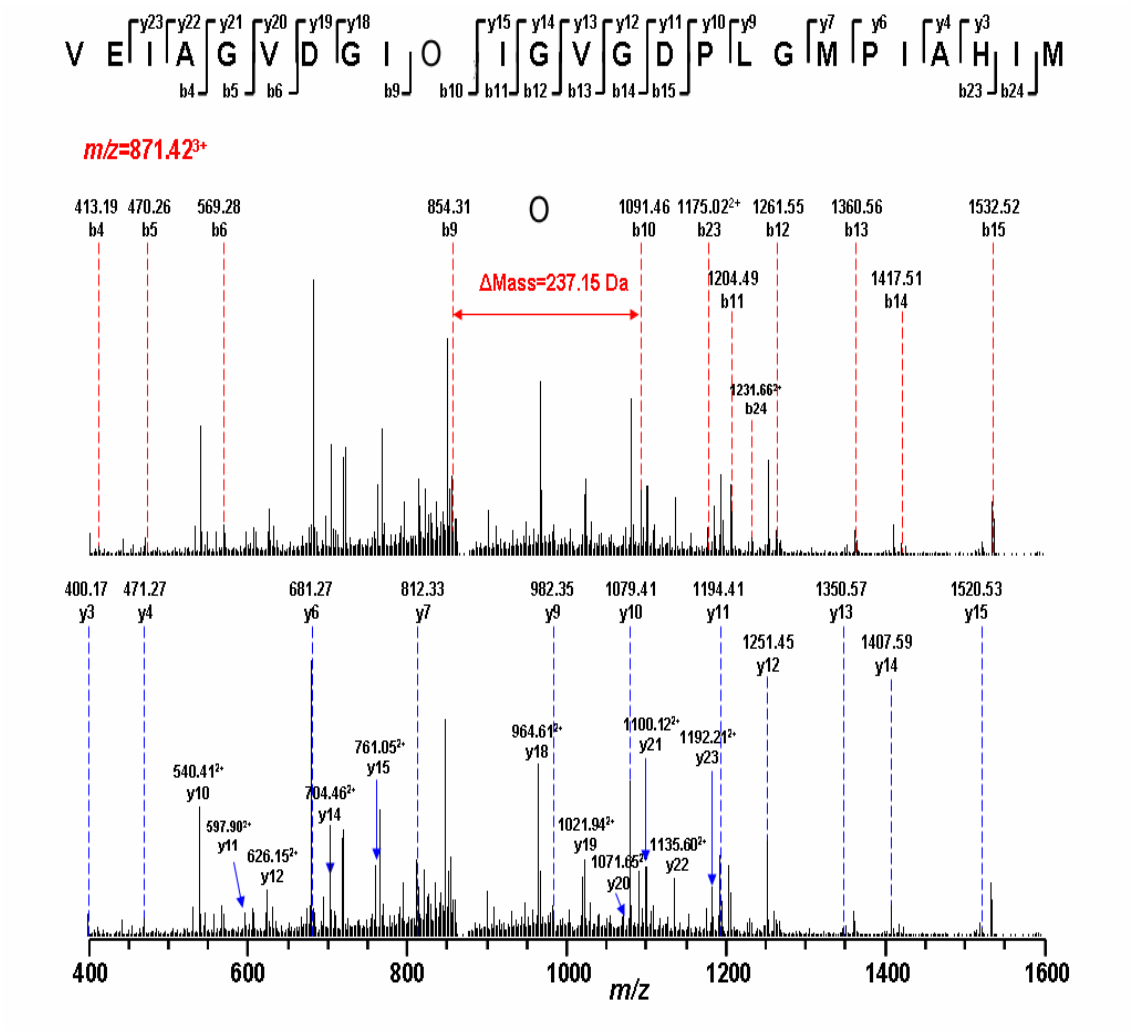

Figure 3.12: Collision-Induced Dissociation Spectrum of the *m/z* = 871.42^{3+} of MtbB (untreated)

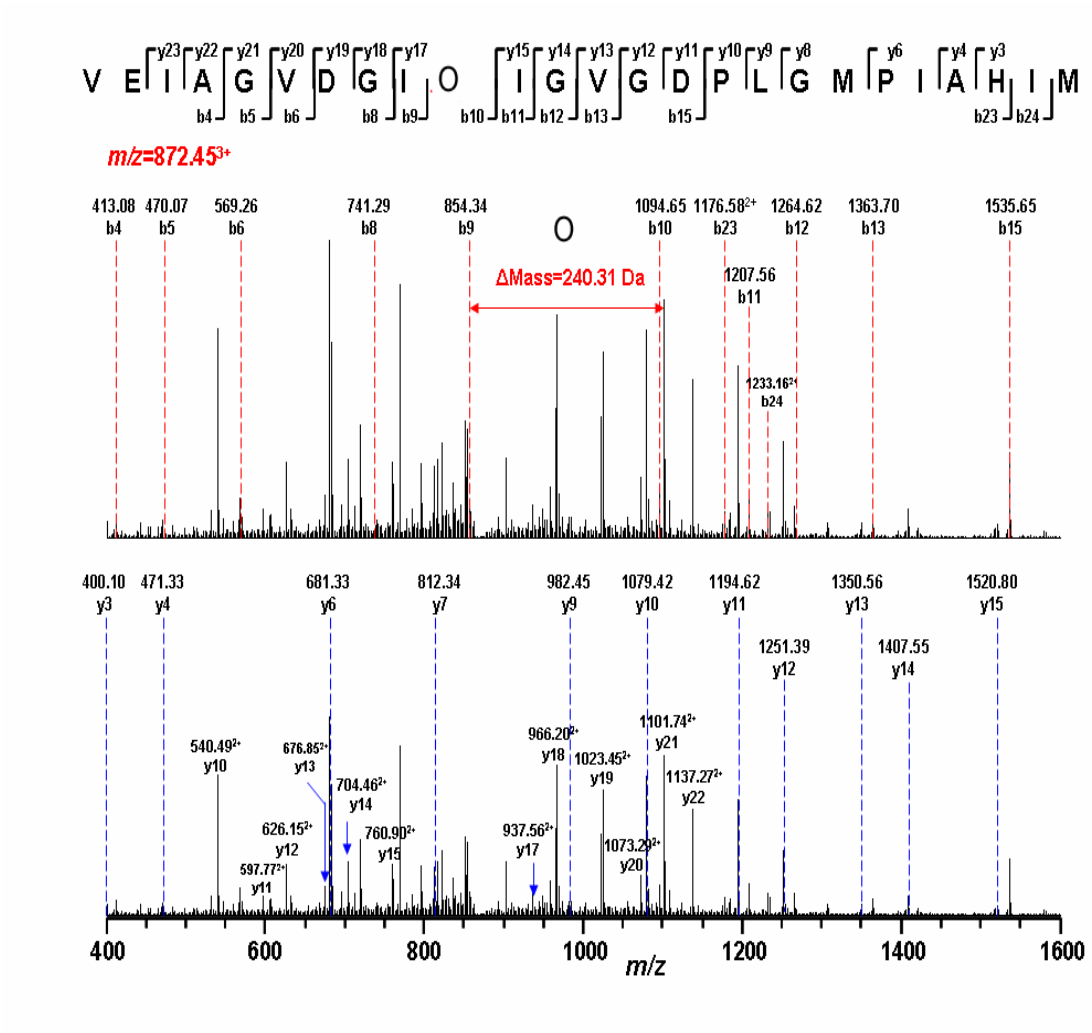

Figure 3.13: Collision-Induced Dissociation spectrum of m/z = 872.45^{3+} of MtbB treated with 10 mM $NaBD_4$

Δm between y-n and yn-1	Fragment Ion	Measured m/z	Sequence	Measured m/z	Fragment Ion	Δm between b-n and bn-1
			Val			
			Glu			
113.22	**y23**	1192.21^{+2}	Ile			
70.96	**y22**	1135.60^{+2}	Ala	413.19	**b4**	
56.94	**y21**	1100.12^{+2}	Gly	470.26	**b5**	57.07
99.42	**y20**	1071.65^{+2}	Val	569.28	**b6**	99.02
114.66	**y19**	1021.94^{+2}	Asp			
	y18	964.61^{+2}	Gly			
			Ile	854.31	**b9**	
			Pyrrolysine	1091.46	**b10**	**237.15**
112.94	**y15**	1520.53	Ile	1204.49	**b11**	113.03
57.02	**y14**	1407.59	Gly	1261.55	**b12**	57.06
99.12	**y13**	1350.57	Val	1360.56	**b13**	99.01
57.04	**y12**	1251.45	Gly	1417.51	**b14**	56.95
115.00	**y11**	1194.41	Asp	1532.52	**b15**	115.01
97.06	**y10**	1079.41	Pro			
170.02 (113+57)	**y9**	982.35	Leu			
			Gly			
131.06	**y7**	812.33	Met			
210.00 (97+113)	**y6**	681.27	Pro			
			Ile			
71.10	**y4**	471.27	Ala			
	y3	400.17	His	1175.02^{+2}	**b23**	
			Ile	1231.66^{+2}	**b24**	113.28
			Met			

Table 3.10: b- and y-ion series of *m/z* = 871.42^{3+} of the untreated MtbB, showing the mass of the UAG-encoded residue pyrrolysine as that of unmodified pyrrolysine.

Δm between y-n and yn-1	Fragment Ion	Measured m/z	Sequence	Measured m/z	Fragment Ion	Δm between b-n and bn-1
			Val			
			Glu			
113.08	**y23**	1193.81^{+2}	Ile	342.12	**b3**	
71.06	**y22**	1137.27^{+2}	Ala	413.08	**b4**	70.96
56.90	**y21**	1101.74^{+2}	Gly	470.07	**b5**	56.99
99.68	**y20**	1073.29^{+2}	Val	569.26	**b6**	99.19
114.50	**y19**	1023.45^{+2}	Asp			
57.28	**y18**	966.20^{+2}	Gly	741.29	**b8**	172.03 (115+57)
353.32 (113+240)	**y17**	937.56^{+2}	Ile	854.34	**b9**	113.05
			Pyrrolysine	1094.65	**b10**	**240.31**
113.25	**y15**	1520.80	Ile	1207.56	**b11**	112.91
56.99	**y14**	1407.55	Gly	1264.62	**b12**	57.06
99.17	**y13**	1350.56	Val	1363.70	**b13**	99.08
56.77	**y12**	1251.39	Gly			
115.20	**y11**	1194.62	Asp	1535.65	**b15**	171.95 (57+115)
96.97	**y10**	1079.42	Pro			
170.11 (113+57)	**y9**	982.45	Leu			
			Gly			
131.01	**y7**	812.34	Met			
210.00 (97+113)	**y6**	681.33	Pro			
			Ile			
71.23	**y4**	471.33	Ala			
	y3	400.10	His	1176.58^{+2}	**b23**	
			Ile	1233.16^{+2}	**b24**	113.16
			Met			

Table 3.11: b- and y-ion series for *m/z* = 872.45^{3+} of the MtbB sample treated with 10 mM $NaBD_4$ showing the specific reduction of pyrrolysine as observed by an increased mass of approximately 3 Da.

Sample	MtmB-dependent CoM methylation Activity (µmol/min.mg)
MtmB (untreated)	1.6
MtmB (500 µM $NaBD_4$)	0.2
MtmB + 100 mM MMA (500 µM $NaBD_4$)	0.1
MtmB + 1M MMA (500 µM $NaBD_4$)	0.1
MtmB + 100 mM NH_4Cl (500 µM $NaBD_4$)	0.1

Table 3.12: Specific activities for CoM methylation of MtmB samples tested for substrate and end-product protection studies from $NaBD_4$. The samples were treated with 500 µM $NaBD_4$ for 2 mins. The MtmB was pre-incubated with MMA or NH_4Cl followed by the addition of $NaBD_4$ for 2 mins. The excess $NaBD_4$ was removed by G-25 gel filtration. These MtmB samples were assayed in vials which contained 2.9 µM MtmB, 4 µM MtmC, 5 µM MtbA, and 0.4 µM RAM.

Figure 3.14: Detection of chymotrypsin generated, doubly charged pyrrolysine-containing peptides MtbB titrated with varying concentrations of $NaBD_4$ by electrospray mass spectrometry. A) A 1:1 mixture of MtbB (untreated) and MtbB (10 mM $NaBD_4$), B) MtbB (10 mM $NaBD_4$ showing 1% cobalamin methylation activity), C) MtbB (untreated), D) MtbB (2 mM $NaBD_4$ showing 52% cobalamin methylation activity) and E) MtbB (4 mM $NaBD_4$ showing 15% cobalamin methylation activity). All peptides shown are doubly charged. Peptides of approximately *m/z* 881^{2+} and *m/z* 882.5^{2+} correspond to the unreduced and reduced form of the peptide ^{347}VEIAGVDGIOIGVGDPL^{363}.

Figure 3.14

A) 1:1 mixture of MtbB (untreated) and MtbB (10 mM $NaBD_4$)

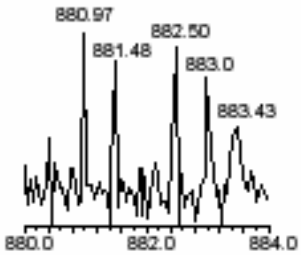

B) MtbB (untreated) 100% activity

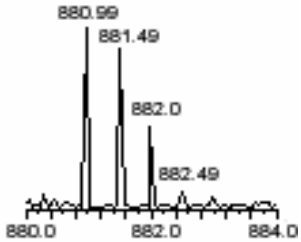

C) MtbB (2 mM $NaBD_4$) 52.7% ± 5.6 activity

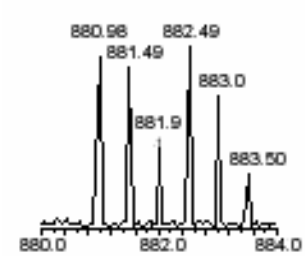

Figure 3.14 continued

D) MtbB (4 mM $NaBD_4$) 15% ± 6 activity

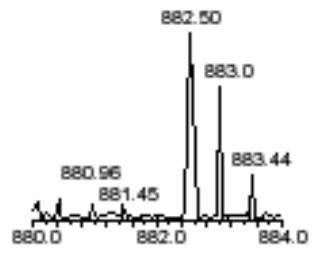

E) MtbB (10 mM $NaBD_4$) 1% activity

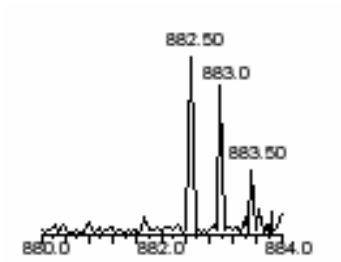

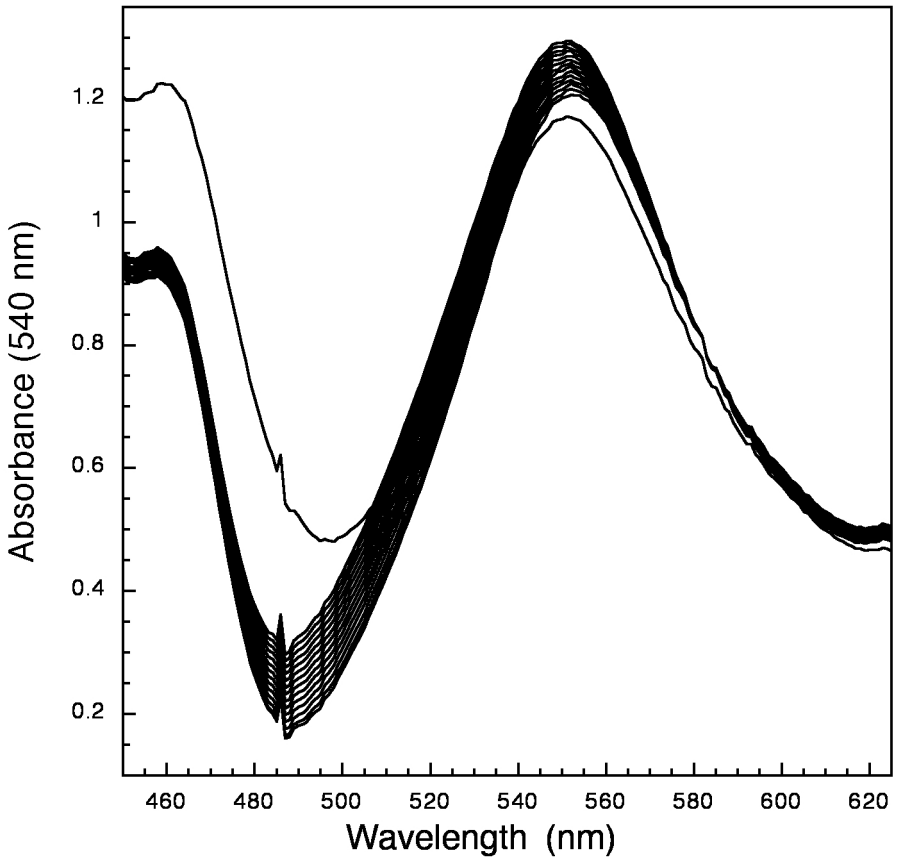

Figure 3.15: Cobalamin methylation by untreated MtbB followed spectrophotometrically by an increase in absorbance at 540 nm

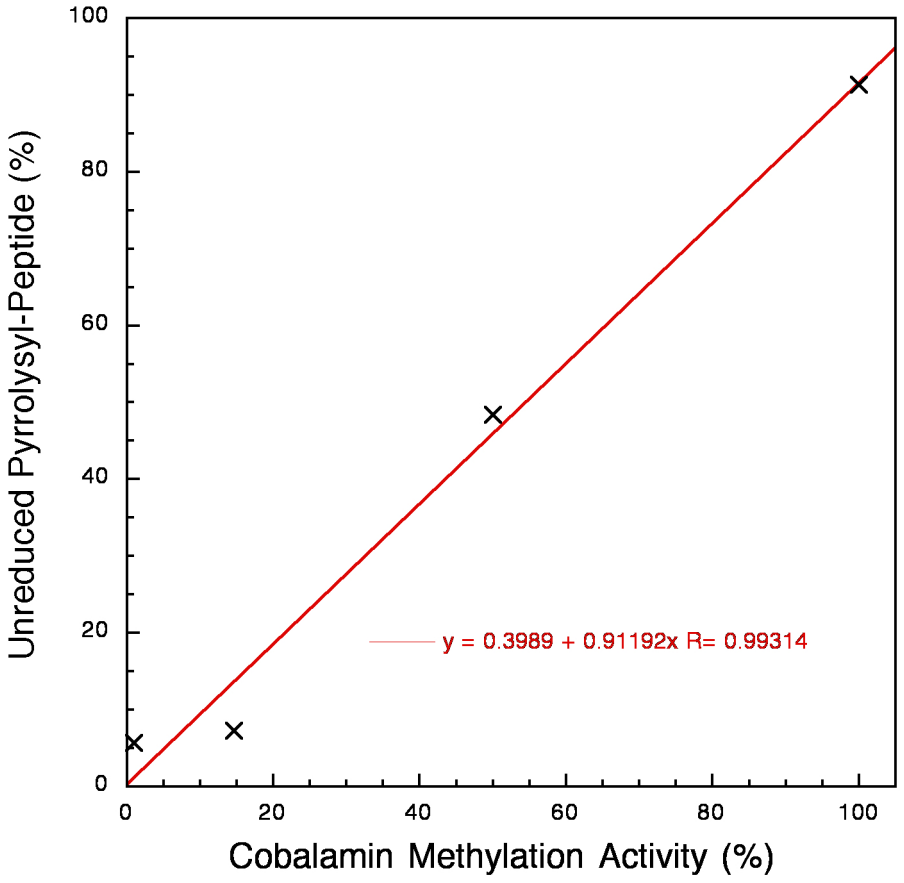

Figure 3.16: Correlation between the cobalamin methylation assay and the reduction of the pyrrolysyl-peptide. The graph was generated by plotting the ratio of the peak intensities of the *m/z* 881.0^{2+} (corresponding to the unreduced pyrrolysyl-peptide) and the *m/z* 882.5^{2+} peak (corresponding to the reduced pyrrolysyl-peptide) versus the corresponding cobalamin methylation activity of the MtbB sample. The graph shows that the two correlate linearly.

The collision-induced dissociation spectra of both *m/z* 871.42^{3+} and *m/z* 872.45^{3+} were studied to determine the site of modification (Figure 3.12 and Figure 3.13). The difference in mass between the b9/b10 ion pairs allowed for the determination of the residue masses of pyrrolysine in the respective proteins. A mass difference of 240.31 Da corresponded very closely with the expected mass of pyrrolysine reduced by $NaBD_4$. Further confirmation was achieved by studying the y-ion series of the peptide. Although the y16 ion was not observed, the difference in masses of the y15 ion (1520.80 Da) and y17 ion (1874.12 Da) allowed for the determination of the mass of pyrrolysine by accounting for the mass of isoleucine in the calculation. Again, the mass of pyrrolysine was approximately 240.32 Da, corresponding closely with the expected mass of pyrrolysine in the reduced form. Similarly, the collision-induced dissociation spectra of the *m/z* 871.42^{3+} peptide of untreated MtbB allowed for the observation of the native pyrrolysine mass, i.e., 237.15 Da based on the mass difference of the b9/b10 ion pair. Thus, a mass increase of 3.16 Da, was observed for the pyrrolysine residue in 10 mM $NaBD_4$-treated MtbB as compared to that of untreated MtbB (Table 3.10 and Table 3.11).

3.3.6 Substrate and end product protection studies for the reduction of pyrrolysine by $NaBD_4$

To study the role of MtmB, and more specifically that of pyrrolysine, in the hypothesized binding of its substrate, monomethylamine, a substrate protection study was carried out. To increase the sensitivity of the assay, 500 µM $NaBH_4$-

treated MtmB was used and approximately 87% reduction in MMA: CoM methyl transfer activity was observed. No significant increase in activity was observed in the presence of 100 mM to 1 M MMA with a 2 min treatment of 500 µM $NaBH_4$, as shown in Table 3.12. A further decrease in activity to approximately 94% was observed. To test whether pyrrolysine might play a role in the binding of NH_4^+, the end product in the MMA: CoM methyl transfer reaction, an end product protection study was conducted. A 100 mM NH_4Cl solution was used to study the effect of end product on the inhibition of 500 µM $NaBH_4$ on MtmB. As was the case with the substrate protection studies, NH_4^+ did not have a significant effect on the inhibition of the $NaBH_4$ as an activity of 0.1 µmol. min^{-1}. mg^{-1} was observed.

3.3.7 Titration of $NaBD_4$ causing partial reduction of pyrrolysine in MtbB correlates with a reduction in catalytic activity

MtbB was treated with 2 mM $NaBD_4$, 4 mM $NaBD_4$ and 10 mM $NaBD_4$ respectively and their cobalamin-methylation activities were studied. The MtbB sample treated with 2 mM $NaBD_4$ showed approximately 52% of the cobalamin-methylation activity as compared to that of the untreated MtmB, whereas the 4 mM $NaBD_4$-treated MtbB sample showed approximately 15% activity. Approximately 1% activity was observed for MtbB treated with 10 mM $NaBD_4$. To check for correlation between MtbB activity and the reduction of pyrrolysine, chymotryptic digests of these samples were studied by electrospray mass spectrometry to study the corresponding ratios of the reduced and unreduced

pyrrolysine-containing peptide. The ratio of the 2 mM $NaBD_4$-treated sample showed a ratio of 50% between the reduced and unreduced peptide ^{347}VEIAGVDGIOIGVGDPL^{363} containing pyrrolysine (Figure 3.14). The identity of the two peptides was confirmed by CID. The residue mass of pyrrolysine was also shown to be the site of $NaBD_4$ induced reduction for the reduced peptide. Similarly, for the 4 mM $NaBD_4$-treated MtbB, 94% of the reduced peptide was observed, which corresponded to the 10% cobalamin-methylation activity observed. The identity of the reduced and unreduced peptides was again confirmed by CID, and pyrrolysine shown to be the specific site of reduction in the reduced pyrrolysyl-peptide. The MtbB treated with 10 mM $NaBD_4$ showed the presence of only the reduced form of the pyrrolysine-containing peptide upon chymotryptic digestion. As a control, a 1:1 mixture of MtbB unreduced and reduced with 10 mM $NaBD_4$ was subjected to chymotryptic digestion, and the ratios studied by mass spectrometry. The observed peaks for the pyrrolysyl-peptide were approximately in a 1:1 ratio as expected.

3.4 DISCUSSION

Enzymes are comprised of amino acids whose side chains consist of exclusively nucleophilic groups. Electrophilic activation of substrates is therefore challenging. Enzymes have circumvented this problem by utilizing metal ions or coenzymes, such as thiamine pyrophosphate and pyridoxal phosphate, to stabilize negative charges (Armstrong 2000, Poppe *et. al.* 2005). Post-translational modification of amino acid side chains have allowed for the

conversion of nucleophilic groups into some fascinating novel electrophilic functional groups. One such modification has been found in enzymes such as histidine ammonia-lyase (HAL), phenyalanine ammonia-lyase, and tyrosine 2,3-aminomutase (Poppe *et. al.* 2005, Christenson *et. al.* 2003 (a), (b)). These enzymes possess a strong electrophile, 5-methylene-3,5-dihyroimidazol-4-one (MIO), which is formed by the cyclization of an internal tripeptide, Ala-Ser-Gly. The first evidence for the presence of an electrophilic group involved in the conversion of histidine to urocanic acid and ammonia by HAL came from the treatment of the enzyme with a specific nucleophile, such as $NaBH_4$, which is known to irreversibly reduce Schiff bases (Wickner *et. al.* 1969). In the reaction catalyzed by acetoacetate decarboxylase, the decarboxylation of acetoacetate to acetone and carbon dioxide is carried out by an electrophilic mechanism. This mechanism was probed with $NaBH_4$ and resulted in the irreversible inhibition of the enzyme along with the detection of a complex between substrate and enzyme via a Schiff base intermediate with a lysine residue (Hamilton *et. al.* 1959, Warren *et. al.* 1966).

The complete inactivation of MtmB and MtbB with low concentrations $NaBD_4$ is consistent with the presence and requirement of the N1-C2 imine bond of pyrrolysine in catalysis. This study corroborates the x-ray crystallographic data demonstrating the presence of an electrophilic imine in pyrrolysine. Based on the data in this study, the structure of the ring linked to the epsilon-nitrogen of lysine in pyrrolysine is predicted to be a pyrroline-ring rather than a pyrrole-ring consistent with the x-ray crystal structure of pyrrolysine in MtmB.

The results of this study are consistent with the idea that *L*-pyrrolysine is involved in catalysis and may be involved in the transfer of a methyl group from the substrate, MMA, to the cobalt atom of the cognate corrinoid protein; MtmC. MtmB has been hypothesized to methylate the cognate corrinoid protein, MtmC, with the involvement of pyrrolysine (Hao *et al.* 2002). It is interesting to note that MtmB is a structural homolog of the methytetrahydrofolate and homocysteine methyltransferase modules of methionine synthase, which directly interact with the cobalamin-binding domain of MetH, a structural homolog of MtmC. Similarly, the inhibition of MtbB by $NaBD_4$ is also consistent with the function of pyrrolysine to binding and orienting methylamines for the methylation of the cognate corrinoid proteins in the nucleophilic Co(I) state (Krzycki *et. al.* 2004). The similarity of the specific activities of MtbB treated with varying amounts of $NaBD_4$ at the level of CoM methylation and cobalamin methylation adds further evidence towards the requirement of pyrrolysine in catalysis. In the case of MtbB, it is reasonable to suggest that pyrrolysine binds DMA and initiates the methylation of MtbC by a mechanism similar to that proposed for the MMA-dependent system. Similarly, pyrrolysine present in MttB may co-ordinate and orient TMA towards the methylation of MttC. Further studies are needed to test the inhibition of MttB catalysis by $NaBD_4$.

One caveat to this study was the reducibility of cysteine-cysteine disulfide linkages by $NaBD_4$, which could potentially result in the inactivation of MtmB or MtbB by destabilizing the overall conformation of the protein. Hao *et. al.* had observed the presence of a partially occupied single disulfide bridge on the

reverse side of the catalytic cleft between the Cys341 and Cys428 residues in MtmB when crystallized in the presence of nucleophiles, hydroxylamine, methylhydroxylamine, and dithionite (Hao *et. al.* 2004). It was suggested that the detection of this disulfide bond might be due to air oxidation, however the role of this possible linkage in catalysis was never directly tested. It is worth noting that this disulfide bond was not observed in the initial crystal structure of 1.55 angstroms, when first crystallized in the native form in NaCl. The treatment of MtmB with DTT did not affect the activity of MtmB, and hence it is likely that this disulfide bond, if present, does not play a significant role in the structure or catalysis of MtmB. Site-directed mutagenesis studies are underway to test the involvement of pyrrolysine in MtmB function. Also, the residues hypothesized to be involved in the hydrogen bonding of pyrrolysine and substrate, and therefore the involvement in catalysis is being tested.

Substrate protection studies were attempted by pre-treating the enzyme with substrate prior to treatment with $NaBD_4$, but no increase in activity attributed to MMA was observed. This result may be owing to the fact that the K_m of MtmB for substrate, MMA, was found to be high, i.e., approximately 50 mM (Burke, thesis 1997). Hence, this protection may not be seen under the conditions tested. Also, following addition of MMA to MtmB, the protein was treated with $NaBD_4$ for 2 mins. It is possible that the substrate protection was not observed under the conditions tested for lack of a more time-resolved reduction with $NaBD_4$. Another possibility for the lack of substrate protection could be due to the base that is hypothesized to be involved in the deprotonation of substrate

causing the formation of methylammonium anion has yet to be determined. This base could be present on a cognate protein of the MMA methyltransferase system such as MtmC or MtbA.

Similar to the substrate protection study, an end product protection study was carried out. Pyrrolysine is suggested to bind the ammonia, and aid in removal of this end product from the active site. End product protection studies by the same method did not yield any increased enzyme activity.

Pyrrolysine, was shown to be charged onto a cognate $tRNA^{pyl}$, encoded by the *pylT* gene, by a novel aminoacyl-tRNA synthetase, PylS (Blight *et. al.* 2004, Polycarpo *et. al.* 2004). This charging was demonstrated to occur *in vivo* in *E. coli* expressing *pylT* and *pylS* when synthetic pyrrolysine was provided exogenously. Pyrrolysine could be used to tag recombinant pyrrolysyl-proteins in *E.coli* expressing *pylT* and *pylS*, to incorporate pyrrolysine for a UAG, and to detect the presence of the protein using tritiated-$NaBH_4$. Given recent data showing that translation of the amber codon can occur at a basal level in a context-independent manner pyrrolysine would be incorporated at the position of the UAG (Longstaff *et. al.* 2007). The incorporation of synthetic amino acids with novel reactive properties has been a goal of several research groups towards the development of engineered enzymes with novel properties. This biotechnology is achieved by modifying tRNA-aminoacyl-tRNA synthetase pairs to specifically incorporate non-cognate amino acids into proteins, often utilizing amber-suppression (Xie *et. al.* 2005). Nature provides us with a system that can

incorporate a novel amino acid with demonstrated unprecedented electrophilic properties by a cognate tRNA-aminoacyl-tRNA synthetase pair.

The apparent importance of pyrrolysine in methylamine methyltransferase catalysis may provide a rationale for the inclusion of pyrrolysine in the genetic code of certain methanogens. The acquisition of this residue allows the function of a set of methyltransferases which permits habitation in the relatively unusual niche of anaerobic methylamine utilization.

CHAPTER 4

RAM, A REDOX ACTIVE PROTEIN REQUIRED FOR ATP-DEPENDENT REDUCTION OF METHYLAMINE CORRINOID PROTEIN TO THE ACTIVE STATE

4.1 INTRODUCTION

Methanogenic archaea are characterized by their ability to form methane as a major end product of metabolism (Thauer, 1998). Methanogens may be responsible for the formation of methane hydrates which are estimated to be in the amount of approximately 10^6 kg globally. This represents one of the largest sources of hydrocarbons on Earth (Marchesi *et. al.*, 2001). Thus, these methane hydrates are potentially an enormous natural gas resource especially keeping in mind the susceptibility to depletion of current energy supplies. Methanogenesis is also important ecologically as methanogens are involved in processes of sewage digestion and the degradation of recalcitrant xenobiotics under anaerobic conditions (Maymo-Gatell *et. al.*, 1995). On the other hand, the generation of

methane also has an adverse effect on the global ecology. Methane is one of the most important greenhouse gases after carbon dioxide and contributes to approximately 16% of the greenhouse effect (Deppenmeier, 2002).

Methanosarcina species are more adaptable than other methanogenic archaea with respect to the catabolism of various substrates such as carbon dioxide (CO_2) and hydrogen (H_2) as well as a variety of methylotrophic compounds such as acetate, methylated thiols, methanol and methylamines. Methanogenesis in *Methanosarcina barkeri* MS occurs by a disproportionation pathway where for every one methylamine molecule oxidized to CO_2, three methylamine molecules are reduced to CH_4. The oxidation of one substrate molecule methyl group of methylamines to CO_2 provides six electrons which supply the reducing equivalents for the reduction of three methyl moieties of methylamines to methane. This is achieved by transferring the electrons to coenzyme F_{420}, a deazaflavin derivative, which functions as a central electron carrier in the cytoplasm of methanogens. The $F_{420}H_2$ is reoxidized by a membrane-bound electron transport enzyme $F_{420}H_2$ dehydrogenase and the electrons are transferred to a heterodisulfide reductase with the involvement of methanophenazine. Heterodisulfide reductase reduces heterodisulfide (CoB-S-S-CoM) generating the methyl carrier, CoM and coenzyme B (Deppenmeier, 2002, Thauer, 1998).

The enzymes involved in methanogenesis from methylamines and methanol in *Methanosarcina* species have been characterized and shown to transfer methyl groups by similar pathways (Sauer *et. al.*, 1998, Burke *et. al.*

1997, Ferguson *et. al.*, 2000). These methyl transfer pathways converge to form methyl-CoM, an important intermediate in the generation of methane. Methanogenesis from monomethylamine (MMA) is initiated by the methylation of MtmC by the methyltransferase MtmB. The methyl-CoM intermediate is formed by the transfer of the methyl group on MtmC to CoM by a CoM methylase, MtbA. The formation of methyl-CoM from methanol is carried out by a pathway similar to that of MMA. Using substrate, MtaB, the methanol methyltransferase methylates the cognate corrinoid protein, MtaC. Subsequently, the methyl group is transferred to CoM by MtaA the corresponding CoM methylase. The central corrinoid protein, MtaC, contains a cobalamin center that cycles between the supernucleophilic Co(I) state and the methylcob(III)alamin form during catalysis (Daas *et. al.* 1996, Keltjens *et. al.* 1993). For the MtaA-dependent transfer of a methyl group to CoM, methylcob(III)alamin undergoes heterolytic cleavage of the Co-C bond, regenerating the highly nucleophilic Co(I) state. As the redox potential of the Co(II)/Co(I) couple is very low, the cobalamin center is prone to oxidation to the Co(II) state, which is catalytically inactive in methyltransferases.

In *Methanosarcina* species, the most predominant species of corrinoid cofactors appear to be a 5-hydroxybenzimidazole cobamide (Daas *et. al.* 1996, Stupperich *et. al.* 1987). The structure of this cofactor consists of a tetrapyrrole ring, with nitrogen from each of the rings coordinated with a central cobalt atom (Drennan *et. al.* 1994, Matthews, 2001). Thus far, the upper ligand of the cobalt has been demonstrated to bind a number of groups such as -CN, -OH, 5'-deoxyadenosyl and -CH_3. The lower cobalt ligand of the cofactor in solution is the

benzimidazole base. In many corrinoid-binding proteins, such as typified by MetH, the benzimidazolyl base is displaced by a histidine residue (Drennan et. al. 1994).

The cobalt center in corrinoid cofactors are present in three oxidation states, namely, Co^{1+}, Co^{2+} and Co^{3+}. One of the groups previously mentioned bind in the upper ligand of the corrinoid cofactor when in the Co^{3+} state and contains six electrons in the 3d orbitals resulting in a diamagnetic state. The Co^{2+} state shows the presence of an unpaired electron in the $3dz^2$ orbital imparting a paramagnetic character to the corrinoid cofactor which is detectable by electron paramagnetic resonance (EPR). The Co^{1+} state has an additional electron in the $3dz^2$ orbital as compared to the Co^{2+} state. This electron is localized perpendicular to the plane of the tetrapyrrole ring in the upper ligand, which imparts a strongly nucleophilic character to the cofactor and is able to take up groups such as $-CH_3$ in the upper ligand. All the electrons in the 3d orbital of cobalt in the Co^{1+} state are paired resulting in a diamagnetic, EPR silent state (Banerjee *et. al.* 2003).

During catalysis in methyltransferase systems, the corrinoid cofactor cycles between the Co(I)-form and the CH_3-Co(III)-form. However, due to the low redox potential of the Co(II)/Co(I) couple, the cofactor is prone to oxidative inactivation to the Co(II) form (Menon *et. al.* 1999). Corrinoid proteins can be converted from the inactive Co(II) state in methyltransferases to the active Co(I) state by a number of different mechanisms. For example, the activation of the cobalamin-binding domain of methionine synthase (MetH) from the Co(II)-MetH

to the methyl-Co(III)-MetH is carried out by methylation with adenosyl-methionine and a concurrent reduction by flavodoxin, that has been demonstrated to preferentially bind to Co(II)-MetH (Banerjee *et. al.* 1990 (a), Jarrett *et. al.* 1998). In the case of the corrinoid/iron-sulfur protein of *Morellia spp.*, CO dehydrogenase/acetyl CoA synthase, low potential electrons from the oxidation of CO were shown to be coupled with the reduction of Co(II) to Co(I) through the iron-sulfur component of this protein (Menon *et. al.* 1998, Menon *et. al.* 1999).

Studies by Daas *et al.* showed that the cell contains an activation system to reduce the inactive corrinoid cofactor of MtaC back to the Co(I) state (Daas *et. al.* 1996). Crude fractions of a methyltransferase activation protein (MAP) were shown to perform an ATP-dependent conversion of MtaC from the Co(II) state to the active Co(I) state in the presence of H_2, ferredoxin and a hydrogenase. Ferredoxin was observed to stimulate activity of MtaC but was not essential. Small amounts of the MAP protein were isolated, and shown to consist of a heterodimeric protein with 60 kDa and 30 kDa subunits. The UV-Vis spectrum of the protein indicated that MAP lacked any prosthetic groups such as iron-sulfur clusters. In the presence of ATP, MAP was suggested to cause a change in the co-ordination of the lower ligand of MtaC, resulting in a change in the redox potential of the Co(II)/Co(I) couple such that reduction could be carried out by H_2, hydrogenase and ferredoxin. MAP could not carry out the direct reduction of corrinoid protein itself. Recently, it has been shown that a partially purified preparations of an oxygen-sensitive “activating enzyme” could reductively

activate the corrinoid protein of veratrol o-demethylase in an ATP-dependent manner (Siebert *et. al.* 2005).

RAM, an enzyme involved in the ATP-dependent activation of MMA: CoM methyl transfer was previously isolated (Ferguson and Krzycki, previously unpublished) and it is hypothesized to be involved in the reduction of the corrinoid center from Co(II) to the active Co(I) state. The RAM protein was isolated to apparent homogeneity by a 9-step column chromatography purification procedure under strict anaerobic conditions as it was found to be sensitive to oxygen. RAM was shown to be an important component involved in the ATP-dependent MMA:CoM methyltransferase reaction catalyzed by MtmB, MtmC and MtbA in the presence of substrate MMA. Before the isolation of RAM, reductive activation of MtmC would be achieved by using Ti(III)-citrate in the presence of a methylviologen as redox mediator. Methylviologen (MV) reduced from MV^{2+} to the highly reducing MV^{0} species with Ti(III)-citrate and activate MMA:CoM methyl transfer in an ATP-independent manner. In the absence of MV, Ti(III)-citrate alone could not activate this reaction.

The UV-Vis absorption spectra of the oxidized and reduced (dithionite treated) forms of the protein strongly suggest the presence of redox-active iron-sulfur clusters. The presence of iron-sulfur clusters was confirmed by conducting phenanthroline and methylene blue assays for iron and sulfur, and was found to contain 6.9 Fe and 7.9 acid labile sulfurs per mol. This suggested that RAM possessed either two Fe_4S_4 clusters, or one Fe_3S_4 and one Fe_4S_4 cluster.

RAM activates the trimethylamine and dimethylamine methyl transfer systems in addition to the monomethylamine system described above. It was found to activate the MMA:CoM methyltransferase system catalytically at ratios of less than 1 pmol RAM in a reaction mixture of 500 pmol MtmC and MtbA, and 1 nmol MtmB. Further addition of RAM caused a linear increase in methyl transfer activity up to a ratio of 1 pmol RAM:25 pmol MtmC. Thereafter the addition of increasing amounts of RAM resulted in saturation of methyl transfer activity.

Ascertaining the direct substrate requirement for the reductive activation of methylamine methyltransferase corrinoid proteins by RAM are of importance towards the better understanding of the underlying mechanism of reductive activation. In this chapter, we demonstrate the direct reduction of MtmC with a purified protein, RAM.

4.2 MATERIALS AND METHODS

4.2.1 Cell cultures and preparation of extracts

M. barkeri MS (DSM 800) was grown in a phosphate buffered medium supplemented with 80 mM MMA. The cells were grown under strict anaerobic conditions, and were harvested 7 days after inoculation. Cell extracts were prepared anaerobically in 50 mM MOPS by lysing the cells by French press under 20,000 psi. The extracts were then subjected to ultracentrifugation at

150,000 xg, and the supernatants were stored in hydrogen-flushed vials at -70 ^{o}C. These supernantents were used to isolate proteins.

4.2.2 MtbC isolation from *M. acetivorans*

MtbC was isolated from extracts of over-expressed hexa-histidine tagged MtbB1 from *M. barkeri* MS in *M. acetivorans* (extracts were a gift from Jodie Lee).

M. acetivorans cells over-expressing N-terminal hexa-histidine tagged MtbB1 from *M. barkeri* MS grown on TMA were harvested at 5 days post-inoculation. These cells (10 g) were lysed by French Press in 10 ml. 50 mM MOPS (pH 7.0), and following ultracentrifugation, the supernatant was loaded onto a 5 ml Ni-NTA column (Pharmacia). On running a 160 ml, 0 to 500 mM imidazole gradient, at a flow rate 1 ml/min., MtbC eluted separately at approximately 20 mM imidazole. The MtbC fractions were pooled and partially exchanged into a 50 mM MOPS (pH 7.0) buffer by first concentrating by ultracentrifugation using a YM-10 membrane (Amicon, Inc., Piscataway, N.J.) and then diluting the concentrated protein 10-fold with MOPS buffer. The MtbC fraction was then loaded onto a 1 x 5 ml hydroxyapatite column (Bio-Rad Laboratories, Inc., Hercules, C.A.) equilibrated with 50 mM MOPS (pH 7.0). A gradient of 0 mM to 250 mM potassium phosphate over 160 ml was applied to the column at 2 ml/min. The MtbC fraction eluted at approximately 25 mM potassium phosphate. This fraction was pooled and exchanged into a 50 mM MOPS (pH 7.0) buffer by ultracentrifugation using a YM-10 membrane and then

loaded onto a Mono-Q HR 10/10 column (Amersham Biosciences, Piscataway, N.J.) equilibrated with 50 mM NaCl in 50 mM MOPS, pH 7.0. A 160 ml 500 mM NaCl gradient in 50 mM MOPS (pH 7.0) was run at a rate of 1 ml/min. MtbC eluted at approximately 250 mM NaCl. The protein preparation was found to be apparently homogenous as determined by denaturing 12.5% polyacrylamide gel electrophoresis followed by Coomassie staining. The activity of MtbC was confirmed by a CoM methylation assay.

4.2.3 CoM methylation Activity Assay

Activity assays were performed under strict anaerobic conditions in 2 ml rubber capped serum vials flushed with N_2. The reaction mixture was comprised of 50 mM MOPS at pH 7.0, 4 mM Ti(III)-citrate, 10 mM ATP, 20 mM $MgCl_2$, 3.2 mM 2-bromoethanesulfonic acid (BES), 2 mM CoM; 100 mM MMA, MtbA and the activation protein, RAM (isolated as described in Section 3.2.6) in a total volume of 125 µl. MtmC was isolated as described in Section 3.2.3. MtmB was added to the assay for testing for MtmC activity in fractions eluting from the Sephacryl S-100 column. Activity assays for MtbB (9 µg) were carried out in the presence of MtbC (9 µg) rather than MtmC and MtbA (10 µg) in a total volume of 125 µl. The assay was carried out at 37°C and 3.5 µl aliquots were periodically removed and added to 250 µl of 5,5'-dithio-bis(2-nitrobenzoic acid) (DTNB). The methylation of the free thiol was monitored by a loss of absorbance at 410 nm.

4.2.4 Determination of molecular mass of RAM

The molecular mass of the RAM monomer was determined by SDS-PAGE analysis with Coomassie staining. The protein markers used for this analysis were myosin (209 kDa), β-galactosidase (124 kDa), bovine serum albumin (BSA) (80 kDa), ovalbumin (49 kDa), carbonic anhydrase (35 kDa), soybean trypsin inhibitor (29 kDa), lysozyme (21 kDa) and aprotinin (7 kDa). A graph of the log molecular weights of the standard proteins were plotted against the distance migrated on the SDS-PAGE to generate a standard curve.

The molecular mass of non-denatured RAM was determined by size exclusion chromatography. Standard proteins (Sigma Chemical Co.) β-amylase (200 kDa), alcohol dehydrogenase (150 kDa), BSA (66 kDa), and carbonic anhydrase (29 kDa) were chromatographed on a (80 x 2.5 cm) Sephacryl S-200-HR (Amersham Pharmacia) column. The void volume was determined by running a sample of Blue Dextran (2000 kDa) on the column. A standard curve was generated, and the molecular mass of RAM was determined based on this standard graph.

4.2.5 *M. barkeri* MS RAM sequence determination

The RAM gene was PCR amplified from *M. barkeri* MS genomic DNA (a gift from Gayathri Srinivasan). Forward and Reverse primers were designed based on the RAM sequence of the *M. barkeri* Fusaro strain with an NdeI restriction site on the 5' end followed by a hexahistidine tag and a SacII site at the 3' end. The sequence of the forward primer was

CATATGCATCATCATCATCATCATCATATGTATGGAATAGCACTTGATCTG and that of the reverse primer was CCGCGGTTATTTCGCTGTGATTTTCAGTTT. The 1.6 kb PCR fragment was excised and gel extracted from a 0.8% agarose gel using the Promega Wizard SV Gel and PCR clean up kit. The purified 1.6 kb fragment was then A-tailed and ligated into a TOPO 2.1 vector (Invitrogen) and sequenced using M13 Forward (5'-GTAAAACGACGGCCAG-3') and M13 Reverse (5'-CAGGAAACAGCTATGAC-3') primers.

4.2.6 Assay of RAM-dependent activation of corrinoid proteins

The assay mixtures were prepared in under strict anaerobic conditions in a quartz cuvette (pathlength =1 cm) and a hydrogen gas phase. MtmC (19 µM) was initially reduced to the Co(II) form in 100 mM Tris-HCl (pH 7.5), 22 mM $MgCl_2$, 4.5 mM ATP and 1 mM Ti(III)-citrate in a total reaction volume of 113 µL. The spectrophotometer was initially blanked with the aforementioned solution lacking MtmC. The spectrophotometer readings were taken at the different time points from 0 min to 160 mins. Similarly the assay was performed for the activation of MtbC from *M. acetivorans* (10 µg) in the presence of RAM (0.8 µg). The time points for this assay were from 0-37 mins. The first two time points were taken at 0 and 1 min respectively and then the rest of the time points were taken at 2 minute intervals thereafter. For the determination of the requirement of ATP in the activation of MtmC, the reaction was started without ATP. At the 22 min. time point, 4.5 mM ATP was added to the reaction cuvette. ADP or 4.5 mM AMP-

PNP were added in the absence of ATP in order to examine the need for ATP hydrolysis during activation. All experiments utilized homogenous RAM as determined by SDS gel electrophoresis, except, those involved with the activation of MtbC with RAM were conducted with approximately 50% pure RAM fractions from the hydroxyapatite stage of purification.

The activity of RAM in the activation of MtmC and MtbC was followed by monitoring the increase in the Co(I) absorbance peak at 386 nm and a corresponding decrease in Co(II) absorbance at 475 nm. The Δε values at 386nm and 475 nm were determined by the relating the differences in absorption at the two wavelengths of the respective absorption maxima to the concentration of MtmC. The specific activities were calculated based on these Δε values.

4.2.7 MtbC-methylation assay

Complete reduction of 11.3 µM MtbC from the Co(II)-form to the Co(I)-form by RAM in the presence ATP and Ti(III)-citrate was carried out as described in section 4.2.6. The reaction was carried out in 150 µl total volume in a pathlength = 1 cm cuvette. 50 mM DMA was added to the cuvette, followed by 0.5 µM MtbB. The methylation reaction was followed spectrophotometrically, with time points being taken every minute.

4.3 RESULTS

4.3.1 RAM catalyzes the formation of Co(I)-MtmC

The reduction of MtmC by RAM was studied spectrophotometrically. The assay was conducted with the addition of ATP and reductant Ti(III)-citrate to the reaction followed by MtmC which was converted to the Co(II)-form as signified by the presence of a strong absorbance band at 475 nm, with the absence of a strong absorbing band at 386 nm that is characteristic of the Co(I) form of the corrinoid cofactor (Figure 4.1). The activation was started with the addition of RAM in catalytic amounts, and the rate of reduction followed by the increase in absorbance at 386 nm corresponding to the Co(I)-form and a corresponding decrease at 475 nm over time. At t=130 mins, the Co(I) peak no longer increased in intensity, coinciding with the loss of the Co(II) peak suggesting that the reaction had ceased. The spectra showed the presence of a clear isosbestic point at 415 nm, and no spectral features corresponding to a Co(III)-form. This isosbestic point remained stable throughout the reaction. Thus all the inactive Co(II)-form MtmC appeared to have being converted to the Co(I)-form.

4.3.2 Determination of RAM specific activity

In order to determine the specific activity of RAM, the reduction of MtmC to the Co(I) state was allowed to go to apparent completion, as indicated by the complete loss of the 475 nm absorbance peak, and no further increase in the peak intensity at 386 nm. No other features were observed to change at reaction

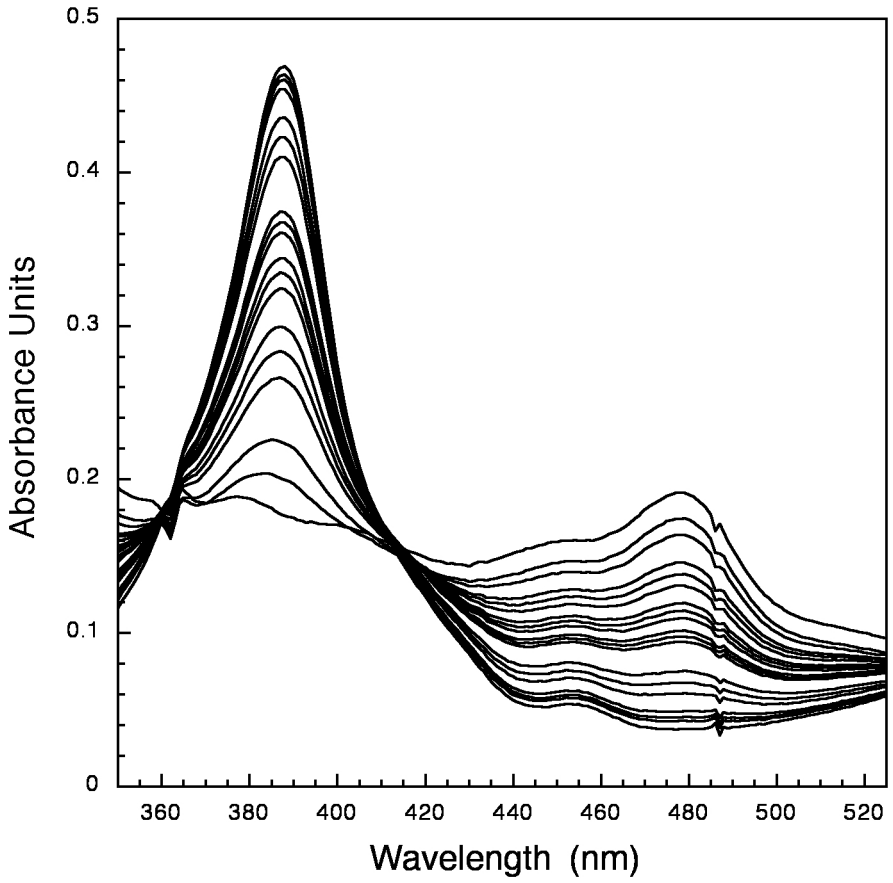

Figure 4.1: The direct reduction of MtmC by RAM. The UV/Vis spectra of MtmC in the Co(II) for at T_o and activation to the Co(I) form (T_{final}) over time in the presence of ATP and RAM. The assay cuvettes contained 19.5 µM MtmC and 0.8 µM RAM.

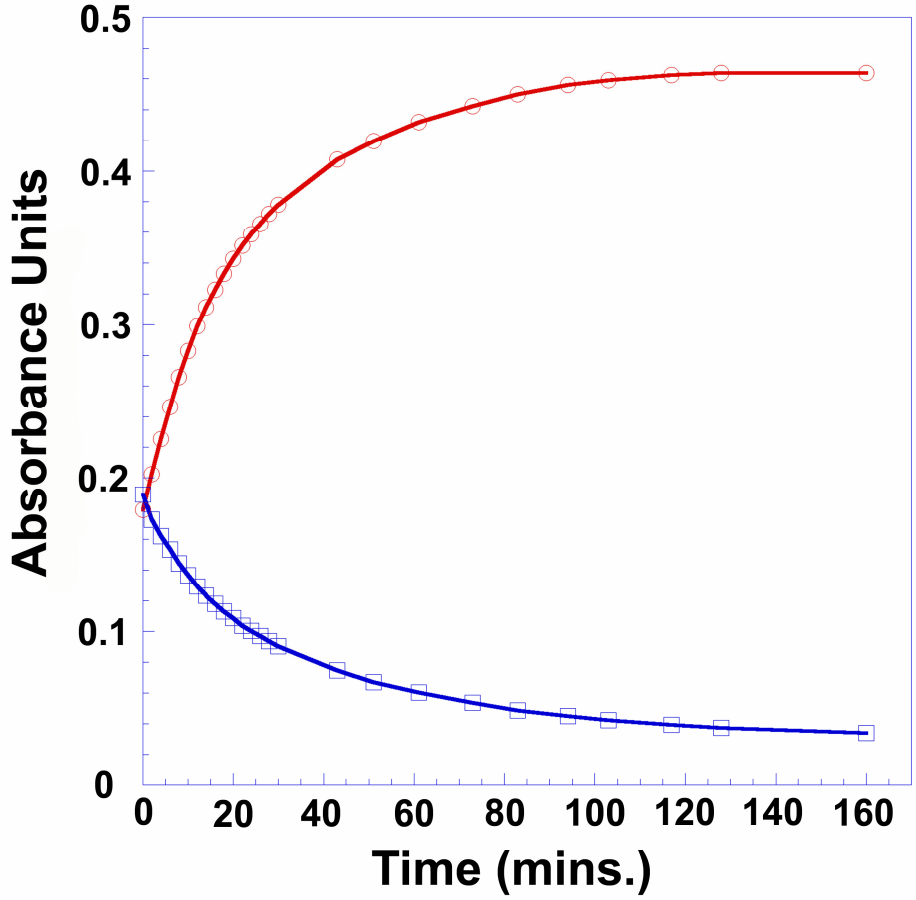

Figure 4.2: Time course of the reduction of MtmC to the Co(I) form as indicated by the increase in absorbance of the UV/Vis spectra at 386 nm (circles), and the decrease in the Co(II) form marked by the decrease in absorbance at 475 nm (squares).

Wavelength (nm)	ε [Co(I)] (mM^{-1} cm^{-1})	ε [Co(II)] (mM^{-1} cm^{-1})	Δε (mM^{-1} cm^{-1})
386	19.32	8.0	11.32
475	1.7	8.1	6.4

Table 4.1: The Δε determined for the redox corrinoid states of MtmC.

end (Figure 4.2). At the start of the reaction the corrinoid protein was in the Co(II)-MtmC form generated with Ti(III)-citrate. MtmC is not reduced to the Co(I)-form in the presence of this reductant unlike MtaC, which is reduced to Co(I) with Ti(III)-citrate (Sauer *et. al.* 1999). In the absence of MV, the Co(II)-form MtmC is stable. due to negative charge. Since all the MtmC present at the start of the reaction was in the Co(II)-form of the enzyme, and that at the end of the reaction the Co(I)-form of the enzyme was the only MtmC redox state present, the $\Delta\varepsilon$ of MtmC at 386 nm and 475 nm were determined as 11.32 mM^{-1} cm^{-1} and 6.4 mM^{-1} cm^{-1} respectively (Table 4.1). The specific activities for the activation of MtmC could be followed by both the increase in the Co(I)-form or the decrease in the Co(II)-form of MtmC. The rates determined were 14.12 ± 3.8 nmol. min^{-1}. mg^{-1} and 14.86 ± 4.6 nmol. min^{-1}. mg^{-1} for the formation of Co(I)-MtmC and the reduction of Co(II)-form MtmC respectively (Table 4.3).

4.3.3 Reductive activation of MtbC to Co(I) by RAM

The conditions used to study the reduction of MtmC spectrophotometrically, were again used to study the reduction of MtbC in the presence of RAM. The study was conducted in the presence of ATP and Ti(III)-citrate. The latter reagent converted MtbC to the Co(II)-form as signified by the presence of a strong absorbance band at 475 nm at T_0 with the absence of a strong absorbing band at 386 nm that is characteristic of the Co(I) form of the corrinoid cofactor (Figure 4.3). The Co(II) absorbance peak was found to be stable indicating that Ti(III)-citrate could not effect the further reduction of MtbC to

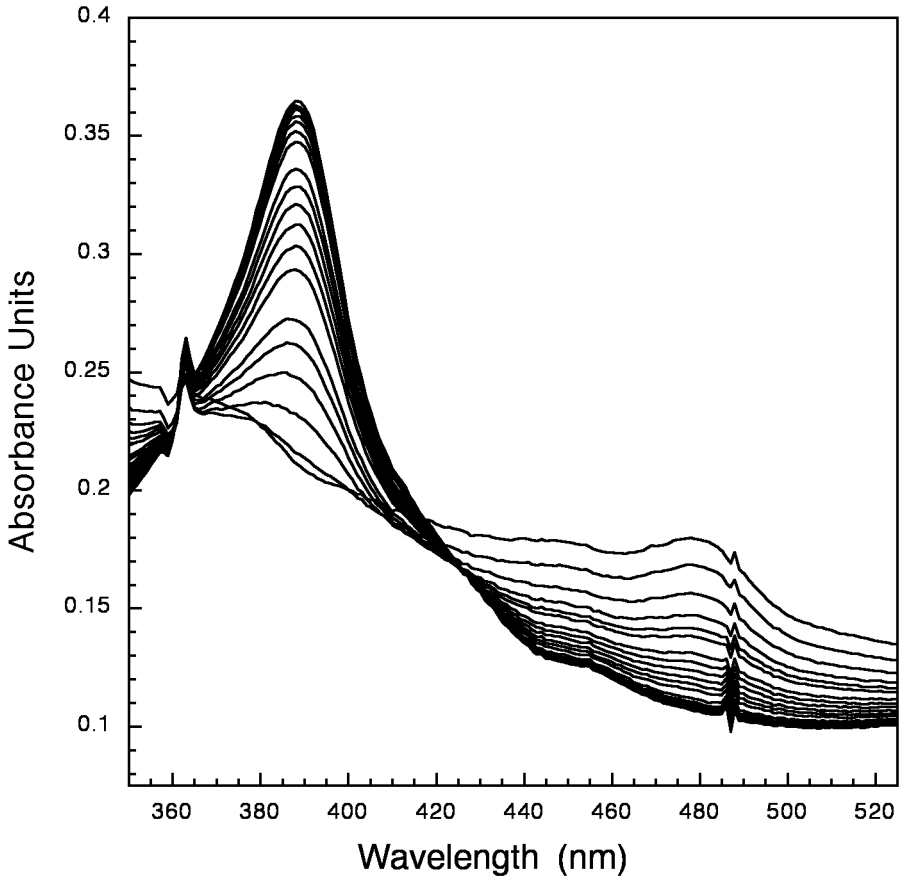

Figure 4.3: The direct reduction of MtbC by RAM. The UV/Vis spectra of MtbC in the Co(II) for at T_o and activation to the Co(I) form (T_{final}) over time in the presence of ATP and RAM. The assay cuvette contained 19 µM MtbC and 0.8 µM RAM.

Wavelength (nm)	ε [Co(I)] (mM^{-1} cm^{-1})	ε [Co(II)] (mM^{-1} cm^{-1})	Δε (mM^{-1} cm^{-1})
386	42.7	23.7	19
475	13	19.3	6.3

Table 4.2: The Δε determined for the redox corrinoid states of MtbC

Corrinoid Cofactor	Specific Activities (nmol. min^{-1}. mg^{-1})
Co(I)-MtmC formation	14.12 ± 3.8
Co(II)-MtmC reduction	14.86 ± 4.6
Co(I)-MtbC formation	8.7
Co(II)MtbC reduction	7.4

Table 4.3: Specific activities for the ATP-dependent reduction of Co(II)-MtmC and Co(II)-MtbC by RAM with the corresponding formation of Co(I)-MtmC and Co(I)-MtbC respectively. The specific activities for MtmC reduction study are based on 5 repeats of the experiment. The MtbC reduction was done twice and the specific activity indicated is an average of the two experimental repeats.

the Co(I) state. The activation was initiated with the addition of RAM (0.8 µM), and the rate of activation followed by the increase in absorbance at 386 nm corresponding to the Co(I)-form and a corresponding decrease at 475 nm over time. RAM fractions of approximately 50% purity as determined by SDS-PAGE and coomassie staining were used to study the activation of MtbC.

In order to determine the specific activity of RAM, the reduction of MtbC to the Co(I) state was allowed to go to apparent completion, as indicated by the complete loss of the 475 nm absorbance peak, and no further increase in the peak intensity at 386 nm. An isosbestic point was observed at 425 nm which was stable throughout the course of the reaction, except the spectrum obtained for T_0 where the line was mildly perturbed on the addition of RAM. No additional feature was observed on the spectrum that signified a transition occurring between the Co(II) and Co(I) forms only. The $\Delta\varepsilon$ of MtbC at 386 nm and 475 nm were determined as 19 mM^{-1} cm^{-1} and 6.3 mM^{-1} cm^{-1} respectively (Table 4.2). The specific activities for the activation of MtmC could be followed by both the increase in the Co(I)-form or the decrease in the Co(II)-form of MtmC. The rates determined were 8.7 nmol. min^{-1}. mg^{-1} and 7.4 nmol. min^{-1}. mg^{-1} for the formation of Co(I)-form MtmC and the reduction of Co(II)-form MtmC respectively (Table 4.3).

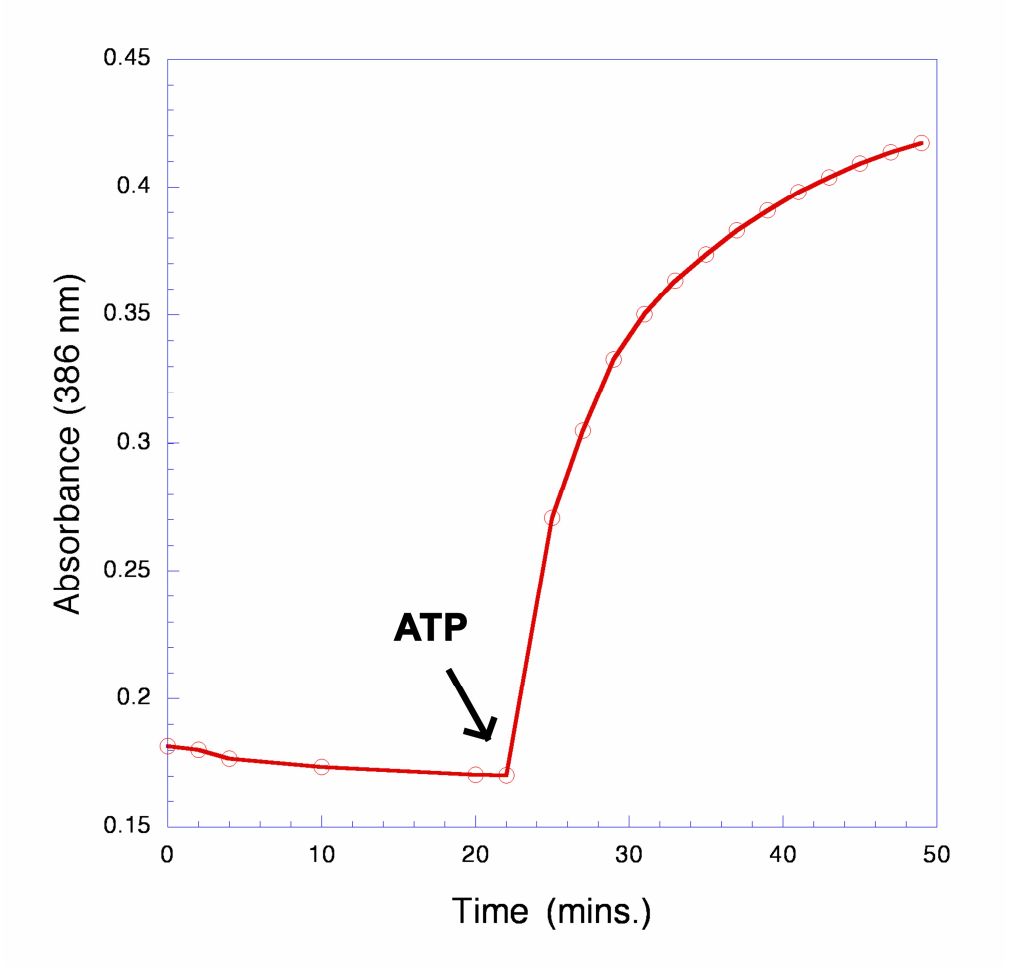

Figure 4.4: Co(II)-MtmC reduction by RAM is ATP-dependent. The RAM-dependent reduction of MtmC from the Co(II)-form to the Co(I)-form was followed by absorbance at 386 nm. The assay was initiated in the absence of ATP, followed by the addition of ATP at t = 22 mins.

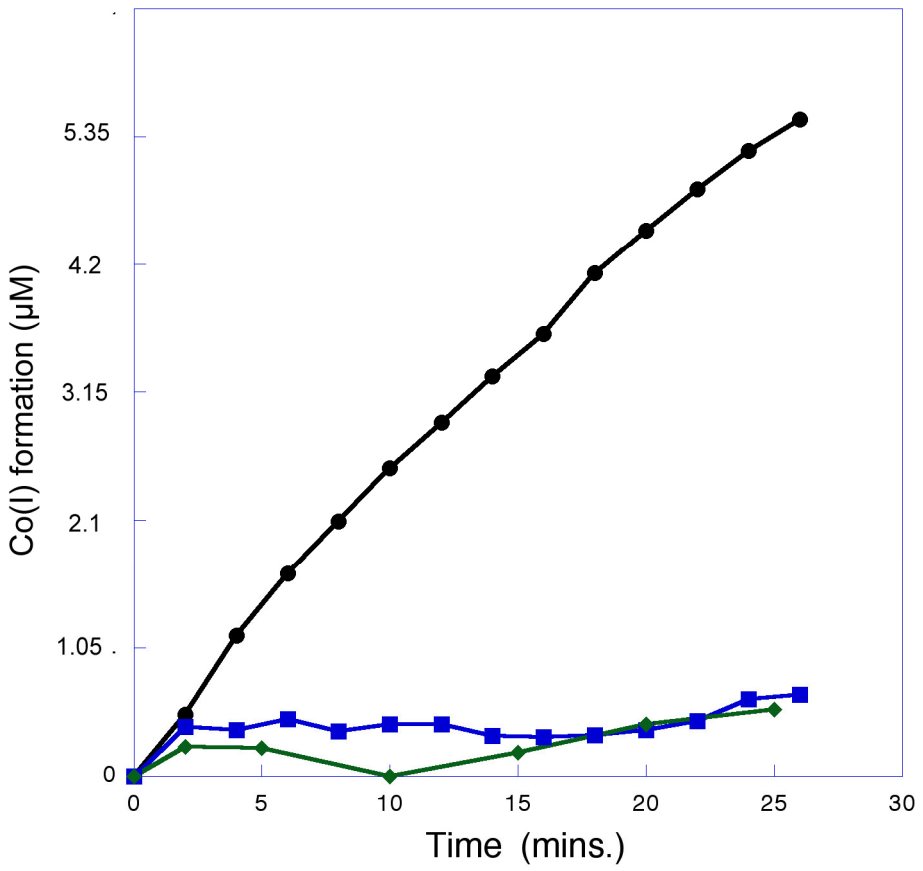

Figure 4.5: Co(II)-MtbC cannot be reduced by RAM when ATP is replaced with an ATP non-hydrolysable analog, 5'-adenylyl-β, γ-imidodiphosphate (AMP-PNP). MtbC reduction by RAM in the presence of ATP (circles), AMP-PNP (squares) and in the absence of ATP (diamonds).

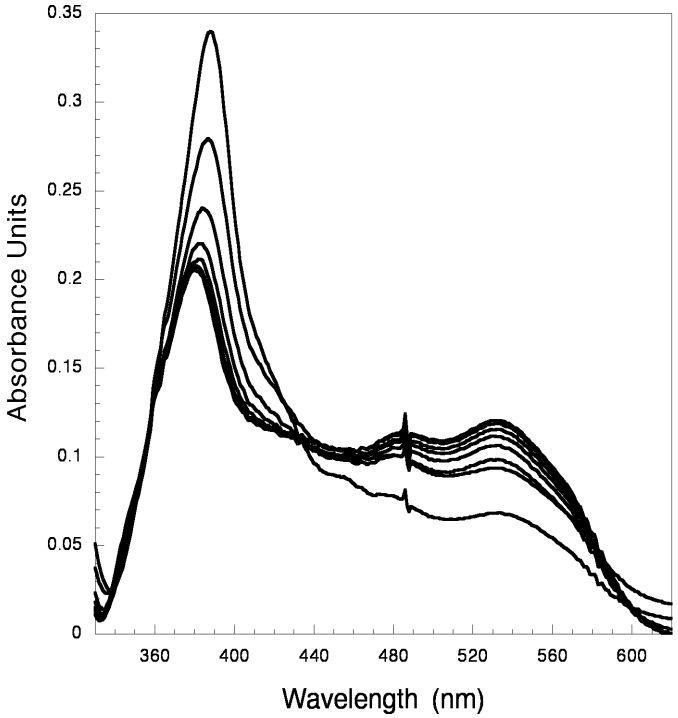

Figure 4.6: Co(I)-MtbC methylation by DMA and MtbB. Co(II)-MtbC was reduced to the Co(I)-form by RAM. This Co(I)-MtbC was present at the start (T_0). On the addition of DMA and MtbB, the spectrum shows the time-dependent conversion to the CH_3-Co(III)-MtbC form (T_{final}).

Figure 4.7: The nucleotide sequence of *ramA* from *M. barkeri* MS following PCR using primers designed based on the *ramA* nucleotide sequence in *M. barkeri* fusaro. The sequences underlined are the nucleotides that were covered by the primers from *M. barkeri* fusaro.

Figure 4.7

ramA sequence from *M. barkeri* MS

5'**ATGTATGGAATAGCACTTGATCTG**GGTACTAGCGGTTTTAGAACCCAGCT
TATTGATCTTGAAACGAAGGAAACCTTAAAGACGGTTATAACCATGGGTCAT
CCCCTCCCCGGGGGAAATGTTATGGATCACCTGGACTTTGCAATCACAACA
GGTGAAGATGTGGCTCATGAGGTAATTATCGAGACAATCAGGAGAATGTTC
CTGCAGTTCGATATTGACCTTTCAAGGGTGGAACGGCTTGCAGTCTGCGGA
AACCCTATCCAGCTTTCCCTTTTCCAGAATACTGAAATAAGGGACCTTGCCT
ATGCAGGAGAAAACAAGCAGAAGATGCTCGGAGTCCGGAATGTGAAAAGAG
ATGCCCGTGTGTTTCCTGCATCTGAAATTTTCGGAGAAAAATACCTGTCTAA
CTGTGAAATCATCGTACCCCCTGCAATAAAGCACGAGATTGGAGCTGACGC
CCTGGCTATGATGCTTGAAACCGATTTTCTTATCCAGCCCGAACCTTCGCTT
GTCACGGATTACGGAACAAATGCCGAAATGGCTCTGAAAATCGGGGATCGA
ATTATCACTGCAAGCGCAGCAGCAGGACCTGCGATTGAAGGACAGGGTATA
AGTTCAGGCATGCTCGCAAGTCCTGGCGCGATCTGTGATGTAAAACCTGAA
GGACAGTACTGGAGAATTATAGTTCTTGACAGGGAAATGGAGAAACAGGAC
GCTTATCTTATCGATCCGGTTAAAGGGGAGATAAAGGATTCCTACGGATTCG
AAGCCGTCGGAATCACAGGCACAGGAGTTATCTCGGCTTTTGCCATGGCAC
TGAAAGGTGGGCTGATTGAAAAATTTCCTAAACTTCCAAATGGAAAACTGAT
CCTGGGTCCTGGGATTGAGATCACTGAAAAGGATGTCGAAGAGGCCGGAA
AGGCTATCGGGGCAATCCGTGCAGCCCATATGACCCTAATCGTTGAATCCG
GAATCAAGTACGAAGACCTGGAATACGCATATATGTCAGGAGCCTCCGGAG
CCTATGTGGACGCTGAAGACGCCCGCAGGCTTGGAGCCGCACCGGGTTAT
GCAAAAAAAATTGTTCAGTTCGGAAATACCTCGCTTGCACTTGCTCGGGAAC
TTGTGCTGGAAAAATCCAGGTTGGATGACGTAATTGAGATTGCAAAGAAAAT
TACTGCCGACCACCTTATGATGGCGACAAGCGAGACTTTCAATAATTTCTAC
CTCTGCGAGCTTTCCTACTGGACTCAGGGCATGCCACTTGAGACGTATGAC
CAGATGCTTGAACTCTACGGCCTGCCTCCTCTTCCAAAAATTCTCGAACATG
TAACCATCGAAAAGCGAGTCAGCAAAGACATAGAAGAGGTCGGGTCAGGTG
GGCTTTCCATTCTCAAAGAAATTGGCATAATCCTTGAAGTCCCGGTTGAAAA
GTGCGTCTACTGCAAAAAATGTGTAAAAGAATGCCCAGAAGCTGCTCTTGAA
ATTGTAGAAAGAGATGGGCAAAGAATCGCAAAATACGACAGCCAGAAATGT
CTTGGTACAAGCTGCCGCCGCTGTGTCGGTGTCTGCCCCGAAGATGCTATC
GATATAACG**AAACTGAAAATCACAGCGAAATAA**-3'

Figure 4.8: The protein sequence of RAM from *M. barkeri* MS. The sequence shows the presence of two iron-sulfur cluster binding motifs in the C-terminal region highlighted by boxes. The underlined residues are those covered by the primers of *M. barkeri* Fusaro primers.

Figure 4.8

Protein sequence of RamA *M.barkeri* MS

M Y G I A L D L G T S G F R T Q L I D L E T K E T L K T V I T M G H P L P G G

N V M D H L D F A I T T G E D V A H E V I I E T I R R M F L Q F D I D L S R V

E R L A V C G N P I Q L S L F Q N T E I R D L A Y A G E N K Q K M L G V R N

V K R D A R V F P A S E I F G E K Y L S N C E I I V P P A I K H E I G A D A L A

M M L E T D F L I Q P E P S L V T D Y G T N A E M A L K I G D R I I T A S A A

A G P A I E G Q G I S S G M L A S P G A I C D V K P E G Q Y W R I I V L D R

E M E K Q D A Y L I D P V K G E I K D S Y G F E A V G I T G T G V I S A F A M

A L K G G L I E K F P K L P N G K L I L G P G I E I T E K D V E E A G K A I G A

I R A A H M T L I V E S G I K Y E D L E Y A Y M S G A S G A Y V D A E D A R

R L G A A P G Y A K K I V Q F G N T S L A L A R E L V L E K S R L D D V I E I

A K K I T A D H L M M A T S E T F N N F Y L C E L S Y W T Q G M P L E T Y D

Q M L E L Y G L P P L P K I L E H V T I E K R V S K D I E E V G S G G L S I L

K E I G I I L E V P V E K C V Y C K K C V K E C P E A A L E I V E R D G Q R

I A K Y D S Q K C L G T S C R R C V G V C P E D A I D I T K L K I T A K

Stop

4.3.4 RAM-mediated reductive activation is strictly dependent on the presence of ATP

The activation of both MtmC and MtbC in the presence of RAM and Ti(III)-citrate were dependent on the presence of ATP. As shown in Figure 4.4, Co(II)-form MtmC in the presence of RAM and Ti(III)-citrate, but in the absence of ATP, showed no activation to the Co(I)-form as there was increase in absorbance over time at 386 nm. At t = 22 mins, 4.5 mM ATP was added to the reaction, and an increase in Co(I)-form MtmC was observed thus proving the absolute requirement of ATP in the reductive activation of Co(II)-MtmC.

Similarly, the activation of MtbC was also dependent on the presence of ATP. Furthermore, MtbC initially reduced to the Co(II)-form with Ti(III)-citrate, was used to study the possible substitution of other nucleotides such as ADP or the non-hydrolysable analog of ATP, AMP-PNP for ATP in this reaction. Activation assays were performed for MtbC in the presence of the aforementioned nucleotides, and no Co(II)-form to Co(I)-form conversion was observed as shown in Figure 4.5.

4.3.5 MtbB-dependent methylation of Co(I)-MtbC in the presence of DMA

The methylation of Co(I)-form MtbC was studied spectrophotometrically in the presence of MtbB and substrate, DMA. At t = 0 mins, Co(I) form of MtbC was observed on the reductive activation in the presence of RAM, Ti(III)-citrate and ATP as the spectra showed the presence of a predominant 386 nm peak. On the addition of MtbB and substrate DMA, a shift in the spectra was observed to 352

nm and a second one at approximately 532 nm which is typical of the Co(III)-methyl form of corrinoid proteins (Steve Burke PhD thesis, 1997, Banerjee et. al. 1990 (c), Fleischhacker *et. al.* 1997, Cao et. al. 1991) (Figure 4.6). The spectrum shows the presence of an isosbestic point at 430 nm, which remained stable throughout the course of the experiment, except for the initial spectrum which was perturbed by the addition of DMA to the assay mixture.

4.3.6 Determination of the molecular mass of RAM

The molecular weight of RAM was determined by size-exclusion chromatography. A Sephacryl-S 200 HR column was used, and molecular weight standards ranging from β-amylase (200 kDa) to carbonic anhydrase (29 kDa) were chromatographed to develop a standard curve. RAM was also chromatographed, and using the standard curve, the molecular weight of the native protein was determined to be 64 kDa. To confirm the molecular weight of the RAM monomer, SDS-PAGE analysis followed by coomassie staining was carried out. The molecular weight was carried out and determined to be 64 kDa.

4.3.7 RAM protein sequence shows the presence of ATP-binding motif and domains for binding iron-sulfur clusters

When RAM was first isolated by Tsuneo Ferguson, the sequence of the first few residues of the N-terminus was determined to be MYGIALNL. Based on this data, the N-terminus sequence of RAM in *M. barkeri* Fusaro was identified to be MYGIALNLGTSGFRTQLINLETKETLKTVITMGHPLPGGN (Tsuneo Ferguson,

unpublished data). The protein sequence was used to identify RAM homologs in the genomes of *Methanosarcina mazei* as well as the incomplete genome of *M. barkeri* Fusaro. Four RAM homologs were identified in *M. barkeri*. Using this information, primers were designed for PCR of the RAM-encoding gene in *M. barkeri* MS present near the monomethylamine methyltransferase genes, as well as the *pyl* gene cluster, using the genome sequence of *M. bakeri* Fusaro. This gene was designated *ramA*.

Following PCR of the *ramA* gene and sequencing (Figure 4.7), the gene was found to be 98% similar to the *ramA* gene in *M. barkeri* Fusaro. The N-terminus of the protein sequence shows the presence of a motif that play a role in binding ATP-phosphates similar to that of benzoyl CoA reductase subunit, BcrD (Boll *et. al.* 1995, Boll *et. al.* 1997) and a subunit of the 2-hydroxyglutaryl-CoA dehydratase, HdgC (Buckel *et. al.* 2004, Hans *et. al.* 2002). The C-terminus of the protein shows the presence of two 4Fe-4S type iron-sulfur cluster motifs (Figure 4.8). This is consistent with previous data that RAM contains 7 Fe and 8 acid-labile sulfurs (Tsuneo Ferguson, unpublished data).

4.4 DISCUSSION

The oxidative inactivation of methyltransferase corrinoid cofactors in cells to the Co(II) state has led to the evolution of different reductive activation systems. In the case of methionine synthase, the activation of Co(II)-form of the cobalamin-binding to the Co(III)-CH_3 form is catalyzed by the methyl donor S-

adenosylmethionine and reduced flavodoxin in *E. coli* (Banerjee *et. al.* 1990 (a), Jarrett *et. al.* 1998, Fujii *et. al.* 1974). In humans, the low potential electron donor is methionine synthase reductase (Olteanu *et. al.* 2001). The reduction requires the cobalt cofactor to be in a benzimidazole-off, His-off form, which makes the reduction more favorable by raising the redox potential of the Co(II)/Co(I) couple. It has been shown that upon the binding of flavodoxin, the Co(II) cofactor goes from the 5-coordinate to the 4-coordinate form with the protonation of the lower axial histidine ligand (Hoover *et. al.* 1997). This transition from the 5-coordinate state to the 4-coordinate state is not required in the acetogenic corrinoid iron-sulfur protein (CFeSP), which is isolated in the 4-coordinate Co(II) state. A low potential ferredoxin transfers an electron to the iron-sulfur cluster in the AcsC subunit of CFeSP, which is turn reduces the corrinoid cofactor to the 4-corodinate Co(I) state (Menon *et. al.* 1999).

RAM is novel class of corrinoid protein-activating enzyme. During isolation, RAM was found in low yields, which is consistent with the low levels of oxidative inactivation of corrinoid proteins. In methionine synthase, it was estimated that oxidative inactivation occurs once every 2000 turnovers (Drummond *et. al.* 1993). The results of this study indicates that RAM and ATP are two requirements in the unfavorable reduction of methylamine-corrinoid proteins MtmC and MtbC in the presence of a reducing agent Ti(III)-citrate. Unlike, the MAP protein, RAM appears to be a monomer in solution. RAM is irreversibly inactivated in the presence of oxygen. This is likely due to the presence of two iron-sulfur clusters which may be prone to disruption in the C-

terminal domain of the polypeptide as shown by the sequenced gene of *ramA.* The presence of these metal clusters was confirmed by the studying iron and sulfur content of the protein conducted by Tsuneo Ferguson and shown to have two 4Fe-4S or one 3Fe-4S and one 4Fe-4S clusters. MAP on the other hand was concluded to be lacking any iron-sulfur clusters, as spectra of the purified preparations did not indicate the presence of a UV-Vis detectable cofactor. RAM can directly reduce Co(II)-MtmC to Co(I)-MtmC, which differs from MAP which was shown to play a role is affecting the co-ordination state of the cobalt center in MtaC. MAP was suggested to change the Co(II)-form of MtaC from the 5-coordinate to the 4-coordinate state, following which the cobalt center was proposed to be reduced to Co(I) in the presence of H_2 and fractions of hydrogenase, ferredoxin. Thus RAM and MAP achieve reductive activation of the MtmC and MtaC respectively by different mechanisms.

The data shows that RAM protein directly reduces methylamine corrinoid proteins from the Co(II)-form to the active Co(I)-form, and thus activates them as substrates for methylamine methyltransferases. The activity Co(I)-MtbC was confirmed by showing that it was now an active substrate for MtbB methylation with DMA. This spectrophotometric assay has now been adapted to study methylation of MtmC by MtmB in the presence of MMA (Dave personal communication). The activation rates for both MtmC and MtbC are likely to be very similar as the rate observed during the activation of MtbC was achieved with 50% pure RAM protein. Thus, RAM is unlikely to discriminate between methylamine-corrinoid proteins when it comes to activation, and the three

corrinoid proteins are likely to share similar structural elements that are recognized and bound by RAM. This is feasible given the close sequence similarity between the methylamine corrinoid proteins and studies done by Tsuneo Ferguson showing that RAM is required to stimulate MMA, DMA and TMA-dependent CoM methyl transfer.

Similar to the MAP enzyme, RAM-dependent activation appears to be strictly dependent on the presence of ATP. The addition of a non-hydrolysable ATP analog, AMP-PNP did not allow for the reduction of the DMA corrinoid protein in the presence of RAM and Ti(III)-citrate. Thus ATP-hydrolysis is likely a part of the activation mechanism. The inclusion of ADP did not allow for activation.

There are a few hypotheses for the mechanism of RAM mediated reduction of corrinoid proteins. Firstly, it is possible that RAM could bind ATP, which causes a conformational change which allows it to bind to the corrinoid protein. The binding could cause the corrinoid protein to change from a 5-coordinate base-off His-on Co(II)-form to the 4-coordinate base-off, His-off Co(II)-form, followed by the reduction of the cobalt cofactor to the Co(I)-form. This is practical possibility as the change in conformation from five-coordinate to four-coordinate corrinoid cofactors raises the potential of the Co(II)/Co(I) couple, making the reduction more feasible. It is possible that much like the case with NifH, RAM could bind ATP, and on hydrolysis, the iron-sulfur clusters are exposed to solvent owing to a conformational change. The ATP-binding motifs of RAM are similar to those of the ASKHA (acetate and sugar kinase/ Hsc 70/ actin)

family of proteins binding ATP. These domains are known to bind ATP, the result of which likely causes conformational change.

The data does not rule out the possibility that RAM on binding and hydrolyzing ATP only causes the corrinoid protein to change to the four-coordinate base-off, His-off Co(II)-form, and a second reducing agent transfers electrons to the cobalt center causing the reduction of the corrinoid protein to the Co(I)-state. It has yet to be demonstrated that pre-reduced RAM can achieve the reduction of Co(II) to Co(I). ATP hydrolysis may take the overall catalyzed reaction over a thermodynamic barrier that helps the reduction reaction to move in the forward direction. A binding and hydrolysis of ATP could cause a change in conformation of the corrinoid protein, either raising the potential of the Co(II)/Co(I) couple, or causing a conformation allowing for binding of RAM. However, given the presence of an ATP-binding domain in the N-terminal of the RAM polypeptide, and the absence of such a motif in the gene of MtmC, this mechanism is unlikely.

Regardless of the mechanism of action, the demonstration that RAM can activate corrinoid proteins as substrates for methylamine methyltransferases will enable assays which directly examine methylation of the corrinoid protein in a highly resolved system. Such assays will be key to future examination of the catalytic mechanism of methylamine methyltransferases, and thereby yield insight into why the functions of these proteins required the recruitment of a novel amino acid into the genetic code of methanogens.

LIST OF REFERENCES

Armstrong, R. N. 2000. Mechanistic diversity in a metalloenzyme superfamily. Biochemistry **39:**13625-32.

Banerjee, R. V., and R. G. Matthews. 1990 (c). Cobalamin-dependent methionine synthase. Faseb J **4:**1450-9.

Banerjee, R., and S. W. Ragsdale. 2003. The many faces of vitamin B12: catalysis by cobalamin-dependent enzymes. Annu Rev Biochem **72:**209-47.

Banerjee, R. V., S. R. Harder, S. W. Ragsdale, and R. G. Matthews. 1990 (a). Mechanism of reductive activation of cobalamin-dependent methionine synthase: an electron paramagnetic resonance spectroelectrochemical study. Biochemistry **29:**1129-35.

Banerjee, R. V., V. Frasca, D. P. Ballou, and R. G. Matthews. 1990 (b). Participation of cob(I) alamin in the reaction catalyzed by methionine synthase from Escherichia coli: a steady-state and rapid reaction kinetic analysis. Biochemistry **29:**11101-9.

Blaut, M. 1994. Metabolism of methanogens. Antonie Van Leeuwenhoek **66:**187-208.

Blight, S. K., R. C. Larue, A. Mahapatra, D. G. Longstaff, E. Chang, G. Zhao, P. T. Kang, K. B. Green-Church, M. K. Chan, and J. A. Krzycki. 2004. Direct charging of tRNA(CUA) with pyrrolysine in vitro and in vivo. Nature **431:**333-5.

Boll, M., and G. Fuchs. 1995. Benzoyl-coenzyme A reductase (dearomatizing), a key enzyme of anaerobic aromatic metabolism. ATP dependence of the reaction, purification and some properties of the enzyme from Thauera aromatica strain K172. Eur J Biochem **234:**921-33.

Boll, M., S. S. Albracht, and G. Fuchs. 1997. Benzoyl-CoA reductase (dearomatizing), a key enzyme of anaerobic aromatic metabolism. A study of adenosinetriphosphatase activity, ATP stoichiometry of the reaction and EPR properties of the enzyme. Eur J Biochem **244:**840-51.

Boone, D. R., W. B. Whitman, and P. Rouviere. 1993. Diversity and Taxonomy of Methanogens. p. 35-80. *In* James G. Ferry (ed.), Methanogenesis. Ecology, Physiology, Biochemistry, and Genetics. Chapman & Hall. New York.

Breaux, G. A., K. B. Green-Church, A. France, and P. A. Limbach. 2000. Surfactant-aided, matrix-assisted laser desorption/ionization mass spectrometry of hydrophobic and hydrophilic peptides. Anal Chem **72:**1169-74.

Buckel, W., M. Hetzel, and J. Kim. 2004. ATP-driven electron transfer in enzymatic radical reactions. Curr Opin Chem Biol **8:**462-7.

Burke, S.A. 1997. Methanogenesis from monomethylamine: Biochemical and molecular characterization of the monomethylamine:coenzyme M methyl transfer activity in Methanosarcina barkeri. PhD thesis, The Ohio State University, Columbus, OH.

Burke, S. A., and J. A. Krzycki. 1995. Involvement of the "A" isozyme of methyltransferase II and the 29-kilodalton corrinoid protein in methanogenesis from monomethylamine. J Bacteriol **177:**4410-6.

Burke, S. A., and J. A. Krzycki. 1997. Reconstitution of Monomethylamine:Coenzyme M methyl transfer with a corrinoid protein and two methyltransferases purified from Methanosarcina barkeri. J Biol Chem **272:**16570-7.

Burke, S. A., S. L. Lo, and J. A. Krzycki. 1998. Clustered genes encoding the methyltransferases of methanogenesis from monomethylamine. J Bacteriol **180:**3432-40.

Cao, X. J., and J. A. Krzycki. 1991. Acetate-dependent methylation of two corrinoid proteins in extracts of Methanosarcina barkeri. J Bacteriol **173:**5439-48.

Christen, P., and P. K. Mehta. 2001. From cofactor to enzymes. The molecular evolution of pyridoxal-5'-phosphate-dependent enzymes. Chem Rec **1:**436-47.

Christenson, S. D., W. Wu, M. A. Spies, B. Shen, and M. D. Toney. 2003(a). Kinetic analysis of the 4-methylideneimidazole-5-one-containing tyrosine aminomutase in enediyne antitumor antibiotic C-1027 biosynthesis. Biochemistry **42:**12708-18.

Christenson, S. D., W. Liu, M. D. Toney, and B. Shen. 2003(b). A novel 4-methylideneimidazole-5-one-containing tyrosine aminomutase in enediyne antitumor antibiotic C-1027 biosynthesis. J Am Chem Soc **125:**6062-3.

Copeland, P. R., and D. M. Driscoll. 2001. RNA binding proteins and selenocysteine. Biofactors **14:**11-6.

Daas, P. J., R. W. Wassenaar, P. Willemsen, R. J. Theunissen, J. T. Keltjens, C. van der Drift, and G. D. Vogels. 1996(a). Purification and properties of an enzyme involved in the ATP-dependent activation of the methanol:2-mercaptoethanesulfonic acid methyltransferase reaction in Methanosarcina barkeri. J Biol Chem **271:**22339-45.

Daas, P. J., W. R. Hagen, J. T. Keltjens, C. van der Drift, and G. D. Vogels. 1996(b). Activation mechanism of methanol:5-hydroxybenzimidazolylcobamide methyltransferase from Methanosarcina barkeri. J Biol Chem **271:**22346-51.

Deppenmeier, U. 2002. The unique biochemistry of methanogenesis. Prog Nucleic Acid Res Mol Biol **71:**223-83.

Deppenmeier, U., T. Lienard, and G. Gottschalk. 1999. Novel reactions involved in energy conservation by methanogenic archaea. FEBS Lett **457:**291-7.

DiMarco, A. A., T. A. Bobik, and R. S. Wolfe. 1990. Unusual coenzymes of methanogenesis. Annu Rev Biochem **59:**355-94.

Dove, J. E., and J. P. Klinman. 2001. Trihydroxyphenylalanine quinone (TPQ) from copper amine oxidases and lysyl tyrosylquinone (LTQ) from lysyl oxidase. Adv Protein Chem **58:**141-74.

Drennan, C. L., S. Huang, J. T. Drummond, R. G. Matthews, and M. L. Lidwig. 1994. How a protein binds B12: A 3.0 A X-ray structure of B12-binding domains of methionine synthase. Science **266:**1669-74.

Drummond, J. T., R. R. Loo, and R. G. Matthews. 1993(a). Electrospray mass spectrometric analysis of the domains of a large enzyme: observation of the occupied cobalamin-binding domain and redefinition of the carboxyl terminus of methionine synthase. Biochemistry **32:**9282-9.

Drummond, J. T., S. Huang, R. M. Blumenthal, and R. G. Matthews. 1993(b). Assignment of enzymatic function to specific protein regions of cobalamin-dependent methionine synthase from Escherichia coli. Biochemistry **32:**9290-5.

Ermler, U., W. Grabarse, S. Shima, M. Goubeaud, and R. K. Thauer. 1997. Crystal structure of methyl-coenzyme M reductase: the key enzyme of biological methane formation. Science **278:**1457-62.

Evans, J. C., D. P. Huddler, M. T. Hilgers, G. Romanchuk, R. G. Matthews, and M. L. Ludwig. 2004. Structures of the N-terminal modules imply large domain motions during catalysis by methionine synthase. Proc Natl Acad Sci U S A **101:**3729-36.

Ferguson, D. J., Jr., and J. A. Krzycki. 1997. Reconstitution of trimethylamine-dependent coenzyme M methylation with the trimethylamine corrinoid protein and the isozymes of methyltransferase II from Methanosarcina barkeri. J Bacteriol **179:**846-52.

Ferguson, D. J., Jr., N. Gorlatova, D. A. Grahame, and J. A. Krzycki. 2000. Reconstitution of dimethylamine:coenzyme M methyl transfer with a discrete corrinoid protein and two methyltransferases purified from Methanosarcina barkeri. J Biol Chem **275:**29053-60.

Ferry, J. G. 1999. Enzymology of one-carbon metabolism in methanogenic pathways. FEMS Microbiol Rev **23:**13-38.

Firbank, S. J., M. S. Rogers, C. M. Wilmot, D. M. Dooley, M. A. Halcrow, P. F. Knowles, M. J. McPherson, and S. E. Phillips. 2001. Crystal structure of the precursor of galactose oxidase: an unusual self-processing enzyme. Proc Natl Acad Sci U S A **98:**12932-7.

Fleischhacker, A. S., and R. G. Matthews. 2007. Ligand trans influence governs conformation in cobalamin-dependent methionine synthase. Biochemistry **46:**12382-92.

Fujii, K., and F. M. Huennekens. 1974. Activation of methionine synthetase by a reduced triphosphopyridine nucleotide-dependent flavoprotein system. J Biol Chem **249:**6745-53.

Galagan, J. E., C. Nusbaum, A. Roy, M. G. Endrizzi, P. Macdonald, W. FitzHugh, S. Calvo, R. Engels, S. Smirnov, D. Atnoor, A. Brown, N. Allen, J. Naylor, N. Stange-Thomann, K. DeArellano, R. Johnson, L. Linton, P. McEwan, K. McKernan, J. Talamas, A. Tirrell, W. Ye, A. Zimmer, R. D. Barber, I. Cann, D. E. Graham, D. A. Grahame, A. M. Guss, R. Hedderich, C. Ingram-Smith, H. C. Kuettner, J. A. Krzycki, J. A. Leigh, W. Li, J. Liu, B. Mukhopadhyay, J. N. Reeve, K. Smith, T. A. Springer, L. A. Umayam, O. White, R. H. White, E. Conway de Macario, J. G. Ferry, K. F. Jarrell, H. Jing, A. J. Macario, I. Paulsen, M. Pritchett, K. R. Sowers, R. V. Swanson, S. H. Zinder, E. Lander, W. W. Metcalf, and B. Birren. 2002. The genome of M. acetivorans reveals extensive metabolic and physiological diversity. Genome Res **12:**532-42.

Goulding, C. W., D. Postigo, and R. G. Matthews. 1997. Cobalamin-dependent methionine synthase is a modular protein with distinct regions for binding homocysteine, methyltetrahydrofolate, cobalamin, and adenosylmethionine. Biochemistry **36:**8082-91.

Hamilton, G. A., and F. H. Westheimer. 1959. On the mechanism of the enzymatic decarboxylation of acetoacetate. J. Am. Chem. Soc. **81:** 6332.

Hans, M., E. Bill, I. Cirpus, A. J. Pierik, M. Hetzel, D. Alber, and W. Buckel. 2002. Adenosine triphosphate-induced electron transfer in 2-hydroxyglutaryl-CoA dehydratase from Acidaminococcus fermentans. Biochemistry **41:**5873-82.

Hao, B., G. Zhao, P. T. Kang, J. A. Soares, T. K. Ferguson, J. Gallucci, J. A. Krzycki, and M. K. Chan. 2004. Reactivity and chemical synthesis of L-pyrrolysine- the 22(nd) genetically encoded amino acid.

Hao, B., W. Gong, T. K. Ferguson, C. M. James, J. A. Krzycki, and M. K. Chan. 2002. A new UAG-encoded residue in the structure of a methanogen methyltransferase. Science **296:**1462-6.

Hodgkin, D. C., J. Kamper, M. Mackay, J. Pickworth, K. N. Trueblood, and J. G. White. 1956. Structure of vitamin B12. Nature **178:**64-6.

Harder, S. R., W. P. Lu, B. A. Feinberg, and S. W. Ragsdale. 1989. Spectroelectrochemical studies of the corrinoid/iron-sulfur protein involved in acetyl coenzyme A synthesis by Clostridium thermoaceticum. Biochemistry **28:**9080-7.

Hoover, D. M., and M. L. Ludwig. 1997(a). A flavodoxin that is required for enzyme activation: the structure of oxidized flavodoxin from Escherichia coli at 1.8 A resolution. Protein Sci **6:**2525-37.

Hoover, D. M., J. T. Jarrett, R. H. Sands, W. R. Dunham, M. L. Ludwig, and R. G. Matthews. 1997(b). Interaction of Escherichia coli cobalamin-dependent methionine synthase and its physiological partner flavodoxin: binding of flavodoxin leads to axial ligand dissociation from the cobalamin cofactor. Biochemistry **36:**127-38.

James, C. M., T. K. Ferguson, J. F. Leykam, and J. A. Krzycki. 2001. The amber codon in the gene encoding the monomethylamine methyltransferase isolated from Methanosarcina barkeri is translated as a sense codon. J Biol Chem **276:**34252-8.

Jarrett, J. T., D. M. Hoover, M. L. Ludwig, and R. G. Matthews. 1998. The mechanism of adenosylmethionine-dependent activation of methionine synthase: a rapid kinetic analysis of intermediates in reductive methylation of Cob(II)alamin enzyme. Biochemistry **37:**12649-58.

Kaufmann, F., G. Wohlfarth, and G. Diekert. 1998. O-demethylase from Acetobacterium dehalogenans--substrate specificity and function of the participating proteins. Eur J Biochem **253:**706-11.

Ketjens, J. T., and G. D. Vogels. 1993. Conversion of methanol and methylamines to methane and carbon dioxide. p. 253-304. . *In* James G. Ferry (ed.), Methanogenesis. Ecology, Physiology, Biochemistry, and Genetics. Chapman & Hall. New York.

Krzycki, J. A. 2004. Function of genetically encoded pyrrolysine in corrinoid-dependent methylamine methyltransferases. Curr Opin Chem Biol **8:**484-91.

Krzycki, J. A. 2005. The direct genetic encoding of pyrrolysine. Curr Opin Microbiol **8:**706-12.

Krzycki, J. A., L. E. Mortenson, and R. C. Prince. 1989. Paramagnetic centers of carbon monoxide dehydrogenase from aceticlastic Methanosarcina barkeri. J Biol Chem **264:**7217-21.

Kunz, R. C., Y. C. Horng, and S. W. Ragsdale. 2006. Spectroscopic and kinetic studies of the reaction of bromopropanesulfonate with methyl-coenzyme M reductase. J Biol Chem **281:**34663-76.

Leigh, J. A., K. L. Rinehart, Jr., and R. S. Wolfe. 1985. Methanofuran (carbon dioxide reduction factor), a formyl carrier in methane production from carbon dioxide in Methanobacterium. Biochemistry **24:**995-9.

Longstaff, D. G., R. C. Larue, J. E. Faust, A. Mahapatra, L. Zhang, K. B. Green-Church, and J. A. Krzycki. 2007 (a). A natural genetic code expansion cassette enables transmissible biosynthesis and genetic encoding of pyrrolysine. Proc Natl Acad Sci U S A **104:**1021-6.

Longstaff, D. G., S. K. Blight, L. Zhang, K. B. Green-Church, and J. A. Krzycki. 2007 (b). In vivo contextual requirements for UAG translation as pyrrolysine. Mol Microbiol **63:**229-41.

Lu-Chang, A. L. 2006. Isolation and analyses of MutY homologs (MYH). Methods Enzymol **408:**64-78.

Lukatela, G., N. Krauss, K. Theis, T. Selmer, V. Gieselmann, K. von Figura, and W. Saenger. 1998. Crystal structure of human arylsulfatase A: the aldehyde function and the metal ion at the active site suggest a novel mechanism for sulfate ester hydrolysis. Biochemistry **37:**3654-64.

Mahapatra, A., A. Patel, J. A. Soares, R. C. Larue, J. K. Zhang, W. W. Metcalf, and J. A. Krzycki. 2006. Characterization of a Methanosarcina acetivorans mutant unable to translate UAG as pyrrolysine. Mol Microbiol **59:**56-66.

Marchesi, J. R., A. J. Weightman, B. A. Cragg, R. J. Parkes, and J. C. Fry. 2001. Methanogen and bacterial diversity and distribution in deep gas hydrate sediments from the Cascadia Margin as revealed by 16S rRNA molecular analysis. FEMS Microbiol Ecol **34:**221-228.

Matthews, R. G. 2001. Cobalamin-dependent methyltransferases. Acc Chem Res **34:**681-9.

Matthews, R. G., R. V. Banerjee, and S. W. Ragsdale. 1990. Cobamide-dependent methyl transferases. Biofactors **2:**147-52.

Maymo-Gatell, X., V. Tandoi, J. M. Gossett, and S. H. Zinder. 1995. Characterization of an H2-utilizing enrichment culture that reductively dechlorinates tetrachloroethene to vinyl chloride and ethene in the absence of methanogenesis and acetogenesis. Appl Environ Microbiol **61:**3928-33.

Menon, S., and S. W. Ragsdale. 1998. Role of the [4Fe-4S] cluster in reductive activation of the cobalt center of the corrinoid iron-sulfur protein from Clostridium thermoaceticum during acetate biosynthesis. Biochemistry **37:**5689-98.

Menon, S., and S. W. Ragsdale. 1999. The role of an iron-sulfur cluster in an enzymatic methylation reaction. Methylation of CO dehydrogenase/acetyl-CoA synthase by the methylated corrinoid iron-sulfur protein. J Biol Chem **274:**11513-8.

Morris, A. J., R. C. Davenport, and D. R. Tolan. 1996. A lysine to arginine substitution at position 146 of rabbit aldolase A changes the rate-determining step to Schiff base formation. Protein Eng **9:**61-7.

Namy, O., J. P. Rousset, S. Napthine, and I. Brierley. 2004. Reprogrammed genetic decoding in cellular gene expression. Mol Cell **13:**157-68.

Olteanu, H., and R. Banerjee. 2001. Human methionine synthase reductase, a soluble P-450 reductase-like dual flavoprotein, is sufficient for NADPH-dependent methionine synthase activation. J Biol Chem **276:**35558-63.

Paul, L. 2000**.** Analysis of the Genes Encoding the Enzymes Initiating Methanogenesisfrom Methlthiols, Trimethylamine, and Dimethylamine in Methanosarcina barkeri MS. Ph.D. thesis, Ohio State University, Columbus, OH

Paul, L., D. J. Ferguson, Jr., and J. A. Krzycki. 2000. The trimethylamine methyltransferase gene and multiple dimethylamine methyltransferase genes of Methanosarcina barkeri contain in-frame and read-through amber codons. J Bacteriol **182:**2520-9.

Paul, L., and J. A. Krzycki. 1996. Sequence and transcript analysis of a novel Methanosarcina barkeri methyltransferase II homolog and its associated corrinoid protein homologous to methionine synthase. J Bacteriol **178:**6599-607.

Polycarpo, C., A. Ambrogelly, A. Berube, S. M. Winbush, J. A. McCloskey, P. F. Crain, J. L. Wood, and D. Soll. 2004. An aminoacyl-tRNA synthetase that specifically activates pyrrolysine. Proc Natl Acad Sci U S A **101:**12450-4.

Poppe, L., and J. Retey. 2005. Friedel-Crafts-type mechanism for the enzymatic elimination of ammonia from histidine and phenylalanine. Angew Chem Int Ed Engl **44:**3668-88.

Ragsdale, S. W., P. A. Lindahl, and E. Munck. 1987. Mossbauer, EPR, and optical studies of the corrinoid/iron-sulfur protein involved in the synthesis of acetyl coenzyme A by Clostridium thermoaceticum. J Biol Chem **262:**14289-97.

Rogers, J. E. and W. B. Whitman. 1991. Microbial production and consumption of greenhouse gases: methane, nitrogen oxides, and halomethanes. American Society for Microbiology, Washington D. C.

Russell, W. K., Z. Y. Park, and D. H. Russell. 2001. Proteolysis in mixed organic-aqueous solvent systems: applications for peptide mass mapping using mass spectrometry. Anal Chem **73:**2682-5.

Sauer, K., and R. K. Thauer. 1998. Methanol:coenzyme M methyltransferase from Methanosarcina barkeri--identification of the active-site histidine in the corrinoid-harboring subunit MtaC by site-directed mutagenesis. Eur J Biochem **253:**698-705.

Sauer, K., and R. K. Thauer. 1999. Methanol:coenzyme M methyltransferase from Methanosarcina barkeri -- substitution of the corrinoid harbouring subunit MtaC by free cob(I)alamin. Eur J Biochem **261:**674-81.

Schuster, B., and J. Retey. 1995. The mechanism of action of phenylalanine ammonia-lyase: the role of prosthetic dehydroalanine. Proc Natl Acad Sci U S A **92:**8433-7.

Shima, S., and R. K. Thauer. 2005. Methyl-coenzyme M reductase and the anaerobic oxidation of methane in methanotrophic Archaea. Curr Opin Microbiol **8:**643-8.

Shima, S., M. Goubeaud, D. Vinzenz, R. K. Thauer, and U. Ermler. 1997. Crystallization and preliminary X-ray diffraction studies of methyl-coenzyme M reductase from methanobacterium thermoautotrophicum. J Biochem **121:**829-30.

Siebert, A., T. Schubert, T. Engelmann, S. Studenik, and G. Diekert. 2005. Veratrol-O-demethylase of Acetobacterium dehalogenans: ATP-dependent reduction of the corrinoid protein. Arch Microbiol **183:**378-84.

Small-Howard, A. L., and M. J. Berry. 2005. Unique features of selenocysteine incorporation function within the context of general eukaryotic translational processes. Biochem Soc Trans **33:**1493-7.

Snell, E. E., and B. M. Guirard. 1986. Pyridoxal phosphate-dependent histidine decarboxylase from Morganella AM-15. Methods Enzymol **122:**139-43.

Soares, J. A., L. Zhang, R. L. Pitsch, N. M. Kleinholz, R. B. Jones, J. J. Wolff, J. Amster, K. B. Green-Church, and J. A. Krzycki. 2005. The residue mass of L-pyrrolysine in three distinct methylamine methyltransferases. J Biol Chem **280:**36962-9.

Srinivasan, G., C. M. James, and J. A. Krzycki. 2002. Pyrrolysine encoded by UAG in Archaea: charging of a UAG-decoding specialized tRNA. Science **296:**1459-62.

Stupperich, E. 1993. Recent advances in elucidation of biological corrinoid functions. FEMS Microbiol Rev **12:**349-65.

Stupperich, E., I. Steiner, and H. J. Eisinger. 1987. Substitution of Co alpha-(5-hydroxybenzimidazolyl)cobamide (factor III) by vitamin B12 in Methanobacterium thermoautotrophicum. J Bacteriol **169:**3076-81.

Tallant, T. C., and J. A. Krzycki. 1997. Methylthiol:coenzyme M methyltransferase from Methanosarcina barkeri, an enzyme of methanogenesis from dimethylsulfide and methylmercaptopropionate. J Bacteriol **179:**6902-11.

Taylor, C. D., and R. S. Wolfe. 1974. Structure and methylation of coenzyme M(HSCH2CH2SO3). J Biol Chem **249:**4879-85.

Thauer, R. K. 1998. Biochemistry of methanogenesis: a tribute to Marjory Stephenson. 1998 Marjory Stephenson Prize Lecture. Microbiology **144 (Pt 9):**2377-406.

Theobald-Dietrich, A., R. Giege, and J. Rudinger-Thirion. 2005. Evidence for the existence in mRNAs of a hairpin element responsible for ribosome dependent pyrrolysine insertion into proteins. Biochimie **87:**813-7.

van Beelen, P., J. F. Labro, J. T. Keltjens, W. J. Geerts, G. D. Vogels, W. H. Laarhoven, W. Guijt, and C. A. Haasnoot. 1984(a). Derivatives of methanopterin, a coenzyme involved in methanogenesis. Eur J Biochem **139:**359-65.

van Beelen, P., A. P. Stassen, J. W. Bosch, G. D. Vogels, W. Guijt, and C. A. Haasnoot. 1984 (b). Elucidation of the structure of methanopterin, a coenzyme from Methanobacterium thermoautotrophicum, using two-dimensional nuclear-magnetic-resonance techniques. Eur J Biochem **138:**563-71.

Warren, S., B. Zerner, and F. H. Westheimer. 1966. Acetoacetate decarboxylase. Identification of lysine at the active site. Biochemistry **5:**817-23.

White, R. H. and D. Zhou. 1993. Biosynthesis of the coenzymes in methanogens. p. 409-444 . *In* James G. Ferry (ed.), Methanogenesis. Ecology, Physiology, Biochemistry, and Genetics. Chapman & Hall. New York.

Wickner, R. B. 1969. Dehydroalanine in histidine ammonia lyase. J Biol Chem **244:**6550-2.

Woese, C. R., L. J. Magrum, and G. E. Fox. 1978. Archaebacteria. J Mol Evol **11:**245-51.

Woese, C. R., O. Kandler, and M. L. Wheelis. 1990. Towards a natural system of organisms: proposal for the domains Archaea, Bacteria, and Eucarya. Proc Natl Acad Sci U S A **87:**4576-9.

Xie, J., and P. G. Schultz. 2005. An expanding genetic code. Methods **36:**227-38.

Zhang, Y., P. V. Baranov, J. F. Atkins, and V. N. Gladyshev. 2005. Pyrrolysine and selenocysteine use dissimilar decoding strategies. J Biol Chem **280:**20740-51.

Zinder, S. H. 1993. Physiological ecology of methanogens. p. 128-206. *In* James G. Ferry (ed.), Methanogenesis. Ecology, Physiology, Biochemistry, and Genetics. Chapman & Hall. New York.